1507 The Expression of Apoptotic Related Proteins and Apoptosis in Human Renal Tissues of Class II and IV Lupus Nephritis.

J Zhang, J Cui, YQ Zhang, Q Qiao. Xijing Hospital, Fourth Military Medical University, Xi'an, Shaanxi, China; Tangdu Hospital, Fourth Military Medical University, Xi'an, Shaanxi, China.

Background: Apoptosis is involved in glomerular injuries leading to glomerulonephritis. The role of renal cell apoptosis in the pathogenesis and progress of human lupus nephritis (LN) is still controversial. Furthermore, in different types of LN renal tissues, the expression of apoptotic related proteins, such as FasL, Bax and caspase-3, is still unknown. We therefore investigated these apoptotic related proteins and apoptosis index (AI) in human renal tissues of class II and IV LN.

Design: The expressions of FasL, Bax and caspase-3 were assessed in forty-two cases of human LN renal tissues (twenty cases of class II, twenty-two cases of class IV) and ten cases of human normal renal tissues by immunocytochemistry. The terminal deoxynucleotidyl transferase dUTP nick end labeling (TUNEL) staining was used to assess AI.

Results: In class II and IV LN renal tissues, the increased expressions of FasL, Bax, caspase-3, and AI were detected in glomerular cells, tubular epithelial cells compared with controls (P<0.05). The expression of Bax, caspase-3 and AI in glomerular cells of class IV LN was significantly higher than class II LN (P<0.05). However, there was no difference in FasL expression between class II LN and class IV LN (P>0.05).

Conclusions: Apoptosis might be induced to LN pathogenesis by FasL, Bax and caspase-3. There might be other pathways except Fas/FasL signaling to initiate apoptosis during LN progress.

1508 Exogenous Ac-SDKP Administration Regulates Profibrotic Molecules in Obstructed Kidneys.

Y Zuo, SA Potthoff, H-C Yang, L-J Ma, AB Fogo. Vanderbilt University, Nashville, TN.

Background: Our previous studies showed that thymosin β4 (Tβ4), a G-actin sequestering protein, is remarkably increased in the obstructed kidney in the unilateral ureteral obstruction (UUO) model of tubulointerstitial fibrosis. Ac-SDKP, the degradation product of Tβ4 by prolyl oligopeptidase (POP), is postulated to have anti-fibrotic effects. Moreover, we found that inhibition of POP shifted the balance of Tβ4 and Ac-SDKP and exacerbated fibrosis in obstructed kidneys. We have now investigated profibrotic molecular gene expression in the UUO kidneys.

Design: Male C57BL/6 mice were sacrificed at day 5 after UUO and treatments: UUO without treatment, UUO+POP inhibitor (S17092, 40mg/kg per day, by gavage), UUO+Tβ4 (150μg/d, i.p.), UUO+combination (POP inhibitor and Tβ4), and UUO+Ac-SDKP (1.6 mg/kg/d, delivered by minipump).

Results: POP activity was significantly decreased in the obstructed kidneys of mice treated with either POP inhibitor or the combination (8% and 21% of levels in untreated UUO, respectively, both p<0.05). Ac-SDKP concentration was significantly reduced by both the POP inhibitor and combination treatment but dramatically increased by Ac-SDKP administration vs. untreated UUO (POP inhibitor, 47%; combination, 61%; Ac-SDKP, 172% of untreated UUO, respectively, all p<0.05). Neither POP activity nor Ac-SDKP was affected by Tβ4 treatment (77% and 78% of untreated UUO, respectively). Ac-SDKP treatment dramatically decreased plasminogen activator inhibitor (PAI-1), transforming growth factor (TGF)-β1, Tβ4, collagen I and III expression assessed by real time PCR vs. untreated UUO. By contrast, PAI-1, TGF-β1 and collagen III expressions were significantly increased by POP inhibitor. Ku80, a potential receptor for Tβ4, was abundantly present in glomerular endothelial cells and peritubular capillary endothelium in UUO kidneys and increased vs. non-obstructed kidneys. Ku80 mRNA in the UUO kidney assessed by real time PCR was dramatically increased by POP inhibitor and Tβ4 treatment vs. untreated UUO.

Conclusions: Our study suggests that exogenous administration of Ac-SDKP inhibits profibrotic factors. We propose that the balance of thymosin β4 and Ac-SDKP is crucial in determining tubulointerstitial fibrosis, and Ku80, a potential receptor for Tβ4, may modulate these processes.

Liver & Pancreas

1509 Site-Specific Subclassification of Ampullary Carcinomas: Delineation of Four Clinicopathologically and Prognostically Distinct Subsets in an Analysis of 249 Cases.

N Adsay, N Ohike, T Tajiri, GE Kim, A Krasinskas, S Balci, O Basturk, S Bandyopadhyay, DA Kooby, SK Maithel, J Sarmiento, CA Staley. Emory, GA; Showa, Yokohama, Japan; UCSF, San Francisco, CA; UPMC, Pittsburgh, PA; MSKCC, NY; WSU, MI.

Background: Ampullary (AMP) carcinomas (ACs) encompass a highly heterogeneous group; there have not been uniformly applied definitions or systematic analysis of the neoplasms arising in different compartments of this region.

Design: 249 strictly-defined primary ACs were analyzed with careful correlation of gross and microscopic findings to determine the tumor epicenter, and if present, extent of involvement by preinvasive neoplasm of the duodenal surface (DS), the edge of papilla of Vater (PV) and intraampullary region (IA). Their prognosis was compared to that of 112 pancreatic carcinomas.

Results: I. Overall, AC cases had significantly better prognosis than pancreatic carcinoma cases (p<0.01). **II.** ACs could be further classified into 4 distinct subtypes (See figure 1 for illustration and clinicopathologic information). **1.AMP-NOS**: Ulcero-fungating tumor located at PV with epicenter of invasion at PV/IA was most common (56%). **2.Intra-AMP:** Invasive carcinomas arising in intraampullary papillary-tubular neoplasms (AJSP, 2010, in press) had the best prognosis. These relatively large overall sized tumors had smaller size of invasion and typically occurred in men. **3.AMP-ductal**: Mucosal-covered, button-like elevation of PV without significant exophytic (preinvasive) growth on DS/PV had plaque-like thickening of intrapancreatic CBD or pancreatic duct walls that formed constructive sclerotic (non-exophytic) tumors. These were the smallest tumors, but had the worst prognosis, presumably due to pancreatobiliary histology/origin, yet prognosis was better than pancreatic carcinomas (p<0.01). **4.PeriAMP-duodenal:** Exophytic (ulcero-fungating) duodenal tumor encasing PV but with bulk of preinvasive tumor (>75%) involving DS, and invasion epicenter away from ampulla itself. These were fairly large tumors with intestinal phenotype and high incidence of LN metastases.

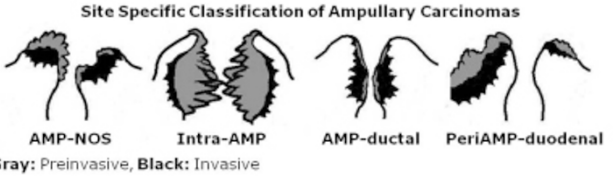

Clinicopathologic Data of Subtypes

	N	Age (y)	M/F	Mean size (mm) Overall/Inv	Invasive Histology (IN/non-IN)	LN Met (%)	T-stage T1+T2/ T3+T4	Survival (median mos/3y%)
AMP-NOS	140	65	1.5	25/18	38/102*	42	86/54	30*/45
Intra-AMP	61	64	2.2	29/15^	33/28^	28	52/9^	50^/69^
AMP-ductal	36	69*	0.9	19^/17	2/34^	41	14/22^	28/32
PeriAMP-duodenal	12	59	1.0	47^/34^	9/3^	50	8/4	46/63

p *<0.05 and ^<0.01; IN=Intestinal; LN=Lymph node; Met=Metastasis

Conclusions: AC comprises 4 clinicopathologic subtypes (*AMP-NOS, intra-AMP, AMP-ductal* and *PeriAMP-duodenal*) that are prognostically distinct.

1510 High Prevalence of IgG4 Positive Immunohistochemical Cholangitis in Liver Explants from Patients with PSC.

S Ali, GM Hirschfield, C Meaney, PD Greig, G Therapondos, SE Fischer. University of Toronto, ON, Canada.

Background: IgG4 associated cholangitis/pancreatitis is a highly steroid responsive inflammatory disease. As many as 10-15% of patients with primary sclerosing cholangitis (PSC) are reported to have elevated serum IgG4 levels, and this subpopulation may have a different natural history. IgG4 deposition histologically has been reported in explants from patients with PSC. The aim of the study is to confirm the prevalence of histological IgG4 associated cholangitis in patients undergoing liver transplantation for PSC.

Design: IgG4 immunohistochemistry was performed on liver explants from patients with PSC (n=123) and unrelated cholestatic and viral liver disease (n=50), using representative sections from the hilum. Positive IgG4 staining was defined either as ³10 positive IgG4 cells per high power field (HPF) or as no staining (<5 cells/HPF), mild staining (5-10 cells/HPF), moderate staining (11-29 cells/HPF) and marked staining (³30 cells/HPF). Immunochemical staining was compared to baseline lymphoplasmacytic inflammation. Clinical correlations with pre- and post-transplant variables were performed.

Results: Of the 50 control liver sections (PBC, n=19; HCV, n=19; HBV, n=8; AIH, n=6) none had marked staining and mild-moderate staining was seen in only one AIH explant, one PBC explant, and three HCV explants. In contrast of the 123 explants from patients with PSC studied, 59 (48.0%) had positive IgG4 immunohistochemical staining in hilar tissue (³10 cells per HPF). Forty two (34.1%) were classified as no IgG4 staining, 22 (17.9%) had mild staining, 28 (22.8%) moderate staining, and 31 (25.2%) had marked staining. Tissue IgG4 positivity was strongly correlated with moderate to marked periductal (hilar) lymphoplasmacytic inflammation (P<0.001) i.e. the inflammation surrounding the large hilar ducts which extends into adjacent tissue. Positive IgG4 staining was more likely in men (P=0.04), and in those with a history of pancreatitis (P=0.03). Other clinical parameters were unrelated to IgG4 staining, in particular age at diagnosis, presence of IBD and presence of recurrent disease.

Conclusions: A large number of patients undergoing transplantation for PSC have marked histological IgG4 plasmacytic cholangitis. Further characterization of the significance of this histological observation is required, as it raises the question of whether steroids may have a role in a sub-population of patients with PSC.

1511 Antibody-Mediated Rejection and Graft Outcome in ABO-Compatible Liver Re-Transplantation.

S Ali, V Shah, K Kantz, A VanDyke, M Mahan, S Skorupski, B Eisenbery, I Lopez-Plaza, G Rada, A Ormsby. Henry Ford Hospital, Detroit, MI.

Background: Unlike kidney, the role of HLA antibody mediated rejection (AMR) in ABO-compatible liver transplantation is still controversial. Limited reports described isolated episodes of AMR with early graft loss requiring re-transplantation (re-tx) despite aggressive therapy. We conducted a retrospective study of re-transplanted patients (pts) to explore similar incidence and effect on transplantation outcome.

Design: Fifty four of 63 Pts who underwent ABO-compatible/identical orthotropic liver re-tx since May 2004 were selected. Pts were classified based on time to graft failure into group; (A) primary non-function graft or graft loss within the first 7 days (ds) from transplantation; (B) re-tx pts within 8-90 ds and (C) re-tx pts > 91 ds. The latter was chosen sequentially based on the UNOS registration number. 142 graft biopsies

and hepatectomy specimens were selected for histological review and C4d staining including all time zero biopsies, graft hepatectomies and post-transplant biopsies. The association between predictor values and graft survival were assessed using ordinal models for multinomial data. Repeated-measures logistic regression was used to examine the association between C4d staining and graft survival. All analyses were completed using SAS 9.2.

Results: All 7 pts met our group A criterion, 12/14 pts in group B and 35/42 were included in group C. Pts demographics: 36 M/18 F, mean 51 years (range 19-71). Elevated native liver ALT, AST, and INR levels prior to transplantation were significantly and negatively associated with first graft survival (p = 0.01, <0.0001, and 0.03, respectively); however, only AST remained significant after combining three parameters (p = 0.003). Albumin levels, ALK, graft cold and warm ischemic time, C4d staining, and HLA class I/II mismatch antigens did not impact graft survival (p-values >0.05*)*. fourteen grafts demonstrated possible evidence of AMR after excluding other causes based on the NIH published consensus. DSA were documented in 13 of them using flow-PRA single antigen beads and anti-human globulin CDC T-cell trays. C4d endothelial and sinusoidal staining was noted in 6/11, 2/2 and 10/23 of specimens with acute cellular rejection (ACR), chronic ductopenic rejection and recurrent HCV, respectively.

Conclusions: Our findings support the concept that liver naturally resists AMR and its impact remains limited to few reported cases. In our cohort elevated native liver ALT, AST and INR made a negative impact on early graft survival. C4d expression, unlike other allografts, is not a predictor of AMR as it can be seen in various other conditions.

1512 Neutrophil Granulocytes Are the Only Source of MPO in Injured Liver.

A Amanzada, IA Malik, S Sultan, G Ramadori. University of Medicine, Goettingen, Germany.

Background: Myeloperoxidase (MPO) is involved in acute and chronic inflammatory diseases. The source of MPO in acute liver diseases is still a matter of debate.

Design: Therefore, we anlaysed MPO-gene expression on sections from normal and acutely damaged [carbon tetrachloride- (CCl_4) or Whole Liver g-Irradiation] rat liver by immunohistochemistry, real time PCR and Western blot analysis of total RNA and protein. Also total RNA and protein from isolated Kupffer cells (KC), hepatic stellate cells, Hepatocytes, endothelial cells and neutrophil granulocytes (NG) was analysed by real time PCR and Western blot, respectively. Sections of acutely injured human liver were prepared for MPO and CD-68 immunofluorescence double staining.

Results: In normal rat liver MPO was detected immunohistochemically and by immunofluorescence double staining only in single NG. No MPO was detected in isolated parenchymal and non-parenchymal cell populations of the normal rat liver. In acutely damaged rat liver mRNA of MPO increased 2,8-fold at 24 hr after administration of CCl_4 and 3,3-fold at 3 hr after g-Irradiation. In acutely damaged rat and human livers MPO was detected immunhistochemically and by immunofluorescence double staining only in NGs. NG identity was confirmed by immmunostaining of neutrophil elastase. Furhtermore, there was no detection of MPO in ED1/CD-68 positive Cells either.

Conclusions: Our results demonstrate that, in contrast to earlier reports (e.g. Hepatology 2009; 50: 1484-1493) expression of MPO in damaged rat and human liver seems to be due to recruited NGs.

1513 Endoscopic Ultrasound-Guided Fine-Needle Aspiration Cytology of Pancreatic Neuroendocrine Tumors.

S Asioli, A Barreca, D Pacchioni, F Maletta, C De Angelis, A Sapino, G Bussolati. University of Turin, Italy.

Background: Pancreatic Neuroendocrine Tumors (PNTs) are relatively uncommon tumors that account for 1 to 2% of all pancreatic neoplasms. The aim of this report is to describe the cytomorphologic and immunocytochemical features of PNTs obtained by endoscopic ultrasound-guided fine-needle aspiration (EUS-FNA) and to compare them with the histological results.

Design: Forty cases diagnosed with PNTs based on EUS-FNA were studied retrospectively (from 2003 to 2010). Clinical data, EUS findings, cytological and immunocytochemical features were reviewed with particular attention to the on-site slides. The final histopathologic diagnosis from twenty-three patients was also available for comparison.

Results: The case series was of 40 patients (20 men, 20 women), ranging in age from 30 years to 75 years. The mean size of the tumors by EUS was 29 mm (range, 8-100 mm). The average number of FNA per patient to obtain adequate material was 3. The most helpful cytologic findings for the diagnosis of PNTs were: i) high cellularity sample ii) monotonous, poorly cohesive population of small or medium-sized cells iii) granular chromatin (salt and pepper) and iv) plasmacytoid morphology. Immunocytochemistry (positivity for chromogranin A and/or synaptophysin) on cell blocks confirmed the neuroendocrine differentiation of tumors in all patients and Ki67 index was effective for distinguishing well differentiated from high/grade PNTs (p=0.001). The cytological diagnosis of PNT was histologically confirmed in 23 cases (57%) submitted to surgical resection

Conclusions: EUS-FNA is an efficient and accurate procedure for the diagnosis of PNTs and may have a role in determining management strategy.

1514 Reduced Angiotensinogen in Neonatal Hemochromatosis Leads to Impaired Development of Proximal Renal Tubules and Compensitory Glomerular Changes.

D Azar, S Bonilla, D Amaro, P Whitington, H Krous. University of California, San Diego; Northwestern University Feinberg School of Medicine, Chicago, IL; Rady Children's Hospital, San Diego, CA.

Background: Neonatal hemochromatosis (NH) is associated with severe liver injury and extrahepatic tissues siderosis. Renal tubular dysgenesis (RTD) is characterized by paucity or absence of proximal renal tubules (PRTs) leading to late onset oligohydramniosis. While five cases of concurrent NH and RTD have been reported, more recently Bonilla et al. showed a larger number of NH patients have reduced PRTs with a correlation between hepatocyte density, hepatic angiotensinogen (AGT) expression, and PRT density. The current study aims to support these results, confirming the correlation between AGT expression and PRT density as well as exploring glomerulocystic change and expression of Fumarylacetoacetate hydrolase (FAH), a PRT specific marker, within the glomerular epithelium as compensatory/metaplastic changes to accommodate for lost PRT function.

Design: Liver and kidney sections from four NH cases and four gestational age-matched controls were examined. Hepatocyte and glomeruli counts and the degree of glomerular cystic change were determined from H+E sections. Immunohistochemically stained sections were assessed to determine hepatic AGT expression, PRT density (FAH), and renal distal tubule density (EMA). FAH staining of glomerular epithelium was also evaluated. A correlation between hepatocyte volume, AGT expression, and PRT density was sought.

Results: NH cases showed reduced hepatocyte volume(P=0.02), AGT expression(P=0.02), and PRT density(P=0.0007) compared to the age-matched controls, with no difference in distal tubules(P=0.26). AGT expression was correlated to hepatocyte volume(R^2=0.85) and PRT density(R^2=0.81). One NH case and all control cases showed no glomerulocystic change and no glomerular FAH staining. Two NH cases with moderately reduced PRTs showed mild glomerulocystic change and occasional glomerular FAH staining. The remaining NH case, with the fewest PRTs, showed moderate glomerulocystic change and a higher density of glomerular FAH staining.

Conclusions: A spectrum of renal pathology is seen in NH patients including reduced PRTs. Fetal liver damage with decreased AGT synthesis is the likely mechanism leading to RTD in NH. Glomeruli in cases with reduced PRTs demonstrate glomerulocystic changes and FAH staining of the glomerular epithelium, possibly in compensation for lost PRT function.

1515 Molecular Analysis of Pancreatic Ductal Carcinoma and Pancreatic Intraepithelial Neoplasia (PanIN): Does PanIN Represent a Precursor to Invasive Ductal Carcinoma or Secondary Cancerization of Ducts.

SJ Bokhari, JF Silverman, SD Finkelstein, A Mohanty. Allegheny General Hospital, Pittsburgh, PA; RedPath Integrated Pathology, Pittsburgh, PA.

Background: PanIN is seen frequently associated with invasive ductal carcinoma of the pancreas in the same specimen, often found adjacent to the foci of invasive ductal carcinoma. PanIN is assumed to be a precursor lesion of invasive ductal carcinoma of the pancreas. However, there is a lack of data in the literature regarding whether PanIN is a definite precursor lesion or represents cancerization of the ducts present in close proximity to the invasive ductal carcinoma. To address this question, we performed comparative mutational profiling of the invasive ductal carcinoma and the adjacent areas with PanIN.

Design: A total of 14 cases of invasive pancreatic ductal carcinoma with associated PanIN were retrieved from the hospital computer system following IRB approval. All cases were confirmed by histology. Tissue sections from 14 pancreatic cancer cases underwent microdissection of both invasive and PanIN foci present adjacent to and at a distance from the invasive tumor. Mutational profiling was performed which consisted of 1) KRAS mutation (1st exon) (DNA sequencing), and 2) allelic imbalance (loss of heterozygosity [LOH]) for a panel of 16 markers situated at 1p, 3p, 5q, 9p, 10q, 17p, 17q, 18q, 21q, and 22q (GeneScan fragment length analysis). For KRAS point mutation, lower threshold of determination of mutant to wild type bases was approximately 10% of mutant to normal. For LOH determination, lower threshold for significant allelic imbalance was at least 2 times the ratio of peak heights for the non-neoplastic DNA for determination of marker informativeness. Mutational clonality (quantitative extent of clonal expansion) was based on the ratio of allele peak heights (LOH) or ratio of mutant and wild type base peaks (KRAS). The mutational profiles between the invasive and PanIN type foci were compared for degree of concordance.

Results: All 14 cases (100%) showed a greater number of cumulative mutations in the foci of invasive ductal carcinoma compared to the cumulative mutations in the foci with PanIN. This finding supports that PanIN is a precursor lesion and not a secondary process arising from cancerization of the ducts by invasive ductal carcinoma.

Conclusions: Our findings support that PanIN is a precursor lesion to invasive ductal carcinoma of the pancreas and does not represent cancerization of the ducts by the invasive ductal carcinoma.

1516 The Nonalcoholic Fatty Liver Disease Activity Score (NAS) and the Histopathologic Diagnosis in Nonalcoholic Fatty Liver Disease: Distinct Clinicopathologic Meanings.

EM Brunt, DE Kleiner, LA Wilson, PH Belt, BA Neuschwander-Tetri. Washington University School of Medicine, St. Louis, MO; National Cancer Institute, Washington, DC; Johns Hopkins University, Baltimore, MD; Saint Louis University School of Medicine, MO.

Background: The diagnosis (dx) of nonalcoholic steatohepatitis (NASH) is characterized by clinical features and the presence and pattern of specific histological

lesions in liver biopsy. Some studies have used threshold values of the nonalcoholic fatty liver disease activity score (NAS), derived from unweighted sum of scores for steatosis (0-3), lobular inflammation (0-2) and ballooning (0-2), specifically NAS ≥ 5, as a surrogate for the histologic dx of NASH. **Aim:** To evaluate the validity of the NAS to replace pattern-based dx of NASH.
Design: Biopsy and clinical data from adults in the NASH Clinical Research Network (CRN) Database and clinical trials were reviewed. Biopsies had been blindly evaluated, scored and dxd by the NASH CRN Pathology Committee. Excluded were biopsies with cirrhosis, or the uncommon "pediatric" pattern of zone 1 accentuation (n=42).
Results: Among 934 biopsies, 543 (58%) were dxd as definite steatohepatitis (SH), 183 (20%) as borderline SH, and 208 (22%) "not SH". The NAS was ≥ 5 in 51% and ≤ 4 in 49%. Among the biopsies of definite SH, 75% had NAS ≥ 5, as did 28% of borderline SH and 7% of "not SH" biopsies. Of all biopsies with NAS ≥ 5, 86% had SH and 3% were "not SH". Forty-two percent of NAS ≤ 4 were "not SH"; in the remaining 58% of NAS ≤ 4, 50% had SH. Thus, NAS ≤ 4 did not always equal a benign dx. Univariate linear regression analysis demonstrated that NAS≥5 and SH were individually associated with an increase in serum levels of ALT and AST ($p<0.0001$). When both the NAS≥5 and SH were included in a multiple linear regression model, both retained a significant association with ALT and AST. In contrast, SH was associated with diabetes ($p<0.0001$), metabolic syndrome ($p=0.03$), and insulin resistance by HOMA-IR ($p<0.0001$) and QUICKI ($p=0.02$), while the NAS≥5 was not associated with any of these.
Conclusions: The results of this study do not validate usage of NAS ≥ 5 as a means to dx SH. The process of histologic dx in SH, as in all forms of liver disease, is derived from evaluation of patterns as well as individual lesions, and differs from that of scoring. Thus, the diagnosis of definite SH does not always correlate with pre-determined values of the semiquantitative NAS.

1517 High Level of Hexokinase 2 (HK2) Expression Is Observed in Diabetes, Biologically Aggressive Hepatocellular Carcinomas (HCC), and in the Progression of HCC.

R Chennuri, A Chan, R Patel, TJ Layden, N Hay, SJ Cotler, G Guzman. University of Illinois (UIC), Chicago; UIC, Chicago.
Background: The mitochondrial high affinity HK2 that catalyzes the first committed step in glycolysis is highly expressed in HCC. Animal studies have shown that normal hepatocytes exhibit only low affinity hexokinase (glucokinase [GK]) but during tumorigenesis, there is a switch from GK to HK2 expression. Aims: To establish the level of HK2 in human liver tissues ranging from cirrhosis to dysplasia & HCC; & to determine whether HK2 expression is associated with clinical parameters or the physical characteristics of the tumor.
Design: We analyzed a liver tissue array derived from 159 subjects with cirrhosis (108 without HCC + 45 with HCC) & 6 with normal liver for the expression of HK2 by standard immunohistochemistry. Cytoplasmic HK2 positivity was quantified by image analysis in normal, cirrhosis, dysplasia, & HCC. One-way ANOVA & independent samples t-tests for normally distributed groups, Kruskal-Wallis tests & Mann-Whitney U tests for non-normally distributed groups, were employed using SPSS Statistics 17.0.
Results: The HK2 mean level in normal liver was 36.67 (±15.20;n=6), cirrhosis 44.18 (±32.71;n=106), dysplasia 59.94 (±39.86;n=143), & HCC 64.42 (±34.89;n=45). In the cirrhosis without HCC group, we found that the HK2 level was higher in dysplasia in DM(+)(82.21) vs DM(-) subjects (56.18)($p=0.018$). In areas of dysplasia, advanced stage HCCs (stage III & IV) have a higher level of HK2 (87.88) in comparison to low stage HCCs (stage 1, 41.34)($p=0.023$). In the HCC group, HK2 expression was higher in poorly differentiated tumors (73.77) in comparison to well differentiated (47.18) and moderately differentiated tumors (70.97)($p=0.033$), & in pleomorphic variant (85.82) vs non-pleomorphic HCC variants (57.03)($p=0.008$). In the cirrhosis without HCC group, HK2 expression was higher in dysplasia (61.76) in comparison to cirrhosis (46.54)($p=0.005$). In the HCC group, HK2 expression was peak in carcinoma (64.42), followed by dysplasia (56.00) & cirrhosis (37.26)($p=0.007$).
Conclusions: This study shows that the level of HK2 is higher in DM(+) subjects, & in biologically aggressive HCCs. Moreover, HK2 may be an important biomarker for assessing the progression of cirrhosis to dysplasia and HCC. Verification of the findings in this study using a larger cohort is necessary to determine whether HK2 is biomarker for hepatocarcinogenesis.

1518 FNH-Like Lesions and Glutamine Synthetase Expression in the Liver in Hereditary Hemorrhagic Telangiectasia.

S-J Cho, I Wanless, V Paradis, R Pai, P Bioulac-Sage, V Alves, T Souza, H Makhlouf, P Schirmacher, K Evason, L Ferrell. Univ Calif, San Francisco; Queen Elizabeth II Health Sciences Center, Halifax, Canada; Hospital Beaujon, Clichy, France; Washington Univ, St. Louis; Hospital Pellegrin, Bordeaux, France; Univ Sao Paulo, Brazil; Hospital Alianca, Salvador, Brazil; AFIP, Washington, DC; Univ Hospital, Heidelberg, Germany.
Background: Hereditary hemorrhagic telangiectasia (HHT) is a familial disease with arterial enlargement and large shunts in many organs, including the liver. In addition to telangiectases, arterialized nodules are often seen on hepatic imaging, some of which have been called focal nodular hyperplasia (FNH). In livers without HHT, FNH shows artery-portal vein shunts and a distinctive pattern of glutamine synthetase (GS) expression. In this study, we describe liver histology from 16 patients with HHT, concentrating on the vascular lesions (telangiectases), FNH-like lesions, and GS expression.
Design: Specimens (16) ranged from wedge biopsies (1/16) to partial (1/16) and total hepatectomies (14/16; including 1 autopsy). H&E, CD34 and GS stains were evaluated.
Results: Telangiectases typical of HHT were present in all cases. Surrounding sinusoids showed dilation and arterialization, as evidenced by increased CD34 staining (10/12). The extent of telangiectases varied from minimal (1/16) to almost confluent (1/16). 5 cases showed FNH-like lesions, defined by a cluster of component nodules forming a ring of hyperplastic hepatocytes surrounding a central fibrous region. Component nodules consisted of hepatocytes in 1-2-cell-wide plates, supplied by a portal tract containing an artery, often with ductular elements at the portal-parenchymal interface. The central fibrous region contained larger arteries, often with ductules but no ducts or portal veins. An obstructed hepatic or portal vein could be seen in the vicinity of each nodule. GS showed decreased staining around telangiectases, but showed characteristic "map-like" staining in the lesions. Obstructed veins were also seen in cases without lesions (5/11); 1 of these cases showed a background of cirrhosis and 2 cases showed ischemic necrosis.
Conclusions: Telangiectases in HHT provide local high flow and pressure, and remodel into a non-communicating shunt over a long period of development. We propose that if this flow pattern is acutely disturbed, by congestive injury or thrombus in a portal or hepatic vein, the flow must be accommodated by collaterals to normal adjacent hepatic vein drainage beds. The new flow causes hepatocyte hyperplasia, with increased GS expression, leading to the formation of FNH-like lesions.

1519 A Novel Monoclonal Antibody, mAb Das-1, Identifies a Colonic Phenotype and Is Specific for Intraductal Papillary Mucinous Neoplasm (IPMN) with a High Risk for Malignant Transformation.

KK Das, G Krings, MB Pitman, M Mino-Kenudson. Massachusetts General Hospital, Boston.
Background: IPMN is a precursor to pancreatic ductal adenocarcinoma, and consists of 4 epithelial subtypes with varying grades of dysplasia. Of those, the intestinal (IPMN-I) and gastric (IPMN-G) types comprise the vast majority of the neoplasms, and IPMN-G is known to have a much lower risk of developing invasive carcinoma than the other types. However, differentiation between subtypes remains a challenge, especially in the preoperative setting. mAb Das-1 is a murine monoclonal antibody that reacts specifically to a colonic epithelial phenotype. It is both sensitive and specific in identifying various pre-malignant and malignant lesions of the upper GI tract including Barrett's esophagus as well as incomplete gastrointestinal metaplasia associated with gastric cancer. The aim of this study was to assess the ability of mAb Das-1 to identify IPMNs associated with a high risk of malignant transformation.
Design: The study cohort consists of 94 distinct IPMN lesions and 13 IPMN-associated invasive carcinomas from 57 patients. A representative section from each lesion was stained with Das-1 by immunohistochemistry with appropriate controls. The cytoplasmic expression of Das-1 in greater than 5% of tumor cells was considered to be positive. Statistical significance was calculated by the Fisher exact test when compared to internal controls of normal pancreatic duct.
Results: Among IPMN-G, 0/14 (0%) lesions with low-grade dysplasia and only 2/20 (10%) with moderate dysplasia were reactive to Das-1. Compared to internal controls and IPMN-G with low-grade or moderate dysplasia, Das-1 expression was significantly higher in high-grade dysplasia (9/12 [75%], $p<0.0005$ and $p<0.001$, respectively). Among IPMN-I, 16/24 (67%, $p<0.0001$) lesions with moderate dysplasia were positive for Das-1 as were 16/18 (89%, $p<0.0001$) with high-grade dysplasia. Oncocytic-type IPMN demonstrated reactivity in 9/12 (75%, $p<0.05$). As for invasive IPMN, Das-1 was positive in 6/8 (75%, $p<0.01$) tubular adenocarcinomas and in 5/5 (100%, $p<0.01$) colloid carcinomas. The sensitivity and specificity of Das-1 in segregating high-risk/grade from low-risk lesions (IPMN-G with low-grade or moderate dysplasia) were 76% and 94%, respectively.
Conclusions: mAb Das-1 reacts with high specificity to high-risk/grade IPMN lesions compared to normal pancreatic ducts and low-risk lesions. The expression of this marker in preoperative samples such as cyst fluid may be useful as a tool to identify IPMN lesions at risk for malignant transformation.

1520 Increased FLK-1, PDGFR-α, and BRAF Expression in Hepatocellular Carcinoma: An Immunohistochemical Molecular Mediator Survey.

MA Delgado, X Li, SH Patel, PJ Kneuertz, NV Adsay, C Cohen, SK Maithel, AB Farris. Emory University Hospital, Atlanta, GA.
Background: Hepatocellular carcinoma (HCC) pathogenesis is thought to be related to a number of molecular mediators, many of which are involved in vascular neogenesis. FLK-1, a vascular endothelial growth factor receptor, and platelet derived growth factor receptors (PDGFR)-α and -β activate signal transduction pathways that stimulate angiogenesis. BRAF is a serine/threonine protein kinase that regulates cellular growth, proliferation and survival. We hypothesized that HCC would exhibit overexpression of these molecular mediators compared to normal liver.
Design: Patients without prior treatment for HCC, who underwent resection from 8/00-3/08, were identified in our clinical and pathology databases. Routinely stained sections were reviewed; and histologic features of the tumor were analyzed, including tumor grade and histologic type. Sections with HCC in relation to non-neoplastic liver were selected. Slides were immunohistochemically stained for FLK-1, PDGFR-α, PDGFR-β, and BRAF. Staining intensities of the tumor and non-neoplastic liver were separately graded on a 5-tier scale from 0-4. The difference in staining expression was analyzed by a matched-pair T-test, with a P-value <0.05 considered significant.
Results: Fifty-seven cases were available for review. Mean patient age was 62.3 ± 11.8 years old (± standard deviation); 65% were male. Tumors exhibited a variety of grades (Grade 1, 2, 3 and 4: 0, 46, 47 and 7 % of cases, respectively) and histologic subtypes (predominantly trabecular, with a minority of other types). There was significantly higher expression of FLK-1, PDGFR-α, and BRAF compared to surrounding non-neoplastic liver [Table]. There was not a statistically significant difference in expression between different tumor grades or histologic subtypes.

Expression of Molecular Mediators in HCC

	Tumoral expression (Mean ± S.D.)	Non-neoplastic tissue expression (Mean ± S.D.)	P-value
Flk-1	2.8±0.9	2.1±0.7	<0.0001
PDGFR-α	2.4±0.8	1.9±0.7	0.0005
PDGFR-β	1.5±0.9	1.5±0.6	0.5
BRAF	0.9±0.6	0.2±0.4	<0.0001

S.D.: standard deviation

Conclusions: FLK-1, PDGFR-a, and BRAF expression are significantly increased in HCC compared to surrounding non-neoplastic liver, suggesting that the expression of these molecules is altered in hepatocellular carcinogenesis. These findings may help to select patients who would benefit from targeted inhibitor therapy.

1521 The Role of the Soluble Epoxide Hydrolase Expression and K55R Genetic Polymorphism in Pancreatic Ductal Adenocarcionma.

X Ding, J Liao, H Li, MS Rao, S Krantz, D Bentrem, G-Y Yang. Northwestern University, Chicago, IL.

Background: Many studies have shown strong association between inflammation and pancreatic tumorigenesis. The soluble epoxide hydrolase (sEH) is an enzyme participating in arachidonic metabolism, particularly metabolism of endogenous signal and inflammatory mediators, 20--HETE (hydroxyeicosatrienoic acid) and EETs (epoxyeicosatrienoic acid). sEH is a 62-Kd protein containing a 35-kd C-termianl domain with epoxide hydrolase activity and a 25-kd N-terminal domain with phosphatase activity. Further, Enzyme activity of sEH is modified by the K55R genetic polymorphism, which is a risk factor for the development of coronary heart disease due to increased systemic inflammation. However the role of sEH in pancreatic carcinogenesis has never been studied. Because strong association between inflammation and pancreatic tumorigenesis, it is conceivable that pancreatic cancer development and progress might be preceded by disregulated sEH expression and activity.

Design: sEH expression was evaluated from pancreatectomy specimens resected for pancreatic ductal adenocarcinoma (28 cases) and chronic pancreatitis (19 cases) including sections containing PanIN (pancreatic intraepithelial neoplasia) lesions by immunohistochemistry. The sEH staining was classified as no staining (0), low intensity staining (+) or high intensity staining (++). K55R genetic polymorphism was evaluated in 70 pancreatic ductal adenocarcinoma specimen by PCR and DNA sequencing.

Results: Distinct over-expression of sEH was identified in infiltrating pancreatic ductal adenocarcinoma compared to normal, chronic pancreatitis, fibrotic, and PanIN lesions. 96% (27/28) pancreatic ductal adenocarcinoma showed strong cytoplasmic sEH staining. Three cases (15%) of chronic pancreatitis showed mild staining in chronic inflammatory cells and reactive stromal cells. 6 PanIN lesions (mainly PanIN I and II lesions) were negative for sEH. No positive staining was identified in normal pancreatic ductal epithelial cells, acinar cells and islets. sEH K55R single nucleotide DNA polymorphism was identified in 11% (8/70) of pancreatic ductal adenocarcinoma.

Conclusions: This study demonstrated significant over-expression of sEH in human infiltrating pancreatic ductal adenocarcinoma, indicating it may serve as a useful biomarker to differentiate pancreatic ductal adenocarcinoma from pre-malignant lesions. The K55R genetic polymorphism is detected in human pancreatic cancer. It further warrants exploring the role of up-regulated soluble epoxide hydrolase expression and sEH polymorphism in pancreatic carcinogenesis.

1522 Hepatic Pigment Accumulation in HIV Patients on HAART Therapy.

AR Doherty, LD Ferrell, CG Morse, DE Kleiner. University of California, San Francisco; National Institute of Allergy and Infectious Diseases, Bethesda; National Cancer Institute, Bethesda.

Background: Several highly active antiretroviral therapy (HAART) agents used in treating human immunodeficiency virus (HIV) inhibit multidrug-resistance protein 2 (MRP2), which functions in bile transport across the hepatocyte membrane. Hereditary defects in MRP2 result in Dubin-Johnson syndrome, which is characterized by accumulation of coarse granular pigment within hepatocytes. Similar pigment accumulation in hepatocytes has never been described in patients with HIV on HAART therapy.

Design: Liver biopsies in patients with HIV without hepatitis virus co-infection were reviewed. Clinical data were gathered including indication for biopsy, history of pre-existing liver disease, medications, and liver enzymes.

Results: We identified fifteen cases that showed coarse golden brown pigment within hepatocytes. The pigment granules tended to be larger and coarser than lipochrome, bile, or the pigment of Gilbert syndrome, and appeared similar to that of Dubin-Johnson syndrome. The pigment mimicked intracellular bile in one case, but was negative for bile on Hall's stain. Eleven cases (73%) showed diffuse distribution of pigment in all zones, three showed predominantly periportal pigment, and one showed predominantly centrizonal pigment. Seven cases also showed steatosis or steatohepatitis, one showed moderate hemosiderosis, and the others showed only mild chronic inflammatory changes. All patients were male with no history of pre-existing liver disease. The most common indication for biopsy was elevated liver enzymes, with average ALT of 128 IU/L (range 43-887 IU/L), AST 92 IU/L (range 29-664 IU/L), alkaline phosphatase 87 IU/L (range 54-136 IU/L), and GGT 143 U/L (range 24-574 U/L). Six patients (40%) had mildly elevated total bilirubin (average 1.3 mg/dL, range 0.3-3.9 mg/dL), which was unconjugated in two cases for whom data was available. One patient presented with jaundice and normal bilirubin. In 13 patients drug regimen data was available, and all were on HAART therapy. Mean duration of treatment was 13.5 years (range 6.3-17.2 years).

Conclusions: Patients with HIV on HAART therapy can develop pigment in the liver similar to that of Dubin-Johnson syndrome. The pigment is distinct from lipochrome or the pigment of Gilbert syndrome and rarely mimics intracellular bile. This finding may reflect altered function of MRP2 by HAART agents. In some cases it can be associated with hyperbilirubinemia or jaundice.

1523 Posttherapy Pathologic Stage and Number of Positive Lymph Nodes Predict Survival in Patients with Pancreatic Ductal Adenocarcinoma Treated with Neoadjuvant Chemoradiation.

JS Estrella, A Rashid, MH Katz, JE Lee, RA Wolf, GR Varadhachary, PWT Pisters, EK Abdalla, J-N Vauthey, H Wang, HF Gomez, DB Evans, JB Fleming, JL Abbruzzese, H Wang. U.T. M.D. Anderson Cancer Center, Houston, TX; The Medical College of Wisconsin, Milwaukee, WI.

Background: Pancreatic ductal adenocarcinoma (PDAC) remains a deadly disease despite recent advances in oncology and operative techniques. The addition of post-operative chemoradiation demonstrated very modest improvement in survival. In our institution, most patients with PDAC are treated with chemoradiation prior to surgery. Neoadjuvant chemoradiation identifies patients who would likely benefit the most from surgery, provides early treatment of micrometastatic disease, and reduces tumor volume. However, analysis of prognostic factors influencing survival is lacking in patients with PDAC treated with neoadjuvant chemoradiation and subsequent pancreaticoduodenectomy (PD).

Design: The study population comprised of 240 consecutive patients with PDAC who received different neoadjuvant chemotherapy/radiation therapy regimens and underwent pancreaticoduodenectomy (PD) between January 1999 and December 2007. Clinicopathologic features were correlated with disease-free and overall survival using Kaplan-Meier method and Cox regression analysis.

Results: Among 240 patients treated with neoadjuvant chemoradiation followed by PD, the median disease-free and overall survival times were 15.1 and 33.5 months, respectively. There was no significant difference in disease-free and overall survival among patients who received different neoadjuvant chemoradiation regimens. In univariate analysis, disease-free survival was associated with age (p=0.002), posttherapy tumor stage (ypT) (p<0.03), regional lymph node status (ypN) (p<0.001), number of positive lymph nodes (p<0.001), and pathologic AJCC stage (p=0.001), while overall survival was associated with intraoperative blood loss (p<0.03), margin status (p=0.02), ypT (p=0.005), ypN (p<0.001), number of positive lymph nodes (p<0.001), and pathologic AJCC stage (p<0.001). By multivariate analysis, disease-free survival was independently associated with age (p=0.004), number of positive lymph nodes (p=0.01), and AJCC stage (p=0.002) and overall survival was independently associated with differentiation (p<0.04), margin status (p=0.04), number of positive lymph nodes (p=0.001), and AJCC stage (p<0.001).

Conclusions: In patients with PDAC who were treated with neoadjuvant chemoradiation and subsequent PD, posttherapy pathologic stage and number of positive lymph nodes are significant independent prognostic factors for both disease-free and overall survival.

1524 Primary Pancreatic Adenocarcinoma, Metastatic Lymph Node and Distant Metastasis May Differ in HER2 Expression, Gene Amplification and CEP17 Copy Number: Possible Implications for Diagnostic Evaluation and Therapy.

F Fedeli, S Boccardo, P Ferro, N Gorji, P Dessanti, MC Franceschini, M Truini, MP Pistillo, S Salvi, S Roncella. ASL5, La Spezia, Italy; IST, Genova, Italy; AIL "Francesca Lanzone", La Spezia, Italy.

Background: Pancreatic adenocarcinoma (PAC) remains an often incurable disease. The development of the new therapy with anti-p185^{HER-2} (p185) monoclonal antibodies (Trastuzumab, Pertuzumab) has been proposed although the status of HER2 gene in PAC and its correlation with clinical history remain not completely defined. In our study we evaluated the expression of p185, HER2 gene amplification and chromosome 17 centromere (CEP17) copy number in PAC. In addition, we compared p185 expression and HER2 gene status of primary PAC, matched lymph node (LN) and unmatched distant metastasis (MTS).

Design: We analyzed 83 PAC (26 tumours at initial diagnosis, 20 LN, 37 MTS). On paraffin-embedded tissues, we performed immunohistochemistry (IHC) using the PATHWAY kit by Benchmark XT system (Ventana). The samples were analysed using standard criteria for HER2 positivity. A score of 0 or 1+ was regarded as IHC negative and 2+ or 3+ as IHC positive. FISH, to evaluate HER2 gene amplification and CEP17 copy number, was performed using the Pathvision® (Abbot) and/or ZytoLight kit (ZytoVision).

Results: We found p185 positive expression in 13/83 (15.7%) (all with 2+ score), gene amplification in 4/83 (4.8%) and increased CEP17 in 11/83 (13.2%) of all tissues. In particular, p185 expression was found in 4/4 (100%) cases of HER2 gene amplified tumours, in 4/11 (36.4%) cases of those with increased CEP17**,** in addition to 1/26 (3.8%) of primary PAC, 1/20 (5.0%) of LN and 11/37 (29.7%) of MTS. HER2 gene amplification was restricted to 4/37 (10.8%) of MTS, whereas increased CEP17 was found only in 8/37 (21.6%) of MTS and in 3/20 (15.0%) of LN. In 3 cases, increased CEP17 was found in LN and not in related primary tumours.

Conclusions: In PAC, p185 positive expression is associated with HER-2 gene amplification but is present only in a set of tumours with increased CEP17. The different HER2 expression observed among primary PAC, LN and distant MTS suggests the need for the pathologist's evaluation of HER2 status in all three tissue samples, as it may cause different responses to HER2 target therapy.

1525 VEGF-C Expression in Advanced and Metastatic Hepatocellular Carcinoma (HCC): An Autopsy Study in Cirrhotic Patients.

A Felipe-Silva, A Longatto-Filho, A Wakamatsu, C Cassol, V Alves. School Of Medicine, University of Sao Paulo, Brazil.

Background: Vascular endothelial growth factor-C (VEGF-C) immune-expression in HCC has been related to poor prognosis, tumor progression, vascular invasion and lymph node metastases. VEGF-C may be a target for anti-angiogenic therapy for HCC.

Design: This retrospective transversal study of autopsied cirrhotic patients with HCC correlates VEGF-C immune-expression to the following clinicopathological variables: gender, age, viral hepatitis, alcoholism, number and size of tumors, histological grade and pattern, extrahepatic metastases (EHM) and large venous invasion (LVI). Samples from 42 patients were cored in a tissue microarray paraffin block. Immunohistochemistry was performed using anti-VEGF-C rabbit antibody (cod182255, Invitrogen, 1:200), amplified by short peroxidase-polymer system (Novolink, Novocastra). VEGF-C immune-expression was estimated in intensity (0-3+) and distribution of HCC cells staining (0-100%). A score from 0 (no staining) to 300 (100% strong staining) was assigned. Scores were considered strongly positive (≥200), moderately positive (100 to 199), weakly positive (<100) and negative. Statistical significance was examined with Fisher's exact *P*-test and Student's t-test.

Results: Median age was 58 years (M:F rate 3.6:1). Viral hepatitis and alcoholism were present in 74% and 33% of cases. A single liver tumor was detected in 40.5%. The largest tumor measured up to 2cm in 26%. Low grade (1-2) and high grade (3-4) tumors were 31% and 69%. EHM were detected in 12% (7.1% to lung, 4.8% to lymph node and 2.4% to small bowel). LVI was detected in 7.1%. VEGF-C staining was strong, moderate, weak and negative in 21.4%, 47.6%, 14.3% and 16.7% of intrahepatic HCC. Strong staining was associated with high grade tumors (p=0.04) and trended to be associated with larger tumor size (p=0.06). Strong staining was observed in 83.3% of EHM (p<0.01) and 33.3% of LVI (p=0.14). Strong staining was observed in 3/3 lung, 1/2 lymph node and 1/1 small bowel metastases. Moderate and strong staining in intrahepatic HCC were associated with the finding of EHM (p=0.04). EHM and LVI had higher staining scores than intrahepatic tumors (p=0.02). HCC with EHM had higher staining scores than tumors without EHM (p=0.02). Correlations with number of tumors and other clinicopathological data were not significant.

Conclusions: In this autopsy series, higher VEGF-C expression scores were observed in high grade tumors, tumors that have metastasized and in EHM, particularly to the lung, thus suggesting VEGF-C as a potential surrogate marker for hematogenous spread.

1526 Progressive Familial Intrahepatic Cholestasis: Detection of New Mutations and Unusual Modality of Transmission.

P Francalanci, I Giovannoni, FM Santorelli, R Mariani, F Gennari, G Torre, M Di Rocco, C Castana, L Zancan, F Callea. Children's Hospital Bambino Gesu', Rome, Italy; Children's Hospital G. Gaslini, Genova, Italy; ISMET, Palermo, Italy; University of Padua, Italy.

Background: Progressive familial intrahepatic cholestasis (PFIC) refers to a heterogeneous group of autosomal recessive disorders of childhood that disrupt bile formation and present with cholestasis of hepatocellular origin. Three types of PFIC have been identified: PFIC 1 is caused by mutation in ATP8B1 gene encoding the FIC1 protein; PFIC 2 in ABCB11 encoding the bile salt export pump protein (BSEP) and PFIC 3 due to a defect in ABCB4 encoding the multi-drug resistant 3 protein (MDR3). Serum γ-glutamyltranspeptidase (γGT) activity is normal in PFIC 1 and 2, while is high in PFIC 3. Liver histology is not specific in each type of PFIC.

Design: We report on 13 children with intrahepatic cholestasis, in whom molecular analyses for PFIC were performed. Denaturing high-pressure liquid chromatography and direct gene sequencing for ATP9B1 and ABCB11 were carried out when γGT activity was normal, whereas the analysis of ABCB4 was done if high level of γGT was present. Genotypes were correlated with data on immunohistochemistry for BSEP and MDR3 deficiency.

Results: In our cohort, 3 cases were PFIC1, 8 showed BSEP deficiency and 2 cases had MDR3 deficiency. In 1 case of BSEP deficiency, we reported a homozygous c.2620C>T transition in exon 21, that was inherited through the rare phenomenon of paternal uniparental disomy (patUPD). In other 4 children, we identified some new mutations: c.1621A>C in 2 sisters, c.154C>T and c.1844A>G, (compound heterozygosity) in 1 child and c.2787_2788ins GAGAT (single heterozygous mutation) in the last one. Two cases of MDR3 deficiency were associated with a novel ABCB4 mutation (p.Arg595X), homozygous in one child and heterozygous in another patient where we also detected a new heterozygous c.937_992ins55/del6 mutation. On immunohistochemical analysis, all patients showed abnormal or absent BSEP or MDR3 staining. Five children underwent to liver transplant due to end-stage liver function.

Conclusions: PFIC are rare forms of cholestasis of hepatocellular origin. Diagnosis can be suspected on clinical manifestations and serology, but only full gene testing is able to offer a more accurate genetic counselling and recognition of rare phenomenon of padUPD.

1527 Hedgehog Signaling Pathway Is Frequently Activated in Pancreatic Neuroendocrine Tumors.

WL Frankel, M Bloomston, X Zhou. The Ohio State University, Columbus.

Background: The Hedgehog (Hh) signaling pathway plays a critical role in embryo development and governs a diverse array of cellular processes including cell proliferation, differentiation, and tissue patterning. Aberrant activation of this pathway, either by ligand expression, activating mutation/amplification or by loss of function of the core components, has been described in a number of human cancers. Small molecule (s) of Hh inhibitor is available and has shown promising in vivo and in vitro anti-tumor activity. We assessed Hh signaling activity in a cohort of pancreatic neuroendocrine tumors (NET) using immunohistochemistry for SHH and PTCH1.

Design: Tissue microarrays were constructed from formalin-fixed, paraffin-embedded blocks of 98 primary pancreatic NET and 7 normal pancreata (controls) from departmental archives and stained with SHH, PTCH1 and Ki-67. Expression intensity for SHH and PTCH1 was scored as 0 (absent), 1+ (weak), and 2+ (modest to high). The proliferation index was assessed using the percentage of tumor cells positive for Ki-67 nuclear labelling and grouped into ≤2%, 3-20%, >20%.

Results: All 7 normal islets expressed weak levels (1+) of SHH and PTCH1. Modest to high levels (2+) of SHH and PTCH1 expression were detected in 48 (49%) and 11 (11%) NET, respectively. No expression of SHH and PTCH1 was seen in 2 (2%) and 15 (16%) tumors, respectively. Seventy-two tumors showed a proliferation index of ≤2%, 24 of 3-20%, and 4 of >20%. No association was observed between SHH or PTCH1 expression and the proliferation index in NET.

Expression of SHH and PTCH1 in pancreatic NET

Staining Intensity	SHH (n = 98)	PTCH1 (n = 97)
2+	48 (49%)	11 (11%)
1+	48 (49%)	71 (73%)
0	2 (2%)	15 (16%)

Conclusions: Aberrant activation of the Hh pathway was present in up to half of pancreatic NET. Our findings suggest that Hh signaling pathway may represent a rational therapeutic target in pancreatic NET.

1528 Immunohistochemical Expression of Insulin-Like Growth Factor (IGF) Messenger Binding Protein-3 (IMP-3), S100A4 and CDX2 in Intrahepatic Cholangiocarcinoma (IHCC) and Extrahepatic Cholangiocarcinoma (EHCC) Cholangiocarcinoma and their Potential Biological Value.

CE Gimenez, SG Karak, D Mandich, R Cartun, S Ligato. Hartford Hospital, CT.

Background: Cholangiocarcinomas (CC) originate from the bile duct epithelium in either intrahepatic or extrahepatic location. In the development of the human biliary system, the extrahepatic bile ducts (EHBD) develop from the embryonic hepatic diverticulum, while the intrahepatic bile ducts (IHBD) originate within the liver from the ductal plate.

Due to this different embryological origin, we postulate that there is also a different immunohistochemical expression of certain markers between the intrahepatic cholangiocarcinomas (IHCC) and extrahepatic cholangiocarcinoma (EHCC). Previous studies have demonstrated an immunohistochemical expression of IMP-3 (also known as KOC), S100A4, and CDX2 in both pancreatic carcinoma and extrahepatic cholangiocarcinoma but no study has examined their expression in terms of IHCC versus EHCC.

Our aim is to investigate the immunophenotype of IHCC and EHCC and to find out new markers for their classification and different biological origin.

Design: We collected 19 cases of cholangiocarcinoma (CC), subdivided into 11 cases of IHCC and 8 cases of EHCC. All cases were immunohistochemicaly analyzed for IMP3 (KOC/L523S clone 69:1 Dako), S100A4 (Dabo polyclonal) and CDX 2 (Biogenex clone: CDX2-88) expression. The antibodies were estimated semiquantitatively: negative (-) if <5%, positive cells, grade 1 (+) between 5 and 20%, grade 2(++) between 20 and 50% and 3 (+++) >50%.

Results: EHCC expressed IMP-3 in 6/8 (75%), S100A4 in 4/8(50%), and CDX2 in 2/8(25%). IHCC expressed IMP-3 in 2/11(18%), S100A4 in 4/11(36%), CDX2 in 0/11(0%). Of all markers studied only the expression of IMP-3 was statistically significant (p<0.02).

	IMP-3*	S100A4	CDX2
IHCC	2/11 (18%)	4/11 (36%)	0/11 (0%)
EHCC	6/8 (75%)	4/8 (50%)	2/8 (25%

*p <0.02

Conclusions: This study has demonstrated that the IMP-3 is preferentially expressed in EHCC, supporting the hypothesis that EHCC is embryologically different form IHCC. This finding could prove valuable when choosing future target therapeutic options for cholangiocarcinomas depending on the tumor location and differential expression of IMP-3.

1529 Immunohistochemical Assessment of DCBLD2 and PDZD3 Expression in Pancreatic Ductal Adenocarcinoma.

P Gopal, TC Cornish, NB Merchant, RH Hruban, C Shi. Vanderbilt University Medical Center, Nashville, TN; Johns Hopkins University, Baltimore, MD.

Background: DCBLD2 is a tyrosine-phosphorylation target of epidermal growth factor (EGF) signaling and is believed to play a role in cancer cell proliferation and metastasis in gastric and lung carcinomas. PDZD3 is a regulatory protein for guanylyl cyclase C and has been associated with colon cancer metastasis. The aim of this study is to correlate DCBLD2 and PDZD3 expression in pancreatic ductal adenocarcinoma (PDA) with prognosis.

Design: Tissue microarrays composed of PDAs from 36 patients and corresponding normal pancreatic tissue were used in this study and were immunohistochemically labeled with antibodies to DCBLD2 and PDZD3. Expression of DCBLD2 and PDZD3 in PDA was correlated with lymphovascular invasion (LVI), perineural invasion (PNI), tumor stage (TS) at diagnosis, and overall survival (OS).

Results: Twenty-one of 36 (58%) PDAs expressed DCBLD2 as compared to 1 of 36 (0.03%) normal pancreatic ducts (p=0.0001). Carcinomas which expressed DCBLD2 had abundant intracytoplasmic mucin. There was no significant association between DCBLD2 expression and LVI, PNI and TS (p>0.05). Mean overall survival was higher for patients with PDAs that expressed DCBLD2 (22 months, SEM=3.342) as compared

to those who did not express DCBLD2 (14 months, SEM=4.087) however this difference was not statistically significant, probably due to small sample size. Eighteen of 34 (53%) PDAs expressed PDZD3 compared to 10 of 33 (30%) normal pancreatic ducts (p=0.08). There was no association between expression of PDZD3 and LVI, PNI, TS, or overall survival (p>0.05).
Conclusions: More than 50% of PDAs express DCBLD2 and PDZD3. The expression of these genes did not correlate with poor prognostic indicators in this sample set. Expression of DCBLD2 was specific for PDA, and this expression trended towards a better overall survival. These findings suggest that further studies on whether DCBLD2 could serve as a potential biomarker and therapeutic target for patients with PDA may be warranted.

1530 Evaluation of Langerhans Cell Infiltration by CD1a Immunostain in Liver Biopsy for the Diagnosis of Primary Biliary Cirrhosis.

RP Graham, TC Smyrk, L Zhang. Mayo Clinic, Rochester, MN.
Background: Primary biliary cirrhosis (PBC) is characterized by chronic nonsuppurative destructive cholangitis, and is thought to be a cell-mediated immune reaction. Antigen-presenting cells, including Langerhans cells and dendritic cells, have been found in portal tracts and in bile duct epithelium, and may play a role in the pathogenesis in PBC. The diagnostic value of detecting Langerhans cells in PBC has not been evaluated in large scale studies.
Design: Needle biopsies of the liver from adult patients diagnosed with PBC (n=39), primary sclerosing cholangitis (PSC, n=17), obstructive cholangitis (OC, n=13), chronic viral hepatitis B and C (CVH, n=19) and autoimmune hepatitis (AIH, n=20) at our institution were retrieved. The histologic diagnoses were confirmed by reviewing the H&E sections as well as clinical and laboratory data. An immunohistochemical stain for CD1a was used to detect Langerhans cells. The distribution of CD1a positive Langerhans cell infiltrate was recorded as lobular, portal with bile duct sparing, and epithelial. The numbers of Langerhans cells in each area were counted.
Results: Langerhans cells were rarely seen in the lobular parenchyma in any case. A portal Langerhans cell infiltrate was identified in most cases of PBC (62%). Although it was seen significantly more often in PBC than in AIH (30%) or CVH (10%), there were no significant differences compared to PSC (41%) or OC (62%). Intraepithelial Langerhans cells were identified in 44% of PBC, 18% of PSC, 15% of OC, 15% of AIH, and none of CVH. The numbers of intraepithelial Langerhans cells were significantly higher in PBC than in other conditions (number of intraepithelial Langerhans cells per bile duct in PBC, median= 4, mean=4.9, range=2-11). Using a cut-off of ≥3 Langerhans cells per bile duct as "positive," gave a sensitivity for PBC of 38% (15/39) and a specificity of 97%, with only rare other biopsies (two AIH) having this density of intraepithelial infiltrate.
Conclusions: A CD1a-positive intraepithelial Langerhans cell infiltrate of ≥3 Langerhans cells in a bile duct is highly specific for PBC, but not very sensitive. This marker may be a useful adjunct to the diagnosis of PBC in cases lacking typical histologic features or serology.

1531 A Novel Immunohiostochemical Staining Pattern for Keratin 8/18 Plus Ubiquitin in Nonalcoholic Fatty Liver Disease Is Associated with Increased Disease Severity and Advanced Fibrosis.

CD Guy, A Suzuki, JL Burchette, EM Brunt, MF Abelmalek, D Cardona, SJ McCall, A Unlap, P Belt, L Wilson, LD Ferrell, AM Diehl. Duke University Medical Center, Durham, NC; Washington University School of Medicne, St. Loius, MO; Johns Hopkins Bloomberg School of Public Health, Baltimore, MD; Univeristy of California at San Francisco.
Background: Nonalcoholic fatty liver disease (NAFLD) is a global health dilemma. The gold standard for diagnosis is liver biopsy. Ballooned hepatocytes (BH) are histologic manifestations of hepatocellular injury and are characteristic features of steatohepatitis (SH), the more severe and potentially more progressive form of NAFLD. Definitive histologic identification of BH on routine stains, however, can be difficult. Immunohistochemical (IHC) staining for loss of the normal hepatocytic keratin 8/18 (K8/18) can serve as an objective marker of BH. We sought to explore the utility of a K8/18 plus ubiquitin (Ub) double IHC stain for the histologic evaluation of adult NAFLD.
Design: Double IHC staining for K8/18 and Ub was analyzed using 40 core liver biopsies from clinically and histologically well-characterized adult patients with NAFLD enrolled in the Nonalcoholic Steatohepatitis Clinical Research Network (NASH CRN) Database study. Our cohort was preselected for a representative range of disease severity. Immunohistochemical staining analysis was performed in a blinded fashion.
Results: Ballooned hepatocytes lack K8/18 staining (KBH), as previously shown by others, but normal size hepatocytes with keratin loss (KH) are approximately five times more numerous than KBH. Linear regression analysis demonstrates that KBH, KH, and Ub deposits show a zonal distribution and are positively associated with each other ($P < 0.0001$). KBH, KH, and Ub deposits are frequently found adjacent to or intermixed with fibrous matrix and linear regression analyses show that these patterns of injury are associated with advanced fibrosis stages ($P = 0.0002$, 0.0032, and < 0.0001, respectively). Furthermore, these patterns of injury correlate with insulin resistance.
Conclusions: This double IHC may be a useful research tool and/or clinical diagnostic confirmatory aid for the identification of hepatocellular injury in nonalcoholic steatohepatitis (NASH).

1532 Histopathologic Predictors of Early Graft Loss in Viral Hepatitis C Patients with Liver Transplant.

S Hafezi-Bakhtiari, G Therapondos, EL Renner, N Selzner, OA Adeyi. University Health Network, Toronto, Canada; University of Toronto, ON, Canada.
Background: Viral hepatitis C (HCV) with or without hepatocellular carcinoma (HCC) is a major indication for liver transplantation, with more than 80% 3-year graft survival, implying a subset of patients experience graft loss within 2 years. Pathologists play a big role in early diagnosis of graft abnormalities. We have reviewed the causes of graft loss with or without patient death occurring within 2 years and looked back at all earlier pathological materials to identify what features were predictive of eventual outcome.
Design: Patients transplanted for HCV or HCV/HCC between 1991 and May 2010 are identified from our hospital's electronic records. Early graft loss is defined as patient death or re-transplantation within 2 years. All explants as well as all available preceding allograft biopsies were reviewed. Immediate graft losses from surgical complications are excluded.
Results: 44 out of 554 transplanted patients for HCV +/- HCC were selected within our criteria. All explants and pre-loss biopsies were reviewed; 25 of the 44 patients had one to multiple HCC in the explants. Respectively 20.5%, 38.6%, and 40.9% of 44 graft losses occurred in less than 3 months, within the first year; and in the second year. The mean biopsy-to-loss period is 207 days (range 2- 644 days). 19 (36.4%) of these patients had cholestasis beyond the first week of transplant +/- brisk hepatitic activity beginning within 6 months and all lost their grafts to progressive fibrosis from recurrent HCV; 11 of the 19 were classified as the fibrosing cholestatic variant. Chronic rejection was preceded in all affected 5 patients by acute rejection of RAI 7 or greater, PTLD, or zone 3-accentauted "hepatitis". Non-caseating granulomas were seen in two explants with both patients dying of disseminated tuberculosis within 5 months. All 6 patients with recurrent HCC had either multiple or single lesion greater than 5 cm in the explant, but nothing in their allograft biopsies predicted tumor recurrence. Hepatic artery thrombosis in 3 patients was confirmed by prior zone 3 necrosis/ ischemic cholangiopathy. One patient had portal vein thrombosis and 8 others died of either unrelated (breast carcinoma; hemolytic anemia) or unknown causes.
Conclusions: Predictive histopathological features of shortened graft survival due to aggressive recurrent HCV, chronic rejection, reactivated tuberculosis, and recurrent neoplasms were often present in earlier biopsies or explant, 2-644 days (mean 207 days) prior to graft loss.

1533 Liver Allografts for Primary Biliary Cirrhosis in 101 Patients: Diagnosis and Followup Outcome of Histopathological Abnormalities.

S Hafezi-Bakhtiari, OA Adeyi. University of Toronto, ON, Canada; University Health Network, Toronto, ON, Canada.
Background: While data exist for post-transplant outcomes in the more common indications for liver transplant, those for primary biliary cirrhosis (PBC) have largely been limited to small case series with varied outcomes. For example recurrent PBC (rPBC) is reported to be as low as 9% and high as 50%. Also other causes of graft abnormalities other than chronic rejection (CR) and rPBC in this patient group have not been documented. This study of a large cohort over a 22-year period aims at addressing these issues.
Design: Patients who received liver transplant from 1987-2009 and with a minimum of 1-year follow-up were identified. Clinical information was retrieved from transplant electronic record and corresponding pathologic material reviewed in cases where these were available.
Results: 101 PBC patients with primary grafts were included. Patients were on Cyclosporin or Tacrolimus-based regimen and followed-up for 133 months (range 12.2 -274 months). All biopsies were performed for indication and available in 71 (70.3%) patients. Of 30 patients with no biopsy, 25 are alive with functioning grafts; 5 died of graft unrelated causes. rPBC was present in 9 (8.9%) patients at a mean of 98.7 months post-transplant, resulting in 1 (0.9%) graft failure 78 after diagnosis. CR was documented in 11 patients (10.3%) after a mean of 96.8 months; 3 (2.9%) resulted in graft failure within 30-60 months. Overall graft failure occurred in 6 patients (5.9%) including 2 from causes other than CR or rPBC. Features favoring CR over rPBC are cholestasis >> fibrosis; absence of ductular reaction; and no periportal copper. rPBC showed ductular reaction in portal tracts with and without florid duct lesions but cholestasis was rare. Late acute cellular rejection that responded to treatment was present in 60.1% of biopsies; de novo HCV (2.8%); and idiopathic hepatitis (2.8%) were some other findings. Only 6 of 33 deaths were due to graft failure; 27 died with functioning graft from sepsis, metastatic carcinoma; myocardial infarction, CVA, and others.
Conclusions: Excellent long-term graft survival for PBC is confirmed. CR and rPBC occurred in 10.3% and 8.9% of patients respectively. Neither was inevitably "fatal" to the graft although CR was 3 times more likely to result in graft loss, and it was possible to histologically differentiate one from the other. Late-occurring acute cellular rejection was a common cause of clinical graft dysfunction, but typically responded to routine treatment.

1534 A and B Glycosiltransferase/Blood Group Antigens in Human Pancreatic Ductal Adenocarcinomas.

A Handra-Luca, S Hong, R Hruban, M Goggins. The Johns Hopkins Medical Institutions, Baltimore, MD; APHP Universite Paris 13/Nord UFR SMBH, Bondy Bobigny, France.
Background: Pancreatic ductal adenocarcinoma (PDAC) is one of the leading causes of digestive cancer-related mortality. Recent studies suggested that patients with blood group non-O have increased risk of development of pancreatic cancers. However, information regarding blood group antigen expression in PDACs is limited.

Design: The aim of this study was to determine the clinicopathological significance of blood group expression patterns in patients with resectable PDAC.
459 patients with PDAC were analyzed for immunohistochemical expression of A and B blood group antigens on tissue microarrays. Correlations were established by Fisher's, chi squared tests, and logistic regression models; relationships to overall survival were analyzed by Kaplan-Meier method, logrank test and multivariate Cox models.
Results: The A blood group antigen was expressed in 43% tumors and B antigen in 13%. Blood group antigen expression in normal pancreatic acini was directly correlated to the corresponding patient's blood group type. Tumor A antigen expression correlated (p=0.01) and predicted a decreased number of lymph node metastases (<3, 3 being the median of metastatic lymph nodes) (p<0.01 HR 0.56, 95% CI 0.37-0.85). Tumor A antigen expression was related to a better survival on univariate (p=0.04) and multivariate analysis (p=0.03, HR 0.77 95% CI 0.62-0.97). Blood group serology was not associated with outcome.
Aberrant tumor expression patterns (defined as compared to the patient's blood group type), present in 24% of the tumors, consisted in loss of expression and de novo expression (19% and 5% of the 356 patients with available blood group type).
Loss of A antigen tumor expression (in A blood group type patients) correlated with vascular invasion (p=0.01).
Conclusions: The results of our study suggest that in patients with PDAC:
- Tumor expression of A blood group antigen correlated to <3 lymph node metastases and to a better outcome,
- Loss of tumor A antigen expression correlated to vascular invasion in patients with A blood group type.

1535 Combined Use of Cytology, IMP3 Immunocytochemistry, and Forceps Biopsy Increases the Diagnostic Yield in the Detection of Pancreatico-Biliary Malignancy.

J Hart, M Parab, D Mandich, R Cartun, S Ligato. Hartford Hospital, CT.
Background: Biliary brushing and EUS/FNA are two common techniques used to obtain material for the cytologic evaluation of biliary stenosis. Due to their low sensitivity in the detection of malignancy, new ancillary techniques such as Spy Glass probe with forceps biopsy during ERCP and immunoperoxidase staining of biliary brushing/aspirated material for insulin-like growth factor messenger RNA binding protein-3 (IMP3) have been used to improve diagnostic sensitivity. In the current study, we compared the individual and combined use of routine cytology, IMP3 staining, and forceps biopsy in the analysis of such specimens.
Design: We retrospectively evaluated 30 patients who underwent ERCP for biliary strictures, in which both cytologic and forceps biopsy material was obtained. Papanicolaou (PAP) staining and immunocytochemical staining for IMP3 was performed on all cytology specimens. Follow up data, including histologic evaluation of primary tissue resection, histologic evaluation of metastatic disease, and radiographic/clinical information, were obtained. Stastical analysis were calculated for the individual and combined methods.
Results: Sixteen of 30 patients (53%) were definitively diagnosed with malignancy by primary or metastatic tissue evaluation and radiographic/clinical information. Routine cytologic diagnoses included 26 cases negative and 4 cases positive for malignancy. Forceps biopsy diagnoses included 23 cases negative and 7 positive for malignancy. IMP3 evaluation yielded 20 negative and 10 positive interpretations. Stastical analysis of individual and combined methods are reported in the table:

Individual and combined methods of the cytologic evaluation of biliary stenosis/bold

	Sensitivity/italic	Specificity/italic	PPV/italic	NPV/italic
Brush Cytology/italic	25%	100%	100%	57.7%
Forceps Biopsy/italic	43.8%	100%	100%	60.9%
Brush Cytology & Forceps Biopsy/italic	56.3%	100%	100%	66.7%
IMP3/italic	56.3%	92.9%	90%	65%
Brush Cytology and IMP3/italic	68.8%	92.9%	91.7%	72.2%
Brush Cytology, Forceps Biopsy, and IMP3/italic	81.3%	92.9%	92.9%	81.3%

Conclusions: The addition of forceps biopsy or IMP3 immunocytochemical analysis to routine cytology markedly improves the diagnostic sensitivity in the detection of malignancy in biliary strictures. Furthermore, in the current study, the combined use of all three modalities maximized diagnostic sensitivity while maintaining a specificity > 90%.

1536 Excision Repair Cross Complementing 1 (ERCC1) and Ribonucleotide Reductase Regulatory Subunit M1 (RRM1) as Predictors of Survival and Response in Pancreatic Ductal Adenocarcinoma Treated with Gemcitabine-Based Chemotherapy.

T Holdbrook, KD Danenberg, S Satti, J Kline, CJ Yeo, JR Brody, P McCue, AK Witkiewicz. Thomas Jefferson University Hospital, Philadelphia, PA.
Background: Gemcitabine-based chemotherapy is a standard treatment for pancreatic ductal adenocarcinoma (PDA). Several biomarkers are currently being evaluated as predictors of survival and response in gemcitabine treated PDA. Two such markers, excision repair cross-complementation group 1 (ERCC1) and ribonucleotide reductase regulatory subunit M1 (RRM1), play a pivotal role in DNA damage repair. The purpose of our study was to correlate ERCC1 and RRM1 expression with survival in gemcitabine treated PDA patients.
Design: We investigated the mRNA and protein expression of ERCC1 and RRM1 by RT-PCR and immunohistochemistry (IHC) in formalin-fixed, paraffin-embedded PDA tissues from patients treated with gemcitabine-based chemotherapy. Relative gene expression quantification was calculated according to the comparative cycle threshold (Ct) method using ß-actin as an endogenous control and commercial RNA controls (Stratagene, La Jolla, CA) as calibrators. IHC was performed using purified RRM1 antibodies (1:150 dilution; Abcam, Cambridge, MA) and ERCC1 antibodies (1:50 dilution; Abcam, Cambridge, MA). RRM1 and ERCC1 immunoreactivity was evaluated semi-quantitatively based on staining intensity and proportion of staining in the area of most intense staining. The stained tumor tissues were scored blindly with respect to clinical patient data.
Results: RRM1 RT-PCR results were available for 26 patients and ERCC1 for 60 patients. IHC stains were performed on all cases. Low RMM1 expression by RT-PCR was associated with a two-fold decrease in risk of mortality compared to high expression; however, due to the small sample size, this difference was not statistically significant. Low ERCC1 expression by RT-PCR was associated with 2.5 times higher risk of mortality than high expression (p=0.031). High expression of RRM1 by IHC was associated with shorter survival (p=0.02). There was no association between ERCC1 expression by IHC and survival. Agreement between mRNA and protein expression was modest for RRM1 (kappa = 0.57) and poor for ERCC1 (kappa=0.14).
Conclusions: PDA patients with low expression of RRM1 derive benefit from gemcitabine chemotherapy. The ERCC1 levels measured by RT-PCR but not by IHC predict survival in these patients.

1537 Sonic Hedgehog (SHH) Expression in Biliary Intraepithelial Neoplasia (BilIN), Peribiliary Glands, and Intrahepatic Cholangiocarcinomas.

M Hsu, M Sasaki, K Harada, S Igarashi, Y Nakanuma. Kanazawa University Graduate School of Medicine, Japan.
Background: SHH is aberrantly activated in pancreatic ductal adenocarcinomas (PDACs) and in the precursor lesion, pancreatic intraepithelial neoplasia (PanIN). The recently characterized pancreatic duct gland (PDG) has also been shown to undergo injury-induced, SHH-mediated mucinous metaplasia and may serve as a possible link between chronic injury and pancreatic duct neoplasia. Similar to the PanIN-PDAC sequence model, cholangiocarcinoma (CC) follows a stepwise carcinogenesis process and arises from the precursor lesion BilIN, graded as BilIN-1, 2, and 3 (mild, moderate, and severe dysplasia). Additionally, analogous to reactive PDGs, florid reactive peribiliary glands (PBGs) are often seen preceding the development of CC, in particular in cases of hepatolithiasis (HL). Due to the similarities between the precursor and background lesions involved in PDAC and CC, the role of the hedgehog pathway was investigated in BilIN, PBGs, and CCs in the setting of HL.
Design: Immunohistochemical expression of SHH was evaluated in lesions with HL: normal bile duct (BD) (20), reactive BD (33), BilIN-1 (24), BilIN-2 (21), BilIN-3 (20), intrahepatic CC (ICC) (30), normal/reactive PBG (13), and atypical PBG, identified as those displaying nuclear atypia beyond reactive changes (15). Also for comparison, PDAC (36), normal BD without HL (28) and ICC without HL (58) were stained for SHH. Expression was evaluated as follows: no staining (0), weak (1), moderate (2), and strong (3), present in ≥25% of the lesion. Immunohistochemical staining for smoothened (Smo), a hedgehog pathway mediator, was also preformed and scored as: negative, present in lesion, or present in the adjacent stromal cells.
Results: In cases with HL, a higher percentage of 2 to 3+ SHH staining, which increased with grade, was identified in ICC (70%), BilIN-3 (85%), BilIN-2 (66.7%), BilIN-1 (37.5%), and reactive BD (27.3%) as compared to normal BD (5%). In cases without HL, 69% of ICCs, as compared to 7.1% of normal BD, and 50% of PDAC had 2 to 3+ SHH staining. Normal PBGs did not stain for SHH, and no correlation was identified among atypical and normal/reactive PBGs. Predominately stromal Smo staining was present in 37.5% of ICCs without HL and 51.2% of PDAC, and no significant Smo staining was found in cases with HL.
Conclusions: SHH is frequently aberrantly expressed in ICC and correlates with increasing grade of BilIN, however, may not be involved in reactive PBG proliferation. Similar to PDAC, the hedgehog pathway appears to play a key role in the development of ICC.

1538 Aberrant Expression of Pancreatic Stem Cell Markers in the Biliary Tree Relates to Intrahepatic Cholangiocarcinogenesis in Hepatolithiasis.

S Igarashi, M Hsu, M Sasaki, K Harada, Y Nakanuma. Kanazawa University Graduate School of Medicine, Japan.
Background: During development, the biliary system and ventral pancreas arise from a contiguous region of the endoderm, and transcription factors, such as pancreatic duodenal homeobox factor 1 (PDX1) and hairy and enhancer of split 1 (Hes1), a downstream target of the Notch signaling pathway, help guide pancreaticobiliary differentiation. Recently, biliary intraepithelial neoplasia (BilIN) has been proposed as a preneoplastic lesion leading to intrahepatic cholangiocarcinoma (ICC) through a dysplasia-carcinoma sequence, and morphologically resembles pancreatic intraepithelial neoplasia (PanIN), a preneoplastic lesion of pancreatic carcinoma. During PanIN development, reactivation of embryonic pancreatic transcription factors and dysregulation of notch signaling has been suggested to play a role in pancreatic carcinogenesis. We hypothesize that the same molecules that are expressed in PanIN and pancreatic cancer, including PDX1, Hes1, Notch, and other stem cell like markers (CD44, cMET and CXCR4), are also involved in the development of BilIN and the carcinogenesis of ICC.
Design: From 90 cases with hepatolithiasis and 40 cases of ICC without hepatolithiasis, normal bile ducts (31), reactive bile ducts (63), BilIN-1 (68), BilIN-2 (47), BilIN-3 (43), and ICC (80) were immunohistochemically examined for PDX1, CXCR4, CD44, cMet, Hes1 and Notch2 expression. RNA samples were extracted from BilIN lesions by laser capture microdissection, and mRNA levels were quantitatively evaluated by real time PCR.
Results: 45% of ICC cases with and without hepatolithiasis were positive for PDX1. Furthermore, PDX1 was more frequently expressed in BilIN-2 (74.0%) and BilIN-3 (79.1%) than in normal bile ducts (22.2%), reactive bile ducts (41.3%), and BilIN-1 (47.1%). Real time PCR revealed that PDX1 expression was significantly greater in

BilIN-2/3 lesions compared to normal/reactive/BilIN-1 lesions. The expression of CXCR4 and cMET tended to increase with higher grades of BilIN, while CD44 tended to decrease. Hes1 and Notch2 was predominantly expressed in normal ducts and BilIN lesions, however there was less and weaker expression in ICC.
Conclusions: Expression of the stem cell like markers and pancreatic specific marker (PDX1) correlated with grades of BilIN lesions, suggesting that ICCs with hepatolithasis express several stem cell like properties in the early steps of carcinogenesis, and that dysregulation of embryonic transcription factors is involved in intrahepatic cholangiocarcinogenesis in hepatolithiasis.

1539 Heterogeneity of Dissemination Patterns in Hepatic Lymphomas in Biopsy Specimens.

S Jakate, D Heagley, J Loew. Rush University Medical Center, Chicago, IL.
Background: Primary hepatic lymphoma is rare but liver is a frequent site of extranodal and extramedullary dissemination of lymphoma. However, since lymphomas constitute a wide morphological, immunophenotypic and clinical spectrum, liver involvement is appropriately varied. We examined 30 cases of hepatic lymphomas in liver biopsy specimens to evaluate the heterogeneity of presentation and dissemination patterns.
Design: Pathology and clinical databases from our medical center from 2000-2010 were searched for liver biopsy specimens with diagnoses of lymphoma. 30 patients were identified (ages 21-88, 18 M & 12 F). Their clinical profiles, available imaging studies, indications for liver biopsy, types of lymphomas and patterns of hepatic involvement were reviewed.
Results: The following lymphomas (with necessary immunophenotypic workup) were detected in the liver biopsies: Diffuse large B-cell (DLBCL) 14/30, Hodgkin's (HL) 6/30, T-cell (TCL) 5/30, post transplant lymphoproliferative disorder (PTLD) 2/30, and small lymphocytic (SLL), marginal zone (MZL) and Burkitt (BL) – 1 case each. 27/30 (90%) cases were disseminations from medullary and/or nodal, splenic or other visceral lymphomas (secondary), but in 3 of these, liver was the first identified organ of lymphoma involvement. In all of these secondary cases, there was variable hepatomegaly but radiographically visible liver masses were infrequent (only 3/27 cases) and the biopsies were random. Histologically, the liver involvement was patchy with variable neoplastic cell infiltrate. HL cases were the most histologically challenging and had the fewest neoplastic cell infiltrates limited to a few portal areas. DLBCL, TCL and BL infiltrates were patchy but present in abundance in the sinusoids and portal areas. SLL, PTLD and MZL infiltrates were mainly portal. In 3/30 cases (10%), after extensive imaging studies and bone marrow biopsies, no other sites of lymphoma were identified (primary hepatic lymphoma). All of these 3 cases were DLBCL and presented with radiographically visible masses and the image-guided biopsies showed dense tumor infiltrates without any native liver tissue.
Conclusions: Lymphomas disseminated to the liver are of a variety of types and rarely produce masses on imaging but primary hepatic lymphomas tend to be DLBCL with radiographic masses and dense tumor infiltrates. HL in liver has the fewest tumor cells in the portal areas and poses the highest diagnostic challenge. While SLL, PTLD and MZL are mainly portal infiltrates, DLBCL, TCL and BL show abundant infiltrates in the sinusoids as well as the portal areas.

1540 Invasive Carcinomas Arising from Pancreatic Mucinous Cystic Neoplasms (MCNS) with Ovarian Stroma: A Clinicopathologic Analysis of 25 Cases with Invasive Carcinoma Identified in 131 MCNS.

K-T Jang, N Dursun, O Basturk, E Stelow, S Bandyopadhyay, N Adsay. Samsung Medical Center, Seoul, Korea; Emory, GA; MSKCC, NY; U of VA; WSU, MI.
Background: The data on the incidence and clinicopathologic characteristics of invasive carcinoma (IC) arising in MCNs is rather limited because they are either concealed in studies analyzing all MCNs, or in those that did not employ the current sampling protocols or criteria (requirement of ovarian type stroma-OTS), or some authors had lumped them together with CIS under "malignant MCNs". Not surprisingly, reported incidence of invasive MCN ranges from 2.9-28.6%.
Design: All 131 MCNs in the authors' files, defined by the presence of OTS were analyzed. Average number of blocks of tumor examined was 18.
Results: 25/131 cases (19%) had IC; the remainders were 78 with low-grade dysplasia (LGD), 20 intermediate, and 8 high-grade dysplasia (HGD/CIS). The cases with IC had the following characteristics (as opposed to the non-invasive MCNs): All female, mean age=53 yrs (vs 49; p=0.228), mean tumor size=9.3 cm (range, 3.5-15 cm; vs 5.5cm; p=0.001), elevated serum CA19-9 detected in 7/10 (vs 8/47; p=0.001). Invasion was suspected preoperatively in 6 cases. MCN component of all 25 IC cases had in-situ papillary areas (9/25 in the form of >0.5 cm florid papillary nodules) and 13/25 had extensive HGD/CIS. In 4 cases, the MCN component was partially obliterated by the IC (IC was larger than MCN component). Mean size of IC was 1 cm; staged (per the recent proposal according to size of invasion) as T1a (<0.5 cm) in 11 cases (77%), T1b (0.5-1 cm) in 2 (12%) and T1c (1-2 cm) in 1 and T2 in 5. Invasion was confined to the mural nodule in 9 cases; showed pericapsular extension in 14, and adjacent organ involvement in 2. 19 ICs were ordinary ductal carcinoma, 1 was papillary (in-situ like), and 4 was undifferentiated (1 osteoclastic-giant cell type; 1 sarcomatous; 2 epithelioid). None was colloid type. Lymph node metastasis was seen in 2, liver metastasis in 3, and peritoneal spread in 3. The actuarial 5-yr survival of IC cases was 26%.
Conclusions: Invasive carcinomas occur in 19% of resected MCNs (with ovarian stroma). These arise in larger MCNs, often in the background of papillary nodules and extensive HGD/CIS. Most (75%) are of tubular (ductal) type, others are undifferentiated, but none are colloid (mucinous). Most are small (<0.5 cm), qualify as T1a; however, even the small ones can lead to fatalities (one death and one recurrence). Invasive carcinomas arising in MCNs are agressive tumors, with 5-yr survival of 26%.

1541 Immunohistochemical Analysis of the Progression of Flat Versus Tumoral Intraepithelial Neoplasia (Intracholecysitc Papillary-Tubular Neoplasm) in Gallbladder Carcinogenesis.

K-T Jang, N Dursun, O Basturk, JC Roa, O Tapia, P Terry, N Adsay. Samsung MC, Seoul, Korea; Emory, GA; MSKCC, NY; UFRO, Temuco, Chile.
Background: It is becoming clear that the dichotomy of "flat" versus "tumoral" intraepithelial neoplasia in early carcinogenesis, which has been well established in pancreatobiliary tract (pancreas;PanIN vs IPMN, and bile duct; BilIN vs IPNB) may also exist in the gallbladder in forms of conventional flat dysplasia/CIS versus intracholecystic papillary-tubular neoplasms (ICPN).
Design: We investigated IHC expression of MUC1 (biliary), MUC5AC (foveolar), MUC6 (pyloric), MUC2/CDX2 (intestinal) and p53 in the progression of these two pathways in 142 resected gallbladders (55 flat IN and 87 ICPNs, as well as 46 and 36 invasive carcinomas associated with these, respectively).
Results: The incidence of invasive carcinoma was significantly higher in flat IN than ICPN (p=0.001). MUC1 expression was also significantly higher in invasive carcinoma arising from flat IN (p=0.001) than in that of ICPN. Conversely, MUC6 expression was higher in ICPN (p=0.001) than flat IN, and there was no invasive carcinoma in flat IN with MUC6 expression. Intestinal differentiation markers of CDX2 or MUC2 were uncommon in both pathways, but if present, they occurred predominantly in the ICPN. There were no significant differences in MUC5AC and p53 expression between both groups. Separately, non-conventional types of invasive carcinoma occurred in 11.4% of ICPN (signet ring cell, 3; mucinous, 1; neuroendocrine carcinoma, 1) but those were uncommon in flat IN.

	No.	MUC1	MUC2/ CDX2	MUC5AC	MUC6	p53
ICPN	87	57 (66%)	11 (13%)	47 (54%)	35 (40%)*	25 (29%)
Flat IN	55	43 (78%)	3 (7%)	23 (42%)	2 (4%)	16 (29%)
Inv C-ICPN	35 (40%)	18 (51%)	4 (11%)	14 (40%)	7 (20%)	14 (40%)
Inv C-Flat IN	46 (84%)*	45 (98%)*	2 (4%)	25 (54%)	0	18 (38%)

(*: p=0.001)
Conclusions: There are two different precursor lesions in early gallbladder carcinogenesis, flat IN and ICPN. Although flat IN is the more common pathway, ICPN also shows high incidence of invasive carcinoma. MUC1, a marker of aggressive phenotype in pancreatobiliary tract, is commonly expressed in the flat IN but not in the ICPN pathway, and in contrast, MUC6, the gastric pyloric type mucin, is the marker of more indolent pathway. Compared to the IPMNs of pancreas and IPNBs of the bile ducts, intestinal differentiation is rarely identified in ICPN. Further studies to elucidate the mechanisms of these two distinct pathways may shed new light to the GB carcinogenesis.

1542 Classification of Tumoral Intraepithelial Neoplasms of the Gallbladder under a Unified Category of Intracholecystic Papillary Tubular Neoplasms (ICPN) with 4 Subsets Discernible by Correlation of Morphology and Immunophenotype.

K-T Jang, N Dursun, O Basturk, JC Roa, O Tapia, P Terry, N Adsay. SMC, Seoul, Korea; Emory, GA; MSKCC, NY; UFRO, Temuco, Chile.
Background: In the WHO-2010, tumoral intraepithelial neoplasms (TIN) of gallbladder are classified under 7 different names, some based on cell lineage (pyloric, foveolar, intestinal, biliary), some by growth pattern (tubulopapillary), and others by degree of dysplasia (non-invasive papillary ca).
Design: 87 cases >1 cm were evaluated by correlation of morphology with IHC for cell lineage markers MUC1 (biliary), MUC2/CDX2 (intestinal), MUC6 (pyloric) and MUC5AC (foveolar), CK7 and CK20.
Results: I. Hybrid and mixed lineages were very common. 49 (56%) had cellular morphology difficult to classify into an established lineage, and this group also showed a complex IHC profile: MUC1 55%; MUC5AC 53%; MUC6 26%, MUC2 14%, and CK20 20%. 74% had recognizable foci of different lineages within the given tumor, 52% with corresponding expected IHC profile. These mixed types were mostly biliary-foveolar type (n=44), 41 of which expressed non-foveolar markers. 22 with intestinal-like features were negative for MUC2/CDX2. **II. Correlation of morphology with IHC allowed the delineation of 4 subtypes.** ***1. Biliary (n=68):*** Papillary/tubulopapillary; most with HG dysplasia; consistent MUC1/CK7; common foci with pyloric or foveolar features (MUC5AC or MUC6) some with pleomorphic clear cells; some with intestinal-like morphology but MUC2/CDX2 (-). ***2. Pyloric complex-tubular (n=13):*** Nodular, pedunculated lesions composed of complex tightly-packed small tubular units with cuboidal nuclei; uniform/diffuse MUC6; 6 with focal MUC1 highlighting the higher grade or biliary type areas; 2 with Brunner-gland and 2 with foveolar features. ***3. Foveolar (n=3):*** Tubulopapillary; abundant apical, pale, MUC5AC (+) cytoplasm. ***4. Intestinal (n=3):*** Papillary/tubulopapillary; all the characteristics of a colonic-type adenoma; MUC2/CDX2 (+).
Conclusions: There are significant phenotypic overlaps, variable growth patterns and intratumoral heterogeneity in TINs of GB, warranting their unification under one category of ICPN. Correlation of IHC with morphology allows the recognition of 4 subtypes of ICPNs, the vast majority of the cases falling into the biliary category, followed by pyloric complex-tubular, and rarely, foveolar or intestinal. Papillary vs tubular patterns and degree of dysplasia are trans-categorical and thus not applicable in the classification. We believe that this definition of ICPN and its subtypes is a more accurate reflection of the TINs of GB.

1543 Vacuolated Cell Pattern as a Diagnostic Feature of Pancreatobiliary Origin for Carcinomas Identified in Liver Biopsies.

T Jazaerly, S Bandyopadhyay, O Basturk, N Dursun, B Albashiti, N Culhaci, V Adsay. WSU/DMC/KCI, Detroit, MI; MSKCC, New York; Emory Univ, Atlanta, GA; WSU/DMC, Detroit, MI; Adnan Menderes Univ, Aydin, Turkey.

Background: Liver is the most common site for metastatic carcinoma. The primary origin and corresponding treatment are commonly based solely on histopathologic evaluation of small, challenging biopsies. Most pancreatobiliary adenocarcinomas (PBA) present with liver metastasis, and PBA is one of the most common and misdiagnosed sources of carcinomas of unknown primary. We recently described a distinctive vacuolated cell pattern (VCP) of PBA (Virchows Arch, in press, 2011).

Design: 209 liver biopsies with metastatic carcinoma were retrieved from our database and reviewed to identify VCP, which is characterized by multicell-size vacuoles with signet-ring appearance occurring in clusters of cells, imparting them a cribriform pattern. The vacuoles often merge to form multilocular spaces separated by a thin rim of cell membrane. The nuclei are hyperchromatic, with significant atypia and are often pushed to the periphery resembling adipocytes (lipoid cell pattern). Many of the vacuoles contain granular secretory material, some with targetoid appearance, admixed with cellular debris, neutrophils and mucin. True lumen formation lined by epithelial cells was not considered as VCP.

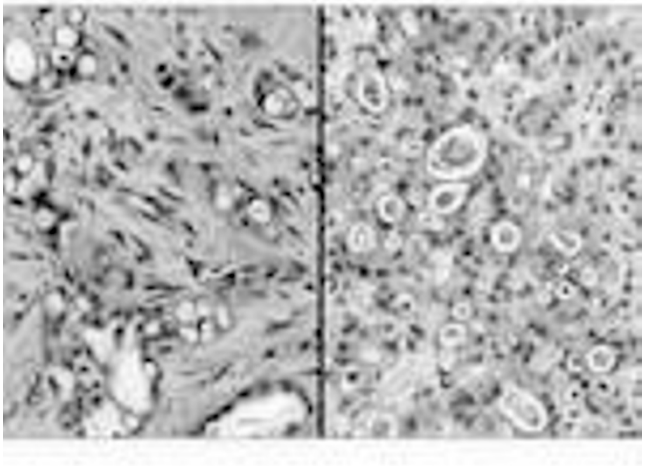

This was confirmed by 2 pathologists after a blinded slide review. The primary site was established by clinical findings.

Results: VCP was identified in 46 of 82 cases of PBA (56%). Occasional vacuoles resembling those of VCP were identified 15 of 127 carcinomas of non-PBA origin (2/15 ovarian, 8/43 colonic, 3/11 upper G.I., 2/15 ovary, 0/5 lung, 0/38 others); however, only 2 of these (colon and upper G.I.primaries) had characteristic features of VCP. Sensitivity and specificity of VCP for PBA was 56% and 88% respectively.

Conclusions: Although not very common, the vacuolated cell pattern is a fairly helpful adjunct in the differential diagnosis of metastatic carcinomas involving the liver. If this pattern is encountered, the possibility of PBA ought to be considered as the most likely primary.

1544 Viral Hepatitis Is Associated with a Distinct Subtype of Intrahepatic Cholangiocarcinoma Characterized by Cholangiolar Differentiation and N-Cadherin Expression.

Y-M Jeng. National Taiwan University Hospital, Taipei, Taiwan.

Background: Viral hepatitis-associated intrahepatic cholangiocarcinoma is thought to have common disease processes with hepatocellular carcinoma, but until now there has been no morphological or molecular evidence to support this hypothesis. The study was performed to identify distinct clinicopathological and molecular characteristics of viral hepatitis-associated intrahepatic cholangiocarcinoma.

Design: From 2000 to 2010, 170 patients with intrahepatic cholangiocarcinoma who received detailed pathological assessment and regular follow-up at the National Taiwan University Hospital were selected for this study. Immunophenotypic features were examined by immunohistochemical stain. Detection of *K-ras and BRAF* gene mutation was performed by polymerase chain reaction and direct sequencing.

Results: Of 170 ICC diagnosed between 2000 and 2010 in Taiwan, 69 (40.6%) were positive for hepatitis B and/or C virus. These patients were younger, were more frequently male, and had elevated serum alpha-fetoprotein levels as compared with seronegative ICC patients. Grossly these tumors were mostly of the mass-forming type, and histologically cholangiolar differentiation was more frequently seen. We identified N-cadherin as an immunohistochemical marker strongly associated with hepatitis virus infection. The prevalence of viral hepatitis in patients with N-cadherin-positive ICC was 70.9%; that in N-cadherin-negative patients was only 33%. N-cadherin-positive patients were younger, had elevated AFP, and had no hepatolithiasis. All N-cadherin-positive ICCs were of the mass-forming type. N-cadherin positivity was strongly associated with cholangiolar morphology and lack of carcinoembryonic antigen and Muc-2 expression, while *K-RAS* mutations were less frequent.

Conclusions: A subgroup of ICC characterized by cholangiolar differentiation and N-cadherin expression is strongly associated with viral hepatitis.

1545 Phosphorylated FOXO1 Is a Novel Prognostic Factor for Patients with Pancreatic Cancer Receiving Multimodal Therapies.

Y-F Jin, M Tomoeda, S Nagata, K Yoshizato, M Kitamura, M Yuki, C Kubo, H Yoshizawa, H Takahashi, H Ohigashi, O Ishikawa, Y Tomita. Osaka Medical Center for Cancer and Cardiovascular Diseases, Japan; Kobe International University, Hyogo, Japan.

Background: Forkhead box O1 (FOXO1), a transcription factor, is a key regulator of cell cycle progression, and apoptosis, thus considered to be involved in cell transformation and tumorigenesis. Correlation of FOXO1 in tumor progression or prognosis has been reported in several human cancers, however, not in pancreatic ductal adenocarcinomas (PDAC).

Design: phosphorylated FOXO1 (p-FOXO1) expression in primary PDAC from 68 patients receiving neoadjuvant chemoradiotherapy, 43 male and 25 female, aged 41 to 81 (median 66) years, was evaluated by immunohistochemistry. Staining intensity of p-FOXO1 in the tumors was judged separately for the nucleus and cytoplasm and categorized as follows: level I, weaker than that of endothelial cells in the same specimen (including absent or faint staining); and level II, equal to or stronger than that of endothelial cells.

Results: Forty-three (63.2%) and 25 (36.8%) cases, and 54 (79.4%) and 14 (20.6%) cases showed p-FOXO level I and II expression in the nucleus and cytoplasm, respectively. Patinets with nuclear p-FOXO1 level I showed a significantly better overall survival rate than those with level II (P = 0.0003). No significant difference was observed in the cytoplasmic p-FOXO1 classification, however correlation between cytoplasmic p-FOXO1 expression and histological assessment of chemoradiation effect grade (I /IIa versus IIb/III) was observed (P = 0.01).

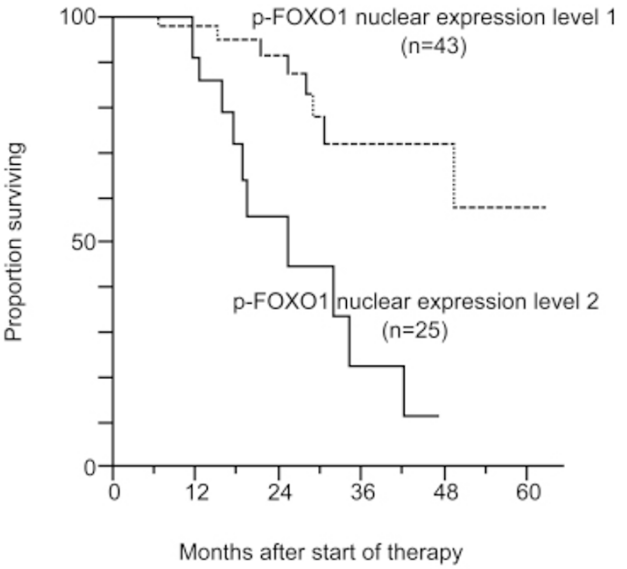

Correlation between cytoplasmic p-FOXO1 expression and histological assessement of chemoradiation effect grade in PDAC

		Cytoplasmic p-FOXO1 expression				p value
		Level I (n=54)		Level II (n=14)		
	I	7	77.8%	2	22.2%	0.01*
Histological Assessment of	IIa	18	64.3%	10	35.7%	
chemoradiation grade	IIb	22	91.7%	2	8.3%	
	III	7	100%	0	0%	

*Level I/IIa versus IIb/III

Multivariate analysis revealed nuclear p-FOXO1 expression as an independent prognosticator together with lymphatic permeation, vascular permeation, lymph node metastasis.

Conclusions: p-FOXO1 expression is a significant prognostic indicator for PDAC receiving multimodal therapy.

1546 Diagnostic Utility of Glutamine Synthetase and Serum Amyloid Associated Protein Immunohistochemistry in the Distinction of Focal Nodular Hyperplasia and Telangiectatic Hepatic Adenoma.

NM Joseph, D Jain, T-T Wu, M Yeh, M Torbenson, S Kakar. UCSF, San Francisco, CA; Yale Univ, New Haven, CT; Mayo, Rochester, MN; Univ of Washington, Seattle; Johns Hopkins, Baltimore, MD.

Background: Telangiectatic/inflammatory hepatic adenoma(THA)can show overlapping features with focal nodular hyperplasia(FNH) including fibrous stroma,ductular reaction and inflammation.Expression of serum amyloid associated protein(SAA)in THA and map-like pattern of glutamine synthetase(GS)in FNH has been reported.We examined SAA and GS in THA and FNH to determine the specificity of these markers and to identify variant staining patterns that can lead to diagnostic errors.

Design: Morphology and immunohistochemistry for GS and SAA was reviewed in 30 FNH(18 biopsy,12 resection)and 42 THA(5 biopsy,37 resection).GS staining was classified as diffuse map-like,perivascular,perivascular with focal map-like, and diffuse. SAA was recorded as negative(0-10%),focal(10-50%)and diffuse(>50%).

Results: Diffuse map-like GS was seen in 28(93%)FNH;2 cases showed focal map-like pattern.30(71%)THA showed perivascular GS which was expanded compared to normal liver.In 8(19%)THA,perivascular staining was accompanied by interconnecting bands of positive hepatocytes focally resembling map-like pattern.Unlike FNH where areas around fibrous septa are GS-negative,GS in these 8 cases was positive around arterioles and map-like pattern was created by negativity in midzonal hepatocytes between perivenular and periarteriolar area.Diffuse GS staining was seen in 4(10%) THA and was easily distinguished from map-like GS pattern.SAA expression was seen in 38(91%)THA and 4(13%)FNH.

	Fibrous stroma	Ductular reaction	Inflammation	Telangiectasia	Steatosis
FNH(n=30)	87	87	47	27	23
T-HA(n=42)	21	50	60	83	55
p-value	< 0.001	< 0.001	0.22	< 0.001	0.005

Numbers reflect percentages

	GS Map-like	GS resembling map-like	Diffuse GS	SAA positive
FNH(n=30)	93	7	0	13
THA(n=42)	0	19	10	91
p-value	< 0.001	0.10	0.09	< 0.001

Figures reflect percentages

Conclusions: Map-like GS pattern is highly specific for FNH and is seen in nearly all cases.Majority of THA show perivascular GS similar to normal liver.Two other GS patterns in THA(perivascular with focal map-like and diffuse)can be mistaken for map-like FNH pattern.Most THA are SAA positive,but this is also seen in 17% of FNH.GS and SAA can distinguish FNH and THA with close attention to variant staining patterns.

1547 Potential Role of p27, PTEN, Cks1 and Skp2 Expression in Hepatocellular Carcinoma.

D Karavias, J Maroulis, C Gogos, V Zolota, D Karavias, C Scopa, A Tsamandas. Patras University Medical School, Greece.

Background: $p27^{Kip1}$ is a cell-cycle inhibitory protein and its downregulation is mediated by its specific ubiqitin subunits Cks1 and Skp2. PTEN is a tumor suppressor gene which upregulates p27. This study investigates p27, PTEN, Cks1 and Skp2 expression in hepatocellular carcinoma (HCC).

Design: Formalin-fixed, paraffin-embedded 4 m sections, obtained from 117 HCC hepatectomy specimens with matched non-neoplastic liver, were subjected to immunohistochemistry using antibodies for p27, PTEN, Cks1 and Skp2. Nuclear staining was considered as positive. Results were correlated with pathologic data and patients survival. Mean follow up time was 42.17 months (range 1-102 months).

Results: Expression of p27, PTEN, Cks1 and Skp2 was recorded in: 88/117(76%), 109/117(94%), 28/117(24%) and 26/117(34%) cases, respectively. PTEN was also expressed in cirrhotic and non-cirrhotic non-neoplastic livers; however its expression was significantly lower compared to that of tumors (HCC: 72.84 38.32, cirrhotic livers: 33.55 14.12, non-cirrhotic livers: 12.13 8.64-p<0.001). Mean values for Cks1, Skp2 and p27 expression in HCC were: 9.2 14.3, 4.33 7.6, 16 8.2 respectively. Cks1, Skp2 and p27 expression in cirrhotic and non-cirrhotic livers was observed in rare instances. Statistical analysis revealed a loss of PTEN and p27 expression in HCC grade 3: [PTEN: grade 1: 96.4 2.3, grade 2: 70.8 21.8, grade 3: 9.1 3.4-p<0.0001. p27: grade 1+2: 20.4 12.4, grade 3: 6.1 4.2-p=0.031]. Loss of PTEN and p27 expression was also related to presence of vascular invasion (VI): [PTEN: VI(-): 92.1 5.6, VI(+): 12.4 1.2-p=0.0012. p27: VI(-): 23.1 4.5, VI(+): 5.2 2.7-p=0.013]. No association was recorded between Cks1 and Skp2 expression and tumor grade or stage. PTEN and p27 expression were reversibly correlated with disease free survival (r=- 0.63, p=0.0041 and r=- 0.45, p=0.014). Cox regression analysis revealed that vascular invasion (CI:1.233-5.402, p=0.017), tumor stage (CI:0.057-0.630, p=0.015) and PTEN expression (CI: 1.059-42.065, p=0.031), were independent prognostic factors.

Conclusions: This study demonstrates that loss of PTEN and p27 expression is associated with adverse pathological parameters and increased risk for tumor recurrence. These results support the importance of PTEN and p27 loss for the progression of HCC in humans. PTEN increased expression in cirrhotic non-neoplastic livers may reflect an effort for control of hepatocyte regeneration associating liver cirrhosis.

1548 Prognostic Significance of Prognostic Significance of Cell Cycle Proteins p53, p21, p27, p14, and p16 in Adenocarcinomas of the Ampulla of Vater and Pancreas (AAVP).

N Katsiakis, J Maroulis, V Zolota, D Karavias, C Scopa, A Tsamandas. University of Patras, Achaia, Greece.

Background: This study investigates the immunohistochemical expression of 5 essential cell cycle proteins p53, p21, p27, p14 and p16 in AAVP and their correlation with classic pathologic tumor features, proliferating index (Ki67 positivity) and patients' survival.

Design: The study included 64 patients with AAVP: group A 14 patients with adenocarcinoma of the ampulla, group B 23 patients with adenocarcinoma of the pancreas head and group C 7 patients with adenocarcinoma of the pancreas body. Patients of groups A/B underwent the Whipple procedure and patients of group C distal pancreatectomy. Eight tumors were TNM-stage I, 19 II, 27 III, and 10 IV; 35 tumors were grade I and II and 29 grade III. Paraffin sections were subjected to immunohistochemistry with antibodies for p53, p21, p27, p14, p16, and Ki67. Nuclear staining was considered as positive. Mean follow-up time was 8.3 months (range 3.5-18 months).

Results: p53, p14, p16, p21 and p27 were detected in: 56%(35/64), 70%(44/64), 65%(41/64), 48%(30/64), and 82%(52/64) of the cases, respectively. Mean index for Ki67 was 29.4±48.2. High grade tumors exhibited higher indices for Ki67 (p=0.004), p53 (p=0.005) and p21 (p=0.024) compared to low grade tumors; p14 and p16 were more frequently present in low grade tumors (p<0.001 in both cases). Ki67, p53, p21 and p27 were more frequently expressed in advanced stage tumors (p=0.002, and p<0.001 in the later three cases). p14 and p16 were more frequently expressed in early stages (p<0.001 and p=0.012). Lower disease-free survival was correlated with high grade (p=0.0007), advanced stage (p=0.0008), and higher Ki67 index (p=0.0075). p53 expression was associated with lower disease-free survival only in high grade p21(+) tumors (p=0.021). Cox analysis revealed that tumor grade, stage, Ki67 and p53 index were independent prognostic factors (CI: 0.032-0.502, p=0.03, CI:1.167-5.408, p=0.019, CI: 1.006-1.057, p=0.016, CI:1.000-1.0044, p=0.028).

Conclusions: The study confirms that in cases of AAVP, tumor grade and stage and Ki67 and p53 indices are independent predictors of the outcome of the patients. p53 is associated with poor prognosis only in tumors overexpressing p21. Thus, high levels of p21 in tumor cells associated with aberrant p53 protein expression may result in tumor recurrence.

1549 The Potential Role of p27, Skp2, and PTEN Expression in Adenocarcinomas of the Ampulla of Vater and Pancreas (AAVP).

N Katsiakis, J Maroulis, V Zolota, D Karavias, C Scopa, A Tsamandas. Patras University Medical School, Greece.

Background: $p27^{Kip1}$ is a cell-cycle inhibitory protein and its downregulation is mediated by its specific ubiqitin subunit Skp2. PTEN is a tumor suppressor gene which upregulates p27. This study investigates p27, Skp2 and PTEN expression in adenocarcinomas of the ampulla of Vater and pancreas (AAVP).

Design: The study included 64 patients with AAVP: group A 14 patients with adenocarcinoma of the ampulla, group B 23 patients with adenocarcinoma of the head of the pancreas and group C 7 patients with adenocarcinoma of the pancreas body. Patients of groups A and B underwent the Whipple procedure and patients of group C distal pancreatectomy. Eight tumors were TNM-stage I, 19 II, 27 III, and 10 IV, whereas 35 tumors were low-grade (high and moderately differentiated) and 29 high grade (poorly differentiated). Paraffin sections were subjected to immunohistochemistry using antibodies for p27, Skp2 and PTEN. Nuclear staining was considered as positive. Results were correlated with pathologic data and patients survival. Mean follow-up time was 8.3 months (range 3.5-18 months).

Results: Expression of p27, Skp2 and PTEN was recorded in 61.4% (39/64), 44.8% (28/64) and 77.9% (49/64), respectively. PTEN and p27 expression was higher and Skp2 expression was lower in tumors of early stage and low grade compared to those of advanced stage and high grade. Skp2 expression levels were inversely correlated to p27 and PTEN in AAVP (p=0.0042 and p=0.0059 respectively). Statistical analysis revealed a positive correlation between PTEN expression and survival (p=0.009); Skp2 expression was negatively associated with survival (p=0.013). Cox regression analysis revealed that tumor grade and stage, and PTEN expression were independent prognostic factors (CI: 0.032-0.502, p=0.03, CI:1.167-5.408, p=0.019, CI: 1.065-41.082, p=0.032, respectively).

PTEN, p27 and Skp2 expression

	PTEN	**p27**	**Skp2**
Low grade AAVP	87.3 ±11.9[a]	79.2 ±13.2[c]	22.41 ±6.3[e]
High grade AAVP	7.4± 2.5[a]	5.3 ±3.1[c]	38.85 ±5.63[e]
TNM stages I+II	86.1± 8.34[b]	73.1± 7.32[d]	22.78± 6.92[f]
TNM stages III+IV	12.4 ±1.2[b]	5.2 ±2.7[d]	53.01 ±7.34[f]

[a], [d], [f]:p<0.001, [b]: p=0.0029, [c]:p=0.0012, [e]: p=0.031

Conclusions: The study demonstrates that in AAVP loss of PTEN and p27 expression and enhancement of Skp2 expression are associated with adverse pathological parameters and increased risk for tumor recurrence. Loss of p27 in AAVP may be mediated by Skp2 overexpression. PTEN is possibly involved in the regulation of p27 levels via negative regulation of Skp2.

1550 Dysplastic Biliary Lesions in Primary Sclerosing Cholangitis Harbor Cytogenetic Abnormalities Similar to Cholangiocarcinoma.

SE Kerr, EG Barr Fritcher, MB Campion, BR Kipp, JS Voss, SC Abraham, KC Halling, JT Lewis. Mayo Clinic, Rochester, MN; The University of Texas MD Anderson Cancer Center, Houston.

Background: Grading criteria for biliary dysplasia (biliary intraepithelial neoplasia, BilIN) have been recently described. This literature suggests a dysplasia-carcinoma sequence in which dysplasia is associated with concurrent or future cholangiocarcinoma (CCA), especially in primary sclerosing cholangitis (PSC). If so, cytogenetic abnormalities similar to those seen in CCA may be present in BilIN.

Design: Nine PSC liver explants in which a previous multi-section gross protocol had identified BilIN grade 3 were selected. One or two formalin fixed, paraffin embedded blocks from each patient represented the following lesions of interest: normal/reactive (N/R) biliary epithelium, intestinal metaplasia without dysplasia (IM), BilIN 1-2 (low grade dysplasia), BilIN 3 (high grade dysplasia), and CCA. Areas of interest were chosen by consensus of two pathologists and circled on H&E stained slides as a template for UroVysion® fluorescence *in situ* hybridization (FISH probes to 9p21 and centromeres 3, 7, and 17). A cytotechnologist scored 50 consecutive well-visualized epithelial cells per lesion.

Results: Mean (range) % of cells with abnormality on a per lesion basis.

		FISH				
HISTOLOGY	Lesions Counted	Hemiz. 9p21 Loss	Homoz. 9p21 Loss	Homoz. 9p21 Loss Only*	Single Locus Gain	Polysomy
N/R	7	14 (4-28)	3 (0-6)	3 (0-6)	5 (0-16)	0 (0-2)
IM	4	20 (6-26)	3 (2-4)	3 (2-24)	11 (0-36)	0 (0-0)
BilIN 1-2	11	32 (0-14)	15 (0-100)	5 (0-14)	5 (0-12)	15 (0-86)
BilIN 3	10	33 (0-56)	35 (0-100)	14 (0-62)	21 (2-38)	34 (0-70)
CCA	1	0 (0)	100 (100)	16 (16)	22 (22)	62 (62)

*Homozygous 9p21 loss as the only abnormality in the counted cell (i.e., not seen in combination with other gains or losses)

Conclusions: Polysomy, a finding strongly associated with CCA, is also detected in some PSC associated BilIN. Homozygous 9p21 loss is seen in some BilIN 3 and CCA. The percentage of abnormal cells is on average higher as the degree of histologic abnormality increases, supporting a dysplasia-carcinoma sequence. Furthermore, cases histologically interpreted as BilIN 1-2 may harbor worrisome cytogenetic abnormalities, while some lesions interpreted as BilIN 3 may not. Although the gold standard is not yet clear, these findings could have important implications for the interpretation of biliary cytology-based FISH.

1551 Weight-Loss Supplement-Induced Hepatotoxicity: A Report of 3 Cases.

A Khan, T Huebner, W Twaddell. University of Maryland, Baltimore.

Background: Unregulated, over-the-counter weight-loss supplements have been associated with hepatotoxicity. We present three new cases of weight-loss supplement-induced hepatotoxicity.

Design: Histomorphologic, clinical and demographic data were compared for 3 new cases of weight-loss supplement-induced hepatotoxicity. H&E and reticulin stained sections of liver explants and biopsies were examined. The institutional records were reviewed for clinical and demographic information.

Results: All patients were female, age 25-40 yrs (mean, 32 yrs). Two were Caucasian and 1 African American (AA). Patient 1: 31 year-old Caucasian female presented with nausea, abdominal cramping, and fatigue, transaminitis (AST 1578 U/L, ALT 1876 U/L) and hyperbilirubinemia (23.6 mg/dL). She had been taking Lipolyze (usnic acid, camellia sinensis) for 2 months prior to admission. Liver biopsy and explant showed extensive parenchymal loss and reticulin collapse indicating severe hepatic necrosis. There was mixed inflammation with prominent eosinophils, suggesting medication-related insult. She was treated with orthotopic liver transplant (OLT). Patient 2: 40 year-old AA female presented with fatigue, jaundice, transaminitis (AST 2933 U/L, ALT 1698 U/L) and hyperbilirubinemia (34.4 mg/dL). She had taken orlistat 2 months prior to admission. Liver biopsy and explant showed severe hepatic necrosis with mixed inflammation, including large numbers of plasma cells and eosinophils, suggesting medication-related injury. The patient was treated with OLT. Patient 3: 25 year-old Caucasian female presented with fatigue, itching, abdominal pain, jaundice (bilirubin 15.6 mg/dL) and transaminitis (AST 1902 U/L, ALT 2180 U/L) after using SlimQuick (camellia sinensis) for 3 months. Liver biopsy showed mixed inflammatory infiltrates including prominent eosinophils, focal necrosis and reticulin collapse. The patient was managed medically and discharged in stable condition.

Conclusions: Weight-loss supplementation with some over-the-counter products has been shown to be associated with liver toxicity in multiple studies. We present three new cases of weight-loss supplement-induced hepatotoxicity, wherein all three patients presented with transaminitis, hyperbilirubinemia, and varying degrees of hepatic necrosis. An eosinophilic inflammatory infiltrate and architectural collapse were also common morphologic features. These cases illustrate the need for regulation of such weight-loss products as the lack of regulation makes it difficult to associate dosages or ingredients with possible side effects, thus complicating identification and reporting of adverse responses.

1552 Telomere Length, TERT and Shelterin Complex Protein Expression in Hepatocellular Carcinomas with Stemness-Related Marker Expression.

H Kim, JY Cho, HS Lee, JJ Jang, SH Jeong, YN Park. Seoul National University Bundang Hospital, Seongnam, Korea; Seoul National University College of Medicine, Korea; Yonsei University Health System, Seoul, Korea.

Background: Hepatocellular carcinomas (HCCs) with expression of stemness-related proteins have been recently associated with aggressive biological behavior and poor prognosis. We examined the relationship between stemness-related protein expression in HCCs and the telomere length, hTERT and shelterin complex protein expression in order to search for any differences in telomere dynamics of these tumors compared to conventional HCCs.

Design: Tissue microarrays were constructed from 139 surgically resected HCCs, and subjected to quantitative fluorescent in situ hybridization for telomere length, immunohistochemistry for stemness-related proteins (K19, EpCAM, CD133 and c-kit), AFP, anti-hepatocyte, hTERT, TRF2 and TPP1, and TUNEL assay for evaluation of apoptotic rate.

Results: The telomere lengths were significantly increased in HCCs expressing stemness-related proteins (K19: p<0.001, EpCAM: p=0.003, c-kit: p=0.040, CD133: p=0.003). K19-expressing HCCs demonstrated more frequent expression of hTERT (p=0.002) and TRF2 (p=0.028) proteins and higher TPP1-labeling indices (p=0.008) compared to K19-negative HCCs. Lower apoptotic rates were seen in HCCs expressing CD133 and c-kit (p=0.014 and p=0.067, respectively), and in HCCs expressing 2 or more stemness-related proteins (p=0.025). HCCs expressing anti-hepatocyte antigen showed shorter telomeres (p=0.014), decreased TPP1-labeling indices and lower Ki-67 labeling indices (p=0.002). Univariable analysis demonstrated a significant relationship between decreased overall survival and expression of at least 2 stemness-related proteins (p=0.035). In addition, a TPP1-labeling index exceeding half of the tumor cells was also associated with a significant poor overall survival compared to HCCs expressing TPP1 protein in less than half of the tumor population (p=0.035).

Conclusions: HCCs with expression of stemness-related proteins are characterized by increased expression of hTERT, TRF2 and TPP1 proteins, increased telomere lengths and decreased apoptosis compared to conventional HCCs.

1553 Immunohistochemical Pitfalls and the Importance of Glypican-3 in the Diagnosis of Scirrhous Hepatocellular Carcinoma.

G Krings, D Jain, T-T Wu, M Yeh, M Torbenson, S Kakar. UCSF, San Francisco, CA; Yale Univ, New Haven, CT; Mayo Clinic, Rochester, MN; Univ of Washington, Seattle; Johns Hopkins, Baltimore, MD.

Background: Scirrhous hepatocellular carcinoma(sHCC)is a rare subtype of HCC which can mimic cholangiocarcinoma(CC)or metastatic adenocarcinoma(MA).sHCC tends to be negative for Hep Par 1(Hep)and often expresses CK7,further confounding the diagnostic dilemma.Glypican-3 (GPC) is an oncofetal antigen that has higher sensitivity than Hep for poorly-differentiated conventional HCC(cHCC).Expression of GPC and other markers used in distinction of HCC and adenocarcinoma including polyclonal carcinoembryonic antigen(pCEA),MOC-31 and CK19 have not been systematically evaluated in sHCC.

Design: Immunohistochemistry for Hep,GPC,pCEA,MOC31,CK7 and CK19 was performed on 12 sHCC cases,and scored as 0(negative),1(weak),2(moderate)and 3(strong).The number of positive cells were recorded as focal(<10%),patchy(10-50%)or diffuse(>50%).Score of at least 2+ in ≥10% of cells was regarded as positive.The results were compared with previously characterized cHCC(n=160)and CC(n=12).

Results: In all sHCC,stroma comprised ≥50% of tumor.In 2 cases,sHCC was admixed with areas of cHCC.Hep was positive in 2(17%)sHCC;GPC3 and pCEA were positive in 12(100%) and 4(33%)cases respectively.Diffuse staining was seen in 10(83%)cases with GPC,compared to 1(8%)with Hep and none with pCEA.Adenocarcinoma markers, MOC31,CK7 and CK19 were positive in 64%,58% and 36% cases respectively. At least one adenocarcinoma marker was positive in 10(83%)cases and at least two in 5(42%)cases.Of 2 cases with admixed cHCC,staining in cHCC was same as sHCC area in 1 case;the other case showed Hep positivity in cHCC area but not in sHCC portion.Staining results in sHCC were significantly different compared to cHCC.All CC were GPC-negative.

	Hep Par 1	GPC3	pCEA(canalicular)	MOC-31	CK7	CK19
sHCC(n=12)	17	100	33	64	58	36
cHCC(n=160)	75	70	54	11	2	2
CC (n=12)	0	0	0	100	100	100
p-value (sHCC vs cHCC)	<0.001	0.02	0.31	<0.001	<0.001	<0.001

Figures reflect percentages

Conclusions: In contrast to cHCC,most sHCC are negative for Hep,and frequently express adenocarcinoma markers like MOC31,CK7 and CK19.This aberrant immunophenotype along with presence of prominent stroma can be confused with CC or MA. GPC is expressed in all sHCC with diffuse expression in most cases.Addition of GPC to the immunohistochemical panel can facilitate the diagnosis of sHCC.

1554 A Comparison of the Immunophenotype of Hepatocellular Carcinoma and Non-Lesional Hepatocytes When Analyzed with Next-Generation Markers.

SM Lagana, M Salamao, F Bao, RK Moreira, JH Lefkowitch, H Remotti. Columbia University Medical Center, New York, NY.

Background: Many novel immunohistochemical stains have recently been introduced to help distinguish hepatocellular carcinomas (HCC) from non-malignant hepatocytes. Among these are Glypican-3 (GPC-3), heat shock protein 70 (HSP-70), and glutamine synthetase (GS). The role of Glucose-transporter-1 (GLUT-1) has been controversial in HCC. In addition, a recent study demonstrated Arginase-1 (Arg-1) to be a more sensitive and specific marker of hepatocellular differentiation than hepatocyte paraffin antigen (HepPar1) in HCC. We undertook a comparative study of these markers in HCC and non-lesional hepatocytes.

Design: Tissue microarrays were constructed from 47 cases (17 high grade, 30 low grade) including both HCC and non-lesional (mostly cirrhotic) liver. Staining was performed for the above markers. A cut-off of 5% was set for positivity.

Results:

Results

		HSP-70	GPC-3	GS	GLUT-1	Hep-Par1	Arg-1
Sensitivity (%)	High grade (17)	53	65	94	6	88	100
	Low grade (30)	47	50	93	0	87	97
Average percentage of cells staining in positive cases	High grade	49	49	72	5	72	90
	Low grade	57	55	74	0	78	91

Conclusions: HSP-70 and GPC-3 are helpful in distinguishing malignant from benign hepatocytes when positive, but suffer from low sensitivity in small specimens. Neither stained non-lesional tissue (100% specificity). GS suffers from lack of specificity as it normally stains benign hepatocytes. Though the pattern in benign tissue is different from that of HCC, this can be difficult to appreciate on small biopsies of cirrhotic liver. However, since GS sensitivity is high, when negative it is helpful in excluding a hepatocellular origin. GLUT-1 immunohistochemistry is non-contributory in HCC. In our cases, Arginase-1 was superior to Hep-Par1, with positive staining in all but one HCC and, importantly, in all cases of Hep-Par1 negative HCC. Hep-Par1 was positive in the only Arginase-1 negative HCC, thus both should be considered together when the index of suspicion is high for a tumor of hepatocellular origin.

1555 Intraductal Papillary Neoplasm of the Bile Duct (IPN): Clinicopathologic Study of 39 Cases in Comparison to Pancreatic Intraductal Papillary Mucinous Neoplasm (IPMN) in a Single North American Institution.

H Lee, FG Rocha, DS Klimstra, GQ Young, WR Jarnagin, N Katabi. Memorial Sloan Kettering Cancer Center, New York, NY.

Background: Biliary Intraductal Papillary Neoplasm (IPN) is the least common subtype of bile duct tumor. Despite controversies on nomenclature and classification, IPN is relatively well-documented in Asia and is considered analogous to pancreatic IPMN by some authors. Comparative studies of IPN with detailed clinical and histologic data are lacking in North American populations.

Design: We identified 39 cases of IPN (1993-2010) and randomly selected 44 cases of IPMN for comparison. Clinicopathologic features were analyzed in both cohorts and survival analysis was performed for IPN in relation to the pathologic parameters. Immunohistochemical (IHC) stains were performed on 33 IPNs.

Results: 39 IPNs were identified among 343 biliary carcinomas (11%), including 23 hilar, 4 intrahepatic and 12 distal bile duct primaries. Mean size was 4.5 cm. 1 case was associated with hepatolithiasis. 69% of IPNs were of pancreatobiliary (PB) type and the remainder were oncocytic (ONC, 15%), gastric (GAS, 10%) and intestinal (INT, 5%) types. All IPNs showed high grade dysplasia and had a predominant papillary architecture in 80%. Invasive carcinoma was present in 74% (90% tubular pattern, 10% colloid) and the invasive component was >10% of the tumor volume in 55%. The IPMNs were more commonly GAS (43%) and INT (29%) types. PB type comprised only 9% of IPMNs. High grade dysplasia and invasive carcinoma were less frequent in IPMNs, 57% and 20% respectively, and >30% of invasive carcinomas were colloid type. CK7 was pos in 88% of IPNs. INT (n=2) were pos for CK20 (2), CDX2 (2) and MUC2 (1). PB (n=23) were pos for MUC1 (22), MUC6 (11), and MUC5AC (6). ONC (n=5) were pos for MUC6 (4), MUC1 (3), MUC5AC (5), and HepPar1 (5). GAS (n=3) were pos for MUC1 (3), MUC5AC (2), and MUC6 (3). Expression of mesothelin, CEA, B72.3, and CA125 was not different between the epithelial types. The IHC profile of epithelial types in IPNs was similar to that reported for pancreatic IPMNs. The presence and depth of invasion (>5mm), margin status, and MUC1 immunolabeling were associated with worse median survival ($p<0.05$).

Conclusions: IPN in the North Americans appears to have no obvious risk factors. Although there is some morphologic overlap with pancreatic IPMNs, the majority of IPNs have a pancreatobiliary phenotype and are invasive at diagnosis, indicative of a distinct carcinogenesis and more aggressive behavior than IPMNs.

1556 CK17, MUC5AC, pVHL, and S100P Are the Effective Antibody Panel in Differentiating Intrahepatic Cholangiocarcinoma from Pancreatic Adenocarcinoma.

F Lin, J Shi, H Liu, JW Prichard, HL Wang. Geisinger Medical Center, Danville, PA; Cedars-Sinai Medical Center, Los Angeles, CA.

Background: Distinction of intrahepatic cholangiocarcinoma (ICC) from ductal adenocarcinoma of the pancreas (DAP) can be very challenging or impossible based on the histomorphology alone. Many biomarkers have been studied in this regard. Unfortunately, no definitive markers have been reported. We have previously reported the diagnostic utility of CK17, MUC5AC, S100P, pVHL, maspin, and IMP3 in confirming the diagnosis of DAP and adenocarcinoma of the common bile ducts (Lin et al. AJSP 2008;32:78-91; Levy et al. Hum Pathol 2010;40:324-329; Lin et al. Modern Pathol 2010;23:363A, #1613). In this study, we attempt to explore the usefulness of this panel of antibodies in differentiating ICC from DAP.

Design: We immunohistochemically evaluated the expression of CK17, MUC5AC, pVHL, S100P, IMP3, and maspin on 30 cases of cholangiocarcinoma on routine histological sections and 70 cases of DAP (50 cases on tissue microarray sections and 20 cases of routine sections). The staining intensity was graded as weak or strong. The distribution was recorded as negative (<5% of tumor cells stained), 1+ (5-25%), 2+ (26-50%), 3+ (51-75%), or 4+ (>75%).

Results: The staining results are summarized in Table 1. Four of 5 CK17-positive ICC cases showed only focal positivity (1+). Six of 7 S100P-positive ICC cases were also negative for pVHL. Fourteen of 18 pVHL-positive ICC cases showed diffuse and strong positivity (3+ or 4+).

Table 1. Summary of the immunostaining results

Antibody	DAP (N=70)	ICC (N=30)
CK17	60% (42/70)	17% (5/30)
MUC5AC	67% (47/70)	10% (3/30)
pVHL	0 (0/70)	60% (18/30)
S100P	96% (67/70)	23% (7/30)
Maspin	100% (70/70)	57% (17/30)
IMP3	90% (63/70)	67% (20/30)

Conclusions: Our data indicate that CK17, MUC5AC, pVHL and S100P are the useful panel of antibodies in distinguishing intrahepatic cholangiocarcinoma from ductal adenocarcinoma of the pancreas.

1557 Utility of pVHL, Maspin, S100P and IMP3 in Diagnosis of Carcinomas from Various Organs.

F Lin, HL Wang, M Wilkerson, H Liu. Geisinger Medical Center, Danville, PA; Cedars-Sinai Medical Center, Los Angeles, CA.

Background: Our studies demonstrated that pVHL, S100P, maspin, and IMP3 were the useful panel of antibodies in confirming a diagnosis of pancreatobiliary adenocarcinoma (AJSP 2008;32:78; Hum Pathol 2010;40:324), and pVHL was a sensitive and specific marker for identifying clear cell carcinoma of the kidney, uterus and ovary (AJCP 2008;129:592). In this study, we investigate the potential utility of these markers in the diagnosis of carcinomas from other organs.

Design: Immunohistochemical evaluation of the expression of pVHL, maspin, S100P and IMP3 was performed on a total of 900 cases of carcinomas from various organs on tissue microarray sections.

Results: The positive immunostaining results (%) and a total number of cases for each entity (N) are summarized in the Table 1. Twenty-two cases of intratubular germ cell neoplasia (ITGCN) were all positive for IMP3.

Table 1. Summary of the immunostaining results

Tumor	pVHL (%)	Maspin (%)	S100P (%)	IMP3 (%)
Lung ADC (N=54)	4	51	4	65
PRCC (N=20)	100	0	0	0
CRCC (N=40)	95	0	0	10
Colonic ADC (N=38)	16	90	55	50
Thyroid papillary CA (N=45)	0	9	0	4
Thyroid follicular CA (N=36)	0	8	0	0
Esophageal ADC (N=30)	13	100	73	57
Gastric ADC (N=18)	0	67	67	56
Pancreatic ADC (N=70)	0	100	96	90
Gallbladder ADC (N=23)	0	100	74	78
Urothelial CA (N=40)	0	65	68	35
Intrahepatic cholangiocarcinoma (ICC) (N=11)	73	27	9	55
Breast ductal CA (N=176)	0	26	24	6
Lobular CA (N=83)	4	31	55	6
Endocervical ADC (N=17)	6	65	47	53
Ovarian serous CA (N=15)	0	27	0	53
Prostatic ADC (N=100)	0	2	1	0
HCC (N=18)	17	0	11	17
Seminoma (N=30)	0	0	0	100
Embryonal CA (N=24)	0	21	0	100
Yolk sac tumor (N=12)	0	17	0	100

ADC-adenocarcinoma; RCC-renal cell CA; CA-carcinoma; HCC-Hepatocellular CA

Conclusions: Our data demonstrate that 1) IMP3 is a sensitive marker for seminomas, non-seminomatous tumors and ITGCN; 2) maspin can be used as a useful marker for esophageal ADC; 3) pVHL can be positive in a small percentage of carcinomas of the colon, esophagus and liver; 4) IMP3 is usually negative in both ductal and lobular CA of the breast and can potentially serve as a marker for differential diagnosis; 5) pVHL is expressed in a high percentage of ICC, which can be useful in differentiating it from other biliary tract ADC if confirmed in a large series of cases.

1558 Congenital Absence of Portal Vein (Abernethy Malformation): A Histopathologic Evaluation.

M Lisovsky, AA Konstas, PF Hahn, J Misdraji. Dartmouth Hitchcock Medical Center, Lebanon, NH; Massachusetts General Hospital, Boston.

Background: Congenital absence of the portal vein, or Abernethy malformation, is a rare malformation in which intestinal and splenic venous blood bypasses the liver and drains into systemic veins. Aside from the absence of portal veins, other histologic features of Abernethy malformation have not been emphasized in the literature. The goal of this study was to detail the liver morphologic changes in 5 patients with Abernethy malformation.

Design: Paraffin-embedded tissue sections from two liver biopsies, two liver tumor resections and one liver explant were evaluated using hematoxylin and eosin stains, elastic and trichrome stains. To identify lymphatic vessels immunohistochemistry for D2-40 was performed according to standard protocols.

Results: There were 2 pediatric and 3 adult patients (3 males, 2 females) ranging in age from 17 months to 53 years. One pediatric patient presented with hepatopulmonary syndrome and the other was diagnosed on postnatal ultrasound. One adult female presented with pulmonary hypertension and two adult males presented with hepatocellular carcinoma (HCC). Small portal veins were absent or rare in all patients. Delicate vascular structures at the edges of some portal tracts proved to be lymphatic channels by D2-40 immunostaining. Medium sized portal tracts in resection specimens and the explant showed absence of portal veins in the majority of portal tracts, but in 2 cases, some portal tracts contained hypoplastic portal veins with small caliber lumina and thickened walls. Naked arterioles were noted in the lobules in all cases, sometimes just outside the portal tracts. In 2 cases hepatic artery branches were abnormally large relative to the paired bile duct. Both resection specimens and the explant showed convergence and crowding of portal tracts indicating a remodeling of liver architecture. Two adult patients had HCC in the absence of cirrhosis. Two patients, one with HCC and one child, had focal nodular hyperplasia.

Conclusions: We conclude that in addition to loss of small portal veins, Abernethy malformation is characterized by multiple vascular abnormalities, such as hypoplastic portal veins, naked lobular arterioles, hypertrophy of hepatic artery branches and global remodeling of the liver architecture. Abernethy malformation can be associated with focal nodular hyperplasia and, in some cases, HCC in the absence of cirrhosis.

1559 Hepatocellular Carcinoma in Noncirrhotic Livers: Morphology, Immunophenotype, and Clinical Outcome.

T-C Liu, N Vachharajani, WC Chapman, EM Brunt. Washington University School of Medicine, St. Louis, MO.

Background: The majority of hepatocellular carcinomas (HCC) arise in the setting of cirrhosis, from an established sequence of premalignant events; liver cell adenomas (LCA) arise in a hormonally or metabolically stimulated liver. Less is understood regarding the pathogenesis of non-cirrhotic (NC) HCC.

Design: Forty consecutive resected or transplanted cases of NC-HCC between 1997 and 2009 were collected. Routine and immunohistochemical (IHC) stains for p53, keratin (K) 19, β-catenin, glutamine synthetase (GS), glypican-3 (GPC-3), and liver fatty acid binding protein (LFABP) were analyzed. Tumor grading was by Edmondson-Steiner (E-S) criteria.

Results: Among the 40 patients, 26 (65%) were men; the mean age at surgery was 66 yrs (range 18 to 77 yr). 34 (85%) had no evidence of liver disease; 2 (5%) had HBV, 3 (7.5%) HCV, 1 (2.5%) had both HBV and HCV. Two (2.5%) with chronic hepatitis also had alcoholic liver disease. Eight (20%) patients were diabetic and 11 (27.5%) were obese. None had cirrhosis. The average tumor size was 7.2 cm (mean 1.5 – 19cm). Seven (17.5%) were E-S grade 1 and had vascular ectasias similar to adenomas; 28 (70%) were grade 2, 2 (5%) were grade 3, and 3 (7.5%) were grade 4. Three cases (7.5%) showed features of combined HCC-cholangiocarcinoma, and two (5%) showed > 50% clear cell changes. Nine cases (22.5%) showed strong nuclear p53 staining in >10% tumor cells. K19 was detected in 7 (17.5%). The majority of the cases showed diffuse cytoplasmic expression of GS (95%), but did not express nuclear β-catenin (95%). Patchy cytoplasmic expression of GPC-3 was seen in 16 (40%), whereas diffuse expression was seen in 11 (27.5%); 13 (32.5%) were negative. Various patterns of LFABP were observed in 23 cases (57.5%). Seventeen patients (42.5%) developed recurrence. The overall survival was 3.5 yrs following surgery. Of all factors, only strong p53 stain correlated with shortened survival by univariate analysis ($p<0.05$).

Conclusions: In this group of 40 noncirrhotic HCC, there was a slight male predominance. Chronic viral hepatitis and/or alcoholism were identified in < 20% of cases; obesity and DM were not features of significance in aggressive behavior. The majority of tumors were E-S grade 2, however, many encapsulated grade 1 NC-HCCs were suggestive of LCA. K19 expression, a marker of aggressive behavior in cirrhotic HCC, was detected in <20% of cases, and only increased nuclear p53 expression correlated with poor outcome.

1560 Sinusoidal Deposition of Complement 4d Is More Commonly Seen in Liver Allografts in Patients with Primary Sclerosing Cholangitis (PSC).

X Liu, L Yerian, A Bennett, J McMahon, R Pai. Cleveland Clinic.

Background: Complement 4d (C4d), a marker of complement activation, has been widely used in renal and heart transplant evaluation for humoral rejection and antibody-mediated acute cellular rejection. While a few previous, small, retrospective studies suggested a role for C4d in diagnosing acute cellular rejection in liver transplants, none correlated C4d deposition in liver allografts with the pretransplant liver disease. This study aimed to determine the association of C4d deposition with the pretransplant liver disease diagnosis.

Design: All liver allograft biopsy cases from 01/2009 to 07/2010 were retrieved from our Database. C4d deposition was analyzed by direct immunofluorescence on frozen liver allograft biopsy material and correlated with the type of pretransplant underlying liver disease as determined by clinical history and/or histologic diagnosis in the explanted native liver.

Results: 569 allograft biopsies from 330 patients were retrieved and classified by native liver diseases. Twenty patients had rare liver diseases and were excluded from further analysis. 506 biopsies from the remaining 310 patients with PSC [PSC alone (n=23) and overlap syndrome (n=2) of PSC and AIH (autoimmune hepatitis)], viral hepatitis [hepatitis C (n=193) and hepatitis B (n=5)], and other liver diseases [non-alcoholic steatohepatitis (NASH), alcoholic cirrhosis, cryptogenic cirrhosis, AIH, acute liver failure, and others, n=87] were studied for C4d by direct immunofluorescence. Sinusoidal C4d deposition was noted in 11.9% of biopsies and 15.2% of patients (in one or more biopsies). Sinusoidal C4d deposition was noted in 26% (9/35), 12% (43/348), and 7% (8/123) of biopsies obtained from patients with PSC, viral hepatitis, and other liver diseases ($p=0.000004$). Approximately 28%, 16%, and 9% of patients with PSC, viral hepatitis, and other liver diseases had at least one biopsy with C4d deposition ($p=0.055$).

Conclusions: C4d deposition in liver allograft is a low frequency event. While our unpublished data show that C4d deposition does not aid in differentiating acute cellular rejection from recurrent hepatitis C, the current data suggest that complement activation occurs in liver allografts in patients with various underlying liver diseases and occurs with greater frequency in patients with PSC than other common liver diseases. These findings suggest that mechanisms other than allo-immunity may activate complement. The mechanism and clinical significance of C4d deposition in liver allografts in patients with PSC remain undetermined and further studies are needed.

1561 Predicting Recurrence-Free Survival in Patients with Well-Differentiated Pancreatic Endocrine Neoplasms without Distant Metastasis: WHO Classification or Two-Tier Grading System?

T-C Liu, N Hamilton, WG Hawkins, D Cao. Washington University School of Medicine, St. Louis.

Background: Well-differentiated pancreatic endocrine neoplasms (WDPENs) are uncommon. In the absence of metastasis or invasion**,** it is difficult to predict their behavior. This study is to compare the ability of two current grading systems, WHO classification and two-tier grading system, to predict recurrence-free survival (RFS) in patients with WDPENs but without distant metastasis (DM) at diagnosis.

Design: The following 11 parameters were analyzed in 94 patients: age, gender, tumor size, T stage, lymph node (LN) status, margin status, vascular invasion (VI), perineural invasion (PI), mitosis, necrosis, Ki-67 proliferation index. Each tumor was graded using the WHO classification [benign behavior (BB): confined to the pancreas, no VI, no PI, <2 mitoses/10HPFs, Ki-67 <2%; uncertain behavior (UB): confined to the pancreas and at least one of the following: ≥ 2 cm, 2-10 mitoses/10 high power fields (HPFs), Ki-67>2%, VI, PI; well-differentiated endocrine carcinoma (WDCA): gross local invasion or metastasis] and the two-tier grading system [low grade (LG): no necrosis and < 2 mitoses/50HPFs; intermediate grade (IntG): with necrosis or 2 to 50 mitoses/50HPFs]. These parameters and tumor grade were correlated with RFS using Kaplan-Meier method and log-rank test. Concordance-index (CI) was calculated for these 2 grading systems.

Results: The mean age (44 M, 50 F) at diagnosis was 53.7 years. The mean tumor size was 2.9 cm (40 T1, 29 T2, 25 T3). Positive margin, VI, PI, necrosis, and LN metastasis was seen in 16, 29, 22, 15, and 29 tumors, respectively. Mitosis was identified in 41 tumors (mean 3.9 per 50 HPFs). Twenty-one, 46, and 27 tumors fell into BB, UB, and WDCA categories, respectively. Sixty were LGs and 34 were IntGs. Average Ki-67 was 6.6%. During followup (1 to 212 months), 22 patients recurred (1/21 BBs, 9/46 UBs, 12/27 WDCAs; 6/60 LGs, 16/34 IntGs). Tumor size, T stage, node metastasis, VI, PI, Ki-67, necrosis, and mitosis strongly predicted RFS ($p<0.01$ for all) where age ($p = 0.38$), gender ($p = 0.18$), and margin status ($p =0.53$) did not. Both WHO classification and two-tier system strongly predicted RFS ($p= 0.002$ and 0.0003, respectively). The CI of the former was 0.69 whereas that of the latter was 0.73. When Ki-67 and the two-tier system were combined, the CI was 0.79.

Conclusions: The two-tier grading system is better than the WHO classification in predicting RFS in patients with WDPCAs without DM. Further predicting accuracy can be achieved by combining Ki-67 and the two-tier grading system.

1562 Inflammatory Pseudotumor (IPF) of Liver: An Entity Distinct from Inflammatory Myofibroblastic Tumor (IMFT): A Clinicopathologic, Immunohistochemical, and Molecular Genetic Study of 145 Cases.

HR Makhlouf, JC Fanburg-Smith, G Wang, M Mujahid, Z Vesoulis, ZD Goodman. Armed Forces Institute of Pathology, Washington, DC; Inova Fairfax Hospital, Falls Church, VA.

Background: Liver pseudotumors are reportedly rare, with less than 200 cases in the literature since 1953, Pack and Baker. There is confusion over these lesions; particularly since IPT has been lumped together as IMFT in the pediatric soft tissue literature. IMFT is a neoplastic process with rearrangement of ALK gene (2p23). We review our experience with hepatic IPT//IMFT.

Design: Cases designated hepatic IMFT or IPF were studied, including patient folders, slides, IHC for IgG4, lymphoid markers, ALK and molecular for ALK and EBV. 0-4+ presence of spindled and specific inflammatory cell components were recorded.

Results: 145 hepatic cases reviewed were all reclassified as IPT variant. The cases included 54F: 91M, with a mean age of 54. Races included Caucasian (n=48 known) followed by Black with fewer Hispanic and Asian. 90 cases were solitary; 40 multiple, 15 not specified; right= left sided. Patients presented with abdominal pain and fever with no known elevation of AST/ALK but mass on imaging, ranging from 0.2 to 20.5 (median, 4) cm. A few patients had known cholelithiasis/cholecystitis. Needle or wedge biopsy was performed. Histologically the lesions could be separated from surrounding liver and were composed of varying proportions of inflammatory cells with fibrosis but without a prominent spindled myofibroblastic component. The lesions were divided into five main groups: plasma cell rich with diffuse or aggregates of lymphocytes (n=67), mixed inflammatory (n=30), granulomatous (n=21), granulomatous with eosinophils (n=15), and predominantly purulent (n=12); all appeared to be resolving inflammatory processes. None of cases studied had positive staining for monoclonal lymphoid population, CD1a, IgG4 in plasma cells, WS, AFB, PAS, GMS, or ALK kinase and none of n=15 showed ALK gene rearrangement. 3/29 cases were positive for EBER in situ. Follow-up to date reveals no patients with subsequent neoplasm, recurrence or metastasis.

Conclusions: Most cases considered as IMFT in liver are better diagnosed as IPT, as a form of resolving inflammatory process. These lesions predominate in middle aged adult males who present with fever, abdominal pain, and mass and may be multiple. While EBV may account for 10% of cases, future study is warranted to delineate possible other specific organisms to hepatic IPF subtypes; there is no IgG4 positive subset to suggest autoimmune process.

1563 Comparison of Changes in the Gene Expression of Transferrin Receptor-1 and Other Iron Regulatory Proteins in the Rat Liver and Brain during Acute-Phase-Response.

I Malik, N Naz, N Sheikh, S Khan, G Ramadori. University Hospital Goettingen, Germany.

Background: Acute phase is clinically characterized by homeostatic alterations such as adinamia, fever, muscular weakness and leucocytosis. Several organs are involved in dramatic changes of iron metabolism such as liver and brain.

Design: Rats were administered turpentine oil (TO) intramuscularly and sacrificed at different time points thereafter. Liver and brain were taken and immediately frozen in liquid nitrogen. Hepatocytes and Kuppfer cells were isolated from normal rat liver. Liver and brain tissue were used for immunohistochemistry, western blot and RNA isolation. RNA from liver and brain tissue was studied by polymerase chain reaction (PCR).

Results: Tissue iron content in the liver and brain increased progressively after the TO administration.By means of immunohistology, an abundant TfR1 expression was detected in membrane and cytoplasm of the liver cells, in contrast to only nuclear expression of TfR1 in the brain and the expression TfR1 increased at protein and RNA level in both organs. In addition, hepcidin-, ferritin H-, divalent-metal transporter-, hephaestin- together with heme oxygenase-1 gene expression was also significantly upregulated while hemojuvelin-, ferroportin-1-, and HFE gene expression was significantly downregulated at the same time points both in the brain and in the liver at RNA level. However, in contrast to what is observed in the liver, expression of main acute phase cytokines (interleukin-6, tumor-necrosis-factor-alpha) in the brain was significantly upregulated.

Conclusions: During acute-phase, iron accumulates in the liver and in the brain and gene expression of TfR1 and iron metabolism proteins is regulated in a way similar to that observed in the liver by locally produced acute-phase cytokines.

1564 Serotonin Expression in Pancreatic Neuroendocrine Tumors Correlates with a Trabecular Histologic Pattern and Fewer Lymph Node Metastases.

CM McCall, C Shi, AP Klein, G Kloppel, B Konukiewicz, BH Edil, T Ellison, RH Hruban. The Johns Hopkins University School of Medicine, Baltimore, MD; Technical University of Munich, Germany.

Background: We recently described a small series of pancreatic neuroendocrine tumors (PanNETs) with prominent stromal fibrosis and serotonin expression. In order to better understand the relationship between tumor histopathological patterns and serotonin expression, we identified all pancreatic NETs with significant stromal fibrosis over the past thirty years at our institution.

Design: All available slides from 361 PanNETs diagnosed at our institution from 1980-2009 were reviewed for prominent stromal fibrosis. 52 cases were identified, and these neoplasms were immunolabeled with antibodies to serotonin and Ki-67. Histology and serotonin and Ki-67 immunoreactivity were examined for each case.

Results: At least focal serotonin immunoreactivity was found in 14 of 52 (26.9%) of the fibrotic PanNETs studied. Two predominant histologic subtypes were identified: 14 of 52 (26.9%) had a trabecular or trabecular-glandular cellular pattern interspersed by fibrosis, while 38 of 52 (73.1%) had a solid architecture. Tumors with predominantly trabecular architecture were significantly more likely to be serotonin-positive (8 of 14 (57.1%)) than those with solid architecture (6 of 38 (15.8%)) ($p<0.01$). Serotonin-positive tumors were less likely to have lymph node metastases (1 of 13 (7.7%)) than serotonin-negative tumors (17 of 35 (48.6%)) ($p=0.026$). There was no significant association of serotonin immunoreactivity with Ki-67 proliferation index, tumor size, or the presence of distant metastases.

Conclusions: Our data demonstrate a correlation between trabecular architecture and serotonin immunoreactivity in pancreatic NETs with stromal fibrosis. Serotonin-positive tumors are also less likely to have lymph node metastases. This subset of pancreatic NETs have no significant difference in distant metastatic potential or Ki-67 proliferation index in our series.

1565 Pancreatic Cyst Fluid Carcinoembryonic Antigen (CEA) Level Obtained by Endoscopic Ultrasound Guided-Fine Needle Aspiration (EUS-FNA) Does Not Predict Grade of Dysplasia in Intraductal Papillary Mucinous Neoplasm (IPMN) of the Pancreas.

C McCarty, J Klapman, M Malafa, J Weber, D Coppola, BA Centeno. Moffitt Cancer Center, Tampa, FL.

Background: Measurement of the CEA level is the most consistently used ancillary study in pancreatic cyst fluids obtained by fine needle aspiration. A level of 192 ng/ml has been reported as an accurate cut-off value for the distinction of mucinous vs. nonmucinous lesions. More controversial is whether the level of CEA can be used to predict the grade of dysplasia in a cyst suspected of being IPMN, and thus guide surgical management. The aim of this study is to determine whether the CEA level predicts the grade of dysplasia in patients with surgically resected IPMN.

Design: Patients were identified by searching an IRB approved database of patients with IPMN at the Moffitt Cancer Center. Patients with a resected IPMN were selected for this study if they had previously undergone EUS-FNA of the cystic mass with CEA measurement of the cyst fluid. All resection specimens were reviewed by two pathologists (CM and BAC) to confirm the pathological diagnosis. IPMN were classified into low grade dysplasia (LG), moderate dysplasia (MD), high grade dysplasia (HG) or invasive carcinoma (INV). One-way ANOVA was performed to examine the differences of CEA levels among pathologic groups.

Results: We identified 47 patients who met these criteria (35 males, 12 females). There were 9 LG, 17 MD, 14 HG and 7 INV. The fluid CEA levels and corresponding surgical pathologic diagnoses are summarized in Table 1.

Table 1: Fluid CEA Levels and Corresponding Surgical Pathologic Diagnoses

Resection Specimen Diagnosis	CEA Ranges, ng/ml	CEA Mean Values, ng/ml	CEA Median Values, ng/ml
LG (N=9)	37.9-4541	1257	458
MD (N=17)	8.5- 90,100	7171	201
HG (N=14)	47.2- 136,441	10806	292.5
INV (N=7)	140- 1866	443	200

The mean level of CEA increased from LG to HG. INV showed CEA levels markedly lower than those in LG. ANOVA statistical analysis showed no significant difference among pathological diagnoses ($p = 0.72$).

Conclusions: This retrospective study shows no statistical significance in the CEA levels among the pathologic groups. Furthermore, not only is a markedly elevated cyst fluid CEA not an accurate predictor of HG or INV, the appearance of INV in IPMN is associated with a decline in mean CEA. Therefore, the decision to observe or resect a pancreatic neoplastic mucinous cyst suspected of being IPMN should not be based on the CEA level.

1566 HuR Regulates IGF1R Expression in Pancreatic Adenocarcinoma.

MJ McDonald, J Kline, S Zaheer, V Patel, CJ Yeo, J Brody, AK Witkiewicz. Thomas Jefferson University Hospital, Philadelphia, PA.

Background: Current therapy for pancreatic ductal adenocarcinoma (PDA) consists of surgery and/or gemcitabine-based chemotherapy. High expression of Hu protein antigen R (HuR) has been recently demonstrated to be a positive predictive marker for overall survival in patients with PDA receiving gemcitabine. In vitro, HuR has been shown to inhibit translation of type 1 insulin-like growth factor receptor (IGF1R), the overexpression of which is associated with invasiveness of PDA. In this study we correlated expression of IGF1R and HuR in PDA and with clincopathological features and patient survival.

Design: IGF1R and HuR expression was evaluated in 98 PDA cases by immunohistochemistry using anti-IGF1R (clone G11, Ventana Medical Systems,) and anti-HuR (clone sc-5261, Santa Cruz Technologies) antibodies. IGF1R was scored on a four-point scale (0, 1+, 2+, 3+) according to the system used for HER-2 evaluation. HuR cytoplasmic staining was scored as low or high as we previously published. For statistical analysis IGF1R scores were dichotomized as low (0-1) vs. high (2-3). Associations between PDA grade and T/N stages and IGF1R and HuR were analyzed using Fisher's exact test. Overall survival was analyzed using LogRank test and Cox proportional hazard model.

Results: High IGF1R expression was associated with low HuR cytoplasmic positivity ($p=0.0085$). High expression of IGF1R correlated with higher tumor grade ($p=0.033$) and high expression of HuR with higher tumor stage. Patients with high IGF1R and low HuR had longer overall survival (median 19.9 months for high IGF1R/low HuR and 15.2 months for lowIGF1R/high HuR), however this difference was not statistically significant.

Conclusions: Our results support in vitro data showing that HuR can repress IFG1R protein expression. This finding should have implications for anti-IGF1R based therapies.

1567 Hyaline Globules in Neuroendocrine and Solid-Pseudopapillary Neoplasms of the Pancreas: A Clue to the Diagnosis.

Z Meriden, C Shi, B Edil, T Ellison, C Wolfgang, R Schulick, RH Hruban. The Johns Hopkins University School of Medicine, Baltimore, MD.

Background: Distinguishing between solid pseudopapillary neoplasm (SPN) and pancreatic neuroendocrine tumors (PanNET) can be problematic. Both can have solid growth patterns, and immunolabel with antibodies to endocrine markers such as synaptophysin and CD56. One established feature of SPN is the presence of hyaline globules.

Design: All available histologic slides from 361 cases originally diagnosed as PanNET were reviewed. Of these, 24 cases had hyaline globules, raising the possibility of SPN. Immunolabeling studies for synaptophysin and beta-catenin were performed on the 24 cases with hyaline globules, and CD10 was used as a confirmatory test in cases with nuclear beta-catenin. PAS, PAS with diastase, and immunolabeling with alpha-1-antitrypsin and trypsin were performed to characterize the hyaline globules. All 24 cases were examined for the pattern of invasion, microcystic change, hemorrhage, cholesterol clefts, clear cells, foam cells, nuclear grooves, and foci of discohesion.

Results: 6 of the 24 cases with hyaline globules had nuclear labeling for beta-catenin, expressed CD10, and were reclassified as SPN. The remaining 18 cases maintained their original diagnosis as PanNET. A subset of these 18 cases had only focal hyaline globules which were absent on deeper levels. Hyaline globules were PAS-positive, diastase resistant (16/16 evaluable cases), and immunolabeled with alpha-1-antitrypsin (12/15 cases) or trypsin (1/16 cases). The mean age of the 24 patients was 54 years, 56 for patients with PanNET, and 48 for patients with SPN. There was no difference in patient gender (SPN: 50% male vs. PanNET: 55.6% male, P=1). When the 24 cases with hyaline globules were compared, 3 features suggestive of SPN emerged: an insidious pattern of invasion wherein normal pancreatic elements are entrapped by the tumor (83.3% SPN vs. 11.1 % PanNET, P=0.003), clear cells (100% SPN vs. 27.8% PanNET, P=0.003), and nuclear grooves (50% SPN vs. 0% PanNET, P=0.010).

Conclusions: The morphologic features of SPN and PanNET overlap. Small SPNs with minimal degenerative changes are particularly hard to recognize. In these cases hyaline globules should raise SPN in the differential diagnosis, and the diagnosis can be established with immunolabeling for beta-catenin. Additionally, the presence of hyaline globules should not be used as a sole diagnostic criterion for SPN, as 5% of PanNETs contain hyaline globules. Features supporting the diagnosis of SPN include nuclear beta-catenin labeling and CD10 expression, an insidious pattern of invasion, clear cells, and nuclear grooves.

1568 Immunohistochemical Study of Maspin for Pancreatic Tumors: Is It Useful for Materials Obtained from Endoscopic Ultrasound Guided-Fine Needle Aspiration?

T Mitsuhashi, H Asamuma, T Hayashi, T Hasegawa. Sapporo Medical University, Hokkaido, Japan.

Background: Differentiating pancreatic invasive ductal carcinoma (IDC) from atypical glands of atrophic acini due to chronic pancreatitis (CP) is always challenging for pathologists. Maspin is known to have tumor-suppressor function and expressed in certain kinds of adenocarcinomas.

Design: Maspin and p53 expression in IDC, pancreatic intraepithelial neoplasia (PanIN), intraductal papillary mucinous neoplasia (IPMN), and CP is evaluated immunohistochemically to distinguish malignant glands from benign glands, using 20 specimens from endoscopic ultrasound guided-fine needle aspiration (EUS-FNA) and surgically resected materials [20 invasive ductal carcinomas, including PanIN and CP in the same specimens, and 15 IPMNs (10 IPMAs and 5 IPMCs)]. Maspin is evaluated as (2+), (1+), pseudo-positive (+-) and (-). p53 is evaluated as positive if distinct strong nuclear stain is seen.

Results: Maspin is (+) or (2+) in IDC (either nuclear or nuclear plus cytoplasmic) and in mucin producing slightly atypical carcinomatous glands. High grade neoplasms (PanIN 2 and 3, borderline IPMN and IPMC) are variably positive for maspin. Atrophic glands of CP and are (+-) or (-). p53 positivity is variable in IDC and adenocarcinoma derive from IPMN, and is negative even in lymph node-positive IDC. Maspin positivity is also recognized in EUS-FNA specimens as shown in Table 2.

Table 1. Expression of maspin and p53 in surgically resected specimens

Surgically resected specimens	Maspin (2+/1+/+-/-)	p53 positive
IDC	100% (15/5/0/0)	45%
IPMA	100% (0/10/0/0)	0%
IPMC(+boderline)	100% (4/1/0/0)	33%
PanIN	100% (4/6/0/0)	20%
CP	0% (0/0/10/10)	0%
Normal pancreas	3%(0/0/1/29)	0%

Table 2. Expression of maspin and p53 in EUS-FNA specimens

EUS-FNA specimens	Maspin(2+/1+/+-/-)	p53 positive
Adenocarcinoma	100% (8/2/0/0)	38%
IPMA	100% (0/5/0/0)	0%
CP	0%(0/0/2/3)	0%
Gastric foveolar epithelium	0%(0/0/0/10)	0%
Pancreatic ductal epithelium	0%(0/0/0/15)	0%
Pancreatic acinar cells	0%(0/0/0/10)	0%

Conclusions: Although the restriction of EUS-FNA specimens, maspin is a very useful marker to differentiate potential malignant glands from benign glands and is better than p53, when it is judiciously applied.

1569 Significance of Obliterative Phlebitis for the Diagnosis of Lymphoplasmacytic Sclerosing Pancreatitis.

K Miyabe, K Notohara, T Nakazawa, T Ando, K Hayashi, I Naitoh, F Okumura, M Yoshida, H Ohara, T Joh. Nagoya City University Graduate School of Medical Sciences, Japan; Kurashiki Central Hospital, Japan.

Background: Obliterative phlebitis is a useful pathological finding for the diagnosis of lymphoplasmacytic sclerosing pancreatitis (LPSP), or type 1 autoimmune pancreatitis. However, little has been discussed so far whether it is specific to LPSP among various pancreatic diseases.

Design: Resection or open biopsy specimens of LPSP (18 patients), chronic pancreatitis (CP; 24), and pancreatic ductal adenocarcinoma (PDA; 45) were gathered. In each case, serial sections were made from a representative block to stain H&E and elastica van Gieson (EVG). The number (/cm^2) and diameter of obliterative venous lesion (OVL), which was defined as presence of inflammatory cells and/or fibrosis inside of tunica adventitia, were evaluated with EVG stain. Each OVL was classified into one of the 3 groups according to the histological findings seen in the affected veins; loosely-arranged lymphoplasmacytic infiltration and fibrosis (type 1), fibrosis and only a few lymphoplasmacytic infiltration (type 2), and densely-packed lymphoplasmacytic infiltration without fibrosis (type 3).

Results: Median number of OVLs in LPSP, CP, and PDA were 5.4, 1.0, and 2.6, respectively. Percentage of types 1/ 2/ 3 of OVLs was 86.2/ 6.8/ 7.0, 14.9/ 54.1/ 31.1, and 9.2/ 54.1/ 37.8 in LPSP, CP, and PDA, respectively. Type 1 OVL was observed in every case with LPSP, although it was less common in CP (5/24) and PDA (12/45) cases. In addition, veins with a diameter of 150μm or larger were affected in 36.2, 0, and 4.2% of type 1 OVLs in LPSP, CP, and PDA, respectively, and 17 out of 18 LPSPs had type 1 OVLs with a diameter of 150μm or larger. From receiver operator characteristic (ROC) analysis, cut off values of average diameter, maximum diameter, and number of type 1 OVL in each case for the diagnosis of LPSP were 84.5μm (sensitivity: 100%, specificity: 88.4%), 150.0μm (94.4%, 98.6%), and 1.6/cm^2 (100.0%, 98.6%), respectively.

Conclusions: Although OVL itself is not specific to LPSP, type 1 OVL is more specific and frequently observed in larger veins in LPSP. We suggest that presence of type 1 OVL with a diameter of 150μm or larger is a highly diagnostic finding for LPSP.

1570 Telangiectatic Variant of Hepatic Adenoma: Correlation between Liver Needle Biopsy and Resection.

T Mounajjed, T-T Wu. Mayo Clinic, Rochester.

Background: Telangiectatic variant of hepatic adenoma (THA) is a benign hepatocellular neoplasm that requires surgical resection. Although the clinical and morphologic features of this entity are well characterized, the role of liver needle biopsy (LNB) in identifying this lesion prior to resection has not been studied in detail.

Design: We identified 52 patients (47 females & 5 males, 18-62 years) who have undergone resection of hepatic adenoma (HA) (31 patients), THA (14 patients) and focal nodular hyperplasia (FNH) (11 patients) following a LNB between 1994 and 2010. If lesions were multiple, we only included cases in which the targeted LNB site was specified and could be correlated with the resected lesion. We evaluated LNB and resection specimens for the following features: 1) abortive portal tracts 2) sinusoidal dilatation 3) ductular proliferation 4) inflammation 5) naked arteries 6) nodules, fibrous septa, and/or central stellate scar 7) steatosis. A diagnosis of HA or FNH was made according to established criteria. A diagnosis of THA was made if the lesion had all of the first 4 criteria (1-4) and lacked criterion 6.

Results: 25 patients had a single lesion (13 HA, 6 THA, 6 FNH) and 27 had multiple lesions (14 HA, 6 THA, 3 FNH, 2 HA & THA, 2 HA & FNH). Lesions ranged in size between 0.2 and 14.4cm, and when multiple, numbered between 2 and >100. All resection specimens diagnosed as THA met the first 4 criteria, lacked criterion 6, and contained naked arteries. Only 27% (8/30) of sampled THAs showed steatosis compared to 76% (51/67) of sampled HAs ($p<0.0001$). All resected HAs and FNHs were correctly diagnosed on LNB. Of the 14 patients receiving resection for THA, all diagnostic criteria for THA (except for inflammation in 1 patient) as well as naked arteries were present on LNB in 6 patients (42.8%). 4 patients (28.6%) had naked arteries only on LNB and lacked all the other criteria (except for sinusoidal dilatation in 1 patient). These were consistent with HA. The remaining 4 patients (28.6%) had some but not all features of THA on LNB (naked arteries & abortive portal tracts: 4/4, sinusoidal dilataion 2/4, ductular proliferation or inflammation: 0/4). No LNB of a THA was misdiagnosed as FNH.

Conclusions: Only 42.8% of resected THAs could be accurately diagnosed on LNB. However, more than half (57.2%) of resected THAs do not have complete diagnostic features on LNB and a subset (28.6%) is misclassified as HA. This is of no clinical consequence because it warrants adequate treatment. Importantly, No THA was misclassified as FNH on LNB. THA is significantly less likely to display steatosis than HA.

1571 Does Rhodanine Stain Help Differentiate Venous Outflow Impairment from Chronic Biliary Disease in Liver Biopsies?

T Mounajjed, TC Smyrk. Mayo Clinic, Rochester, MN.

Background: Venous outflow impairment (VOI) can occasionaly mimic chronic biliary disease (CBD) histologically and by liver biochemistry profile. In this study, we ask whether histochemical demonstration of copper accumulation in hepatocytes by rhodanine stain can aid in differentiating between VOI and CBD.

Design: Pathology files were searched for liver cases demonstrating all stages of VOI and CBD [including primary biliary cirrhosis (PBC) and primary sclerosing cholangitis (PSC)] between 1987 and 2010. We applied a rhodanine stain to all biopsies, and scored stainable copper as follows: no copper = 0, copper accumulation in rare periportal hepatocytes =1, patchy periportal staining = 2, circumferential periportal staining =3; diffuse staining in periportal and non-periportal hepatocytes =4. Clinical and laboratory data as well as H&E and trichrome stained slides were reviewed to confirm diagnosis and stage of disease.

Results: Prevalence and mean score of stainable copper in 64 VOI patients (13 acute & 51 chronic; 26 veno-occlusive disease + 21 Budd-Chiari + 9 congestive heart failure + 8 amyloidosis; 33 female & 31 male; 18 to 84 years) and 123 CBD patients (51 PBC & 72 PSC; 66 female & 57 male; 22 to 87 years) is demonstrated in table 1.

Prevalence and (mean score) of copper in VOI and CBD patients

Stage (S)	VOI	CBD
S1	0/15 (0)	14/37 (0.6)
S2	1/14 (2)	24/32 (1.1)
S3	1/9 (1)	30/33 (2.6)
S4	5/13 (1.6)	21/21 (3.3)

Rhodanine was negative in all cases of acute VOI. Stainable copper was detected in 7/51 chronic VOI patients (5 veno-occlusive disease, 1 Budd-Chiari, & 1 heart failure) and in 89/123 CBD patients (35 PBC & 54 PSC). In all stages, the prevalence of stainable copper was significantly higher in CBD patients compared to VOI patients (stage 1: $p=0.0005$, stage2, 3, & 4: $p<0.0001$). Similarly, the mean copper score was significantly higher in CBD patients compared to VOI patients ($p<0.0001$). With only 2 exceptions, rhodanine was always negative in stage 1-3 VOI. An unusual pattern of sub-capsular copper accumulation was observed in 2 stage 4 VOI cases.

Conclusions: In all stages of liver disease, copper accumulates in hepatocytes more frequently and more extensively in CBD compared to VOI. In liver biopsies displaying stage 1-3 fibrosis, rhodanine stain is a valuable aid in differentiating between VOI and CBD. In contrast, once stage 4 fibrosis has evolved, copper accumulation can be observed in 38.5% of VOI patients, and is therefore less reliable in differentiating VOI from CBD.

1572 Malignant Perivascular Epithelioid Cell Tumor (PEComa) of the Pancreas: First Report in Patient with BRCA2 Mutation.

N Mourra, T Lazure, F Paye, C Colas, L Arrive, A de Gramont, J-F Flejou. Hop. St-Antoine, Paris, France; Hop. Kremlin Bicêtre, Kremlin-Bicêtre, France, Metropolitan.

Background: PEComas (perivascular epithelioid cell tumors) encompass a group of rare mesenchymal neoplasms, sharing cellular characteristics of perivascular epithelioid cells and distinctive immunophenotypic features of both muscular and melanocytic differentiation. They have been found in numerous anatomic sites throughout the body with a striking female predominance, even after excluding PEComas arising in gender-specific sites. Pancreatic PEComas are exceedingly rare neoplasms, only five cases have been described before, all were benign and occurring in women.We report the first malignant pancreatic PEComa, which is the first one occurring in patient with BRCA2 mutation.

Design: A 51-year-old woman with a recent history of jaundice (1 month) complained of right hypochondric pain and prurit. Her medical history was remarkable for bilateral ductal breast adenocarcinoma treated with surgery, chemotherapy and irradiation in 2003. She was tested positive for BRCA2 mutation, and preventive bilateral oophorectomy was performed. Imaging studies (Ultrasound, CT-scan and MRI) showed dilatation of common and intrahepatic bile ducts related to an intrapancreatic mass, consistent with endocrine or secondary tumor.

Results: Endoscopic ultrasound guided biopsy demonstrated a neoplasm with microscopic and immunophenotypic features typical of PEComa. Pathologic examination of Wipple procedure confirmed the diagnosis of a 6 cm intrapancreatic PEComa with abundant granular eosinophilic cytoplasm and eccentric nuclei with few mitotic figures (2/50 HPF).Tumor cells were strongly positive on immunohistochemistry with Hmb45 and negative for all other markers, including muscular ones. The tumor invaded duodenal wall with extensive necrosis and vascular invasion, leading to classify this PEComa into “malignant” category, according to Folpe’s classification. The patient received no adjuvant therapy and she is still alive and well after 7 months of follow-up.

Conclusions: Carriers of BRCA2 mutations, who are at very high risk for hereditary breast and ovarian cancer, also face an increased risk of pancreatic adenocarcinoma compared with the general population. PEComas has never been described in BRCA mutation carriers before, but BRCA mutations were not tested in the previously reported pancreatic PEComas. Furthermore, the undertaking of preventive mastectomy and

oophorectomy by female BRCA1/2 carriers may "unveil" more pancreatic tumors in these families, including a novel member such as PEComas, emphasizing the need for close lifelong surveillance.

1573 Pathologic and Phenotypic Characteristics of Intrahepatic Cholangiocarcinoma Arising in Chronic Advanced Liver Disease and Cholangiocarcioma Component of Combined Hepatocellular-Cholangiocarcinoma.

Y Nakanuma, J Xu, K Harada, Y Sato, M Sasaki, J-H Kim, E Yu. Kanazawa University Graduate School of Medicine, Ishikawa Prefecture, Japan; Shanxi Medical University, Shanxi, Taiyuan, China; University of Ulsan College of Medicine, Seoul, Korea.

Background: Intrahepatic cholangiocarcinoma (ICC) is known to arise in non-biliary, chronic advanced liver diseases (CALD), while its pathological features remain unexplored.

Design: We tried to characterize the pathologic and phenotypic features of ICC arising in non-biliary CALD in comparison with ICC arising in almost normal livers (non-CALD) and also ICC component of combined hepatocellular cholangiocarcinoma (HC-CC). A total of 471 cases of ICC were examined, and ICC component of HC-CC (30 cases) was compared with ICC.

Results: It was found that 53 cases of ICC were associated with non-biliary CALD, while the remaining 418 cases of ICC arose in non-CALD. When ICCs were classified into bile duct (conventional) adenocarcinoma, bile ductular adenocarcinoma, variants, and intraductal papillary neoplasm of bile duct (IPNB), a whole spectrum of such subtypes of ICC were found in non-CALD and also non-biliary CALD. A majority of ICCs belonged to bile duct type in both groups (67.9% in non-biliary CALD and 64.1% in non-CALD). Interestingly, bile ductular type was rather frequent (22.6%) in non-biliary CALD in comparison with non-CALD (8.4%). In contrast, IPNB was rather frequent in non-CALD (22.5%) in comparison with non-biliary CALD (3.8%). Comaparison of ICC component of HC-CC (30 cases) with ICC showed that expression of mucin was higher in ICC with **non-CALD**, while such expression was relatively lower in ICC with CALD and CC component of HC-CC. Expression of biliary markers (CK7, CK19, EMA and EpCAM) was relatively lower in CC with CALD and higher in CC component of HC-CC cases in comparison with CC with **non-CALD**. ICC with CALD and CC component of HC-CC showed higher expression of hepatic progenitor cell markers (NCAM and c-kit), while such epxression was lower in ICC with **non-CALD.**

Conclusions: A whole pathological spectrum of ICC arising in non-CALD were also found in non-biliary CALD. Bile ductular type was rather specifically frequent in non-biliary CALD, suggesting this type was rather characteristic to non-biliary CALD, probably involving hepatic progentitor cells. ICC arising in CALD and ICC component of combined HC-CC showing similar features, may have the cholangiocarcinogenesis involving hepatic progenitor cells.

1574 Distinction of Lymphoplasmacytic Sclerosing Pancreatitis from Other Mass-Forming Inflammatory Diseases by CD163 and -Smooth Muscle Actin Immunohistochemistry.

K Notohara, L Zhang, K Miyabe, S Nakamoto, T Nakazawa. Kurashiki Central Hospital, Japan; Mayo Clinic, Rochester, MN; Nagoya City University Graduate School of Medical Sciences, Japan; Tottori Prefectural Central Hospital, Tottori, Japan.

Background: Lymphoplasmacytic sclerosing pancreatitis (LPSP) and idiopathic duct-centric pancreatitis (IDCP) are recognized as different clinicopathologic entities, and have recently been designated as type 1 and type 2 autoimmune pancreatitis (AIP), respectively. However, histological distinction of LPSP and IDCP is sometimes difficult even for pathologists who are familiar with AIP. $CD163^+$ macrophages are a major component of storiform fibrosis that characterizes LPSP, and therefore CD163 may be useful for the differential diagnosis.

Design: Resected specimens of LPSP (21 patients), IDCP (12), and mass-forming chronic pancreatitis, not otherwise specified (MCP; 17) were gathered. Immunostaining for CD163 and α-smooth muscle actin (ASMA) was carried out with a representative block.

Results: In 17 cases with LPSP, spindle-shaped $CD163^+$ macrophages were numerous, and formed bundle-shaped aggregates that corresponded to storiform fibrosis. Proliferation of $CD163^+$ macrophages, which was observed mainly in the lobules and peripancreatic adipose tissue, and sometimes in the pancreatic ducts, was so prominent that the borders of these structures were often obscure. ASMA, however, could highlight the borders of relatively well-preserved pancreatic lobules. In the remaining 4 cases with LPSP, $CD163^+$ cells were less numerous, and did not form bundle-shaped aggregates, suggesting a regression process of LPSP. Even so, these cells were more numerous than those in IDCP and MCP. In IDCP, $CD163^+$ macrophages were seen isolated in the fibrotic areas and occasionally in the lobules and ducts. Aggregates of $CD163^+$ macrophages were sometimes encountered, but usually consisted of more plump cells. Obliteration of the pancreatic structures by proliferating macrophages was not a feature of IDCP. The distribution of $ASMA^+$ cells in IDCP was denser compared to that in LPSP. $CD163^+$ cells were a few in cases with MCP.

Conclusions: Bundle-shaped aggregates of spindle-shaped macrophages that obscure the pancreatic structures are a characteristic and diagnostic feature of LPSP that correspond to storiform fibrosis. CD163 is useful for recognizing this pattern.

1575 Increased RFC4 Expression in Hepatocellular Carcinoma.

J Ouyang, DE Burstein, MI Fiel, SN Thung, SC Ward. The Mount Sinai Medical Center, New York, NY.

Background: Replication factor C (RFC) is a five-subunit protein complex required to coordinate leading and lagging strand DNA synthesis during S phase and DNA repair in eukaryotic cells. Genome-wide analyses and PCR studies show that RFC4 is consistently upregulated in hepatocellular carcinoma (HCC). Inhibition of RFC4 expression by siRNA correlated with decrease in HepG2 (human liver cancer cell line) proliferation, increased apoptosis and increased sensitivity to DNA-damaging chemotherapeutic agents. RFC4 may therefore be important in hepatocarcinogenesis and could serve as a novel target for cancer therapeutics. There is currently no immunohistochemical data in the literature on RFC4 protein expression in human HCC.

Design: Formalin fixed paraffin embedded tissue from 42 HCCs (12 well-, 19 moderately-, and 11 poorly-differentiated), 10 high grade dysplastic nodules (HGDN), 10 low grade dysplastic nodules (LGDN), 10 HCV related cirrhotic livers without HCC and 10 normal livers (from resection for metastasis) were stained with antibody to RFC4 (Santa Cruz Biotechnology,Inc., Santa Cruz, CA). Of the HCCs, 27 were HCV+, 9 were HBV+ and 6 were negative for both. The expression of RFC4 was graded as: 0 (negative), 1+ (weak), 2+ (moderate), or 3+ (strong) based on intensity of nuclear staining. High expression was defined as 2+, or 3+.

Results: Overall 52.4% (22/42) of HCC cases showed high expression of RFC4, compared with only 2.5% (1/39) of adjacent non-tumor liver, 0% (0/10) of normal liver, 20% (2/10) HCV-related cirrhosis, 0% (0/10) LGDN, and 10% (1/10) HGDN. High expression of RFC 4 was significantly elevated in HCC compared to adjacent non-tumor liver ($p<0.0001$), normal liver ($p<0.005$), and dysplastic nodules ($p<0.0005$). There was a trend toward higher expression of RFC4 in HCC compared to cirrhotic liver without tumor ($p = 0.06$). RFC4 high expression rate in well, moderately, and poorly differentiated HCC was 33.3%, 42.1 %, and 90.9% respectively ($p=0.007$; Cochran-Armitage trend test). We found that 48% (13/27) of HCV+ cases, 67% (6/9) of HBV+ cases and 67% (4/6) HBV/HCV negative cases showed high expression of RFC4. There was no significant difference in RFC4 expression based on etiology of liver disease ($p=0.51$).

Conclusions: We show that RFC4 expression is higher in HCC than adjacent non-tumor liver, normal liver, and dysplastic nodules. Further, increased RFC4 expression is associated with less differentiated tumors and is not specific for etiology of underlying liver disease. These data suggest that RFC4 plays a role in hepatocarcinogenesis. HCC with high RFC4 expression may benefit from novel targeted therapeutics.

1576 Hepatic Biliary Cystadenoma: A Clinico-Pathological and Immunohistochemical Study.

J Ouyang, D Cannan, SC Ward, SN Thung, MI Fiel. The Mount Sinai Medical Center, New York, NY.

Background: Biliary cystadenoma is a rare lesion. This is a retrospective study aimed at characterizing the clinical and histological features of liver cystadenomas and their mucin (MUC) profile by immunohistochemistry.

Design: The pathology database from 1995-2010 was searched and clinical data was gathered from medical records. Detailed histological assessment was performed; when available, immunostains for estrogen and progesterone receptors (ER/PR) were evaluated. Immunostaining using antibodies to MUC2, MUC6, MUC5AC were performed.

Results: In total, 22 cases of cystadenoma were found and 12 were available for review. Eleven of 12 were female, mean age 45 years (range:33-62). Six of 12 were located in the left lobe, 3/12 in the right lobe, and 3/12 in the porta hepatis. The tumors were all multilocular, ranging from 1-29 cm in size (mean 8 cm). A single layer of lining epithelium was present throughout; 7/12 were of the mixed gastric foveolar (mucinous) and pancreatobiliary type having focal intestinal metaplasia in one case, 4/12 was pure pancreatobiliary type. One case (male) was exclusively lined by gastric foveolar type epithelium. Ovarian type stroma was present in all cases. No epithelial dysplasia or carcinoma was found in any case. ER/PR expression was seen in 4 of 4 cases. The period of follow-up ranged from 2 months to 15 years; only 1 of 12 had recurrent disease, 3 years after the initial resection. The MUC immunostaining results and staining expression of other pancreatobiliary neoplasms are presented in Table 1.

Mucin profile in liver cystadenoma and adjacent bile duct

	MUC2	MUC5AC	MUC6
Intrahepatic cystadenoma	8.3%	50%	42%
Adjacent bile duct epithelium	0%	0%	58.3%
Cholangiocarcinoma*	23.5%	66.1%	14.1%
Pancreatic invasive ductal carcinoma*	0%	92%	56%
Intraductal papillary mucinous neoplasm,pancreas*	96%	92%	37%
Mucinous cystic neoplasm of pancreas*	0%	37.5-100%	few cells
Normal pancreatic ductal epithelium*	0%	0%	67%

* From medical literature

Conclusions: Liver cystadenomas are clinically and histologically similar to cystadenomas from other organs; the majority occurs in females and ovarian type stroma is typically present. Liver cystadenomas are often lined by mixed type epithelium and only infrequently with pure pancreatobiliary or gastric foveolar lining. ER/PR expression is universally expressed in the ovarian stroma. Liver cystadenomas are more common in the left lobe. Liver cystadenomas may demonstrate either a predominant MUC5AC or MUC6 expression pattern. Normal bile ducts have similar MUC expression as normal pancreatic ducts.

1577 Complement 4d Deposition in Liver Transplant Is Independent of Ischemic Injury or Biliary Disease.

RK Pai, J McMahon, L Yerian, AE Bennett, X Liu. Cleveland Clinic, OH.

Background: Complement 4d (C4d), a marker of complement activation, has been widely used in renal transplant evaluation for humoral rejection and antibody-mediated acute cellular rejection. While there have been some studies analyzing deposition of C4d in acute cellular rejection and recurrent hepatitis C, little is known about deposition of C4d in other diseases of the allograft liver. Furthermore it is unclear of C4d deposition is related to the time after transplantation. Aims: to determine 1) the overall positive rate of C4d in liver allograft biopsies, 2) the association of C4d deposition with the interval

between the biopsy and transplantation, and 3) the association of C4d deposition with ischemic injury and biliary impairment, two clinicopathologic diagnoses other than acute cellular rejection and recurrent hepatitis C commonly seen in allograft liver biopsies.
Design: All liver allograft biopsies from 01/2009 to 07/2010 were retrieved from our Pathology Database and C4d testing rates and positive rates determined. In addition, C4d positive rates were correlated with the interval between the biopsy and transplantation and ischemic injury and biliary flow impairment.
Results: 674 liver allograft biopsies were retrieved and 569 cases (84.2%) had immunofluorescence testing for C4d on frozen biopsy material. Positive C4d staining is noted in 12.4% of biopsies. C4d deposition was only observed in hepatic sinusoids with no portal vessel or stromal staining. C4d positivity is more frequently observed in biopsies with significant pathologic findings (ACR, recurrent hepatitis C, ischemic injury, and/or biliary flow impairment, n=340) than biopsies with normal histology or mild nonspecific findings (n=127; 15.18% vs 3.14%, p=0.0007). The frequency of positive C4d was independent of the interval of the biopsy and transplantation (10%, 14.3%, 11.9% for biopsies taken < 1 week, between 1 week and 1 month, and ≥1 month, respectively, p=0.85). Five out of 39 (12.8%) biopsies with ischemic injury and 6 out of 42 (14.3%) biopsies with biliary flow impairment showed C4d deposition, similar to the C4d positive rate in the entire cohort.
Conclusions: The positive rate of C4d in liver allograft biopsies by immunofluorescence is low and is independent of the interval between the biopsy and transplantation. C4d deposition is more commonly seen in biopsies with histologic abnormalities. C4d deposition is seen in ischemic injury and in biopsies with bilary tract abnormalities; however, the percentage of positive cases is not significantly different from the overall percentage with positive C4d staining.

1578 Utility of C4d Immunofluorescence in the Diagnosis of Recurrent Hepatitis C and Acute Cellular Rejection in Liver Transplantation.

RK Pai, J McMahon, L Yerian, A Bennett, X Liu. Cleveland Clinic, OH.
Background: Complement 4d (C4d), a marker of complement activation, has been widely used in renal and heart transplant evaluation for humoral and antibody-mediated acute cellular rejection. Recently, some studies have suggested that C4d may be helpful in distinguishing acute cellular rejection from recurrent hepatitis C infection in allograft liver biopsies. However, the studies were quite small and the techniques used to detect C4d varied. In addition, the location of C4d positivity varied considerably. As our protocol for liver allograft biopsies includes submitting frozen tissue for C4d direct immunofluorescence, we determined the rate of C4d positivity in patients with recurrent hepatitis C and acute cellular rejection.
Design: Liver allograft biopsies with C4d direct immunofluorescence results from 1/2009 to 7/2010 with a diagnosis of acute cellular rejection (n = 56) and recurrent hepatitis C (n = 208) were retrieved from our files. The result of C4d immunofluorescence on frozen tissue was recorded. C4d immunofluorescence was also correlated with severity of acute cellular rejection and recurrent hepatitis C.
Results: Of the 208 recurrent HCV liver biopsies, 16% demonstrated positivity for C4d. Of the 56 biopsies with acute cellular rejection, 13% were positive for C4d. These results were not statistically significant (p=0.7). C4d positivity was restricted to the hepatic sinusoids and no stromal reactivity or staining of the portal vessels was observed. There was no correlation between C4d positivity and degree of rejection or recurrent HCV activity.

Correlation of C4d positivity with severity of recurrent hepatitis C and acute cellular rejection

Recurrent HCV			Acute Cellular Rejection		
Degree of Activity	Total	C4d positive (%)	Degree of Rejection	Total	C4d positive (%)
Minimal activity	83	16 (19%)	Mild	35	4 (11%)
Mild activity	100	17 (17%)	Moderate	15	2 (13%)
Moderate to Marked activity	24	5 (21%)	Severe	1	0 (0%)
			Resolving	5	1 (20%)

Conclusions: While several small studies using immunohistochemistry have suggested that C4d may be helpful in distinguishing acute cellular rejection from recurrent hepatitis C, our study analyzes a large number of liver allograft biopsies for C4d deposition by direct immunofluorescence using frozen tissue (gold standard). Our study clearly shows that C4d has no role in distinguishing between acute cellular rejection and recurrent hepatitis C in allograft liver biopsies.

1579 Accuracy of MR Imaging and Liver Biopsy in Hepatocellular Adenomas Subtyping.

V Paradis, M Ronot, S Bahrami, O Farges, J Belghiti, P Bedossa, V Vilgrain. Beaujon Hospital, Clichy, France; APHP, Paris, France.
Background: Hepatocellular adenomas (HCAs) are divided into 4 genotype/phenotype subtypes associated with different evolutive profiles, especially regarding malignant transformation. Therefore, recognition of subtype is of clinical importance in patient management. The **purpose of our study** was to assess the diagnostic performance of Magnetic resonance imaging (MRI) and liver biopsy, with a special focus on the input of the immunohistochemical analysis, in a consecutive series of resected HCAs.
Design: 47 HCAs with preoperative MRI and biopsy were retrospectively included. MRI data were reviewed independently by two abdominal radiologists blind to the pathological results and classification. Subtyping of HCAs on liver biopsy was made blindly to clinical, biological, imaging data and to final classification which was obtained on the surgical specimen. Histologic subtyping was based on morphological criteria and immunohistochemistry using the 4 antibodies panel (LFABP, SAA, βcatenin and glutamin synthetase) was systematically performed when enough tissue was available (n=38).
Results: On surgical specimens, HCAs were subtyped into telangiectatic/inflammatory in 34 (72%) cases, steatotic LFABP negative in 11 (23%) cases, and 2 (4%) were unclassified (LFABP positive, SAA negative, β-catenin inactivated).Radiologists correctly classified HCAs in 85%. Interobserver Kappa correlation coefficient was .86. Routine histologic analysis led to 76.6% of correct classification and 81.6% when immunophenotypical characteristics were taken into account. Agreement between MRI findings and routine histologic analysis was observed in 74.5% leading to a likelihhod ratio of subtyping higher than 20.
Conclusions: MRI and biopsy analysis are two efficient methods in subtyping HCAs and their association increases the diagnosis confidence. Interobserver variability in MRI criteria is very low. Additional value of immunophenotypical markers is best in HCAs containing steatosis.

1580 Ki-67 Proliferation Index in Pancreatic Endocrine Tumors: Comparison with Mitotic Count, Interobserver Variability, and Impact on Grading.

TA Rege, EE King, JA Barletta, AM Bellizzi. Brigham and Women's Hospital, Boston, MA.
Background: The biologic potential of pancreatic endocrine tumors (PETs) is notoriously difficult to predict. Several grading schemes exist, including those proposed by the World Health Organization (WHO) and European Neuroendocrine Tumor Society (ENETS). Mitotic count (MIT) and Ki-67 proliferation index (PI), among the best studied prognostic features, are essential components of these classifications. Despite this, many laboratories do not routinely perform Ki-67 immunohistochemistry (IHC), and if done, quantification methods vary. Ideal PI cutpoints are debated. Much remains to be learned about the relationship between MIT and PI, reproducibility of PI assessments, and impact of PI on grading.
Design: PETs were retrieved and the following recorded: age, sex, tumor size, metastases. One pathologist performed a mitotic count (MIT). Ki-67 IHC was performed on a representative block, and 3 study pathologists each quantified the PI by 2 separate methods: gestalt estimate and computer-assisted formal quantification (QUANT) based on counting ≥ 200 tumor cells. PI was assessed in areas of highest labeling. Correlation coefficients and kappa statistics were calculated; $p<0.05$ was considered significant.
Results: 55 PETs were evaluated (26M, 29F; mean age 58.1 [range 26-88]; mean size 4 cm [range 0.5-18 cm]; metastasis 16). MIT significantly correlated with gestalt PI and QUANT: r^2 0.7677, 0.7774 ($p<0.05$). The gestalt PI and QUANT were nearly perfectly correlated: r^2 0.9911. The gestalt under- and overestimated QUANT in 37 and 15 cases. Kappas for various 2 and 3-tiered Ki-67 cutpoints and a case-by-case comparison of MIT vs QUANT are presented below.

Kappas for Various Ki-67 Thresholds

	Kappa	
Category	Gestalt	Formal
≤2% vs >2%	0.7789	0.7329
≤5% vs >5%	0.7348	0.8073
≤2% vs >2-20% vs >20%	0.7404	0.6641
≤5% vs >5-20% vs >20%	0.6435	0.6990

Comparison of Mitotic Count to Ki-67 Index by ENETS Grade

	Ki-67 Index		
Mitotic Figures per 10 HPF	G1 ≤2%	G2 >2-20%	G3 >20%
G1 (<2)	25	16	0
G2 (2-20)	0	9	4
G3 (>20)	0	0	1

values refer to number of cases (n=55)

Conclusions: MIT and PI correlate in PET. PI assessment by either gestalt or QUANT is reproducible with kappas indicating substantial agreement, although gestalt may tend to underestimate it. Performing Ki-67 IHC results in the reclassification of a significant number of tumors (20/55, 36.3%), suggesting an important role for Ki-67 in accurate grading.

1581 Effects of mTOR Inhibitors on the Biliary Cystogenesis of the Polycystic Kidney Rat, an Animal Model of Caroli's Disease.

XS Ren, Y Sato, K Harada, M Sasaki, Y Nakanuma. Kanazawa University Graduate School of Medicine, Japan.
Background: The polycystic kidney (PCK) rat is an animal model of Caroli's disease as well as autosomal recessive polycystic kidney disease (ARPKD). The activation of the AKT-mTOR signaling pathway has been well documented in the patients with autosomal dominant PKD (ADPKD), and the mTOR inhibitors, sirolimus(SL) and everolimus(EL), have been indicated as potential therapeutic agents. However, the involvement of the AKT-mTOR signaling pathway in the biliary dysgenesis of Caroli's disease has not been fully clarified.
Design: In vivo, immunostaining of p-AKT and p-mTOR was performed using liver sections of the PCK and control (SD) rats. In vitro, biliary epithelial cells (BECs) of the PCK and SD rats were treated with the mTOR inhibitors (SL, EL and PP242). The mTOR have two complexes TORC1 and TORC2, and the both complexes are known to act independently in association with AKT. SL and EL are inhibitors of TORC1, while PP242 is a dual inhibitor of TORC1 and 2. The cell proliferative activity was measured using the WST-1 assay. Phospholyration of AKT, mTOR and P70S6K was examined using Western blotting. The effects of the inhibitors on the biliary cyst formation were determined using the 3-D cell culture system. Apoptosis and autophagy of the BECs were evaluated using the ssDNA ELISA kit and the Western blotting of cleaved caspase 3 for apoptosis, and the Western blotting of the light chain 3B for autophagy.
Results: Both in vivo and in vitro, the phosphorylation of AKT and mTOR of the cholangiocytes was increased in the PCK rat compared to those of the SD rat. In vitro, treatment with mTOR inhibitors induced significant reduction in the cell proliferative activity of the BECs of the PCK rat. Western blot analysis showed that the phosphorylation of AKT, mTOR and P70S6K was inhibited following the

treatment. Notably, PP242, but not SL and EL, showed significant inhibitory effects on the biliary cyst formation of the PCK rat in the 3-D cell culture system. PP242 induced both apoptotic and autophagic cell death in the BECs, while EL induced only apoptotic cell death.

Conclusions: A recent study showed that in vivo administration of SL, failed to improve the biliary cystogenesis of the PCK rat (Reken C et al. Nephrol Dial Transplant 2010). Our data suggest that the dual inhibition of TORC1 and TORC2 may be required for the inhibition of the biliary cystogenesis of the PCK rat, and PP242 may be an effective therapeutic agent.

1582 Rokitansky Aschoff Sinus Involvement in Early Gallbladder Carcinoma (EGBC) as a Prognostic Factor: A Concurrent Cohort Study of 190 EGBC.

JCS Roa, OE Tapia, CD Manterola, MH Villaseca, P Guzman, JCO Araya, N Adsay. Universidad de La Frontera, Temuco, Chile; Emory University, Atlanta, GA.

Background: Studies from high-incidence regions including Chile have shown that early gallbladder cancers (EGBC), i.e., carcinomas confined to the muscularis, including frank CIS, intramucosal adenocarcinoma (IMA) and those that expand/replace the mucosa to abut and push into the muscularis (MP) have a very good prognosis with 10-year survival approaching 90%. Factors associated with recurrence and metastases in this group have yet to be determined.

Design: 190 EGBCs (identified in a database of 953 GBCs), which have been processed with a uniform approach (sampled entirely, and mapped according to a previously established protocol) were analyzed.

Results: F/M=157/33. Mean age=58 (vs 65 in advanced GBC, confirming the continuum). Most were inapparent clinically, and some also macroscopically (60%). In a median follow up of 144 months, the actuarial survival was 92 % at 5-year and 90% at 10-year. There was no significant survival difference between non-complex IMA (n=78) vs complex IMA (n=31) vs MP cases (n=81; p=0.4). The prognosis of well differentiated/gland-forming EGBCs (n=128) was better than that of the moderate and poorly differentiated (n=62; p=0.026). The extent of carcinoma [diffuse (>75% of the entire GB mucosa; n=72) vs substantial (25-75%; n=101) vs focal (<25%; n=17)] was not significant (p=0.3). Extension to RAS was identified in 34 cases; rare (<3 RAS foci) in 5 and substantial (>3 RAS foci) in 29, and was deep extending to the level of muscle in 19 and level of subserosa in 15. The presence of RAS involvement had significant correlation with adverse outcome ($p=9{,}7X10^{-8}$) with an odds-ratio of 7.3 (CI 95% 3-17). The disease related mortality in these RAS+ cases occurred late (median, 48 mos), and thus was not attributable to missed foci of invasion. When the RAS+ cases were eliminated from the survival analysis, the survival at 10-year increased from 92% to 100% for IMA and 88% to 93% for MP.

Conclusions: EGBC exhibits variable histologic patterns, grade and extent. While EGBC has a very good overall prognosis, with a 10-year survival of 90%, those patients with RAS involvement are much more likely to die of disease, highlighting the importance of thorough examination of these cases and the proper documentation of this finding. We propose that in patients with EGBC and RAS involvement, additional radical surgery, or at minimum, close long-term surveillance is warranted.

Financed by DIUFRO and Fondecyt Grant 1090171.

1583 The Spectrum of Hematologic Malignancies Involving the Pancreas: Potential Clinical Mimics of Adenocarcinoma.

JB Rock, TS Chang, G Lozanski, MP Bloomston, WL Frankel. The Ohio State University Medical Center, Columbus.

Background: Hematologic malignancies (HM) often involve the pancreas including up to 1/3 of lymphoma patients. HM may present as a solitary mass and as the initial manifestation of disease, leading to diagnostic pitfalls. Histologic distinction between HM and pancreatic adenocarcinoma (PAC) is usually straightforward, but resections may occur based on clinical suspicion without tissue diagnosis. We reviewed HM involving the pancreas to describe the spectrum of disease and determine features useful in distinction from PAC.

Design: Archived material (1965 to present) was retrieved for HM involving the pancreas, and clinical, pathologic and radiologic data was reviewed. Data from 157 PAC was evaluated for comparison. Student's t-test and Fisher's exact test were used for comparisons.

Results: 42 HM of the pancreas included 29 High Grade B-Cell Lymphomas (HGBCL; Diffuse Large B-Cell and Grade 3 Follicular), 6 Low Grade B-Cell Lymphomas (LGBCL; Small Lymphocytic, Grade 1-2 Follicular, Marginal Zone), 2 Myeloid Sarcomas, 2 EBV-related Post-Transplant B-Cell Lymphomas, and one each of Plasma Cell Myeloma, Chronic Myelomonocytic Leukemia, and Nodular Sclerosing Hodgkin Lymphoma (Other).

Hematologic Malignancies in the Pancreas

	M:F Ratio	Mean Age (yrs)	Mean Size (cm)	Localized to Pancreas	HM History	HM Suspected	# Resected
HGBCL (n=29)	0.8:1	58	6.5	7	5	16	7
LGBCL (n=6)	2:1	58	3.9	1	3	5	3
Myeloid Sarcoma (n=2)	2:0	70	0.9	1	2	1	1
Transplant (n=2)	2:0	40	12.3	1	0	2	2
Other (n=3)	2:1	62	3.1	1	2	3	0

HM was diagnosed by FNA in 4 cases, biopsy in 27 and resection in 11. Clinical/radiologic data led to suspicion of HM in 27 patients (64%). Of 15 with no suspicion for HM or tissue diagnosis, 4 had resection for presumed PAC. Remaining resections were clinically indicated even with suspicion or diagnosis of HM. Diagnoses were confirmed in all with preoperative diagnosis. Patients with HM were significantly younger with larger tumors and lower CA 19-9 than those with PAC.

Hematologic Malignancies of Pancreas vs. Adenocarcinoma

	M:F Ratio	Age (yrs)	Size (cm)	CA 19-9 (U/mL)
HM	1.2:1	58 ± 15*	7.3 ± 3.8**	118 ± 158**
PAC	1.3:1	65 ± 11*	3.9 ± 1.6**	1162 ± 3426**

*p<0.05; **p<0.001

Conclusions: A variety of HM involve the pancreas, most commonly HGBCL. Surprisingly, 11/42 cases were localized to the pancreas and 15/42 were not suspected prior to tissue diagnosis, resulting in 4 resections for presumed PAC. Age, tumor size and CA 19-9 may be useful in distinguishing PAC from HM or may suggest the need for tissue or FNA diagnosis.

1584 Patterns and Significance of Eosinophils in Gallbladder Injury: An Analysis of 1050 Cholecystectomies.

B Saka, N Dursun, O Basturk, JC Roa, O Tapia, S Bandyopadhyay, L Ducato, P Bagci, N Adsay. Emory, GA; MSKCC, NY; UFRO, Temuco, Chile; WSU, MI.

Background: There is minimal data in the literature regarding the role of eosinophils (EOS) in gallbladder (GB) injury. The term "eosinophilic cholecystitis" has been used variably with the reported incidence ranging from 0.5-6.4 %.

Design: 1050 GB resections composed of 895 chronic cholecystitis (CC), 100 subacute cholecystitis (SC) and 55 acute cholecystitis (AC) were reviewed, and > 40 EOS/HPF was regarded as eosinophilia. Those with numerous foci of eosinophilia in the background of diffuse but lesser amount of EOS were classified as **CC with prominent eosinophilia**, and those that had diffuse and massive eosinophilia throughout the GB, as **eosinophilic CC**.

Results: I. Eosinophilia was significantly more common in SC (63%) than in AC (35%) and in CC (6%; p=0.000). **II.** In SC, EOS were concentrated in the areas of denuded epithelium, where stones were dislodged, and where the signs of subacute disease such as tissue culture fibroblasts were more prominent. Similarly, in AC, they were mostly in the areas of ulceration. **III.** Among CC cases, 6 qualified as **CC with prominent eosinophilia**, and these were relatively young (mean age=45 vs 49 in ordinary cholecystitis) females (F/M=5 vs 3.1), 4/6 with history of allergies (including one with asthma) and with relatively uninjured gallbladders with a wall thickness of 3.4 mm (vs 5.2 mm). All were associated with stones. **IV.** Four cases had massive EOS, classified as **eosinophilic CC**, and these were even younger patients (mean age=41 vs 49 in ordinary cholecystitis); all females; 2/4 with history of allergies, and one with ulcerative colitis. None of the CC with prominent eosinophilia or eosinophilic CC cases had blood eosinophilia, gastroenteritis, history of parasites, or eosinophilia-myalgia syndrome.

Conclusions: There are 2 distinct mechanisms with which eosinophils participate in GB injury. One, in the setting of acute and subacute disease associated with breached epithelial integrity leading to exposure of GB wall to the chemical effects of the bile and chemotaxis of eosinophils. Second, in the setting of chronic cholecystitis with relatively uninjured gallbladders, and occurs in younger females with associated allergic conditions. True eosinophilic cholecystitis (with diffuse and massive eosinophilia) is a very uncommon condition (0.4% of cholecystectomies) that may have allergic basis.

1585 Steatohepatitic Hepatocellular Carcinoma: A Novel Histologic Variant Associated with Steatohepatitis and Metabolic Syndrome.

M Salomao, A Siegel, JH Lefkowitch, RK Moreira. Columbia University Medical Center, New York, NY.

Background: We recently described a histologic subtype of hepatocellular carcinoma (HCC) termed "steatohepatitic HCC" (SH-HCC) with features resembling steatohepatitis (SH) in the non-neoplastic liver, including steatosis, hepatocyte ballooning, Mallory bodies, inflammation, and trabecular/pericellular fibrosis. Our initial SH-HCC cases were described in hepatitis C-related cirrhosis. The present study was undertaken to comprehensively assess the overall prevalence of SH-HCC among resected HCCs as well as possible associations with underlying SH and clinical features of metabolic syndrome (MS).

Design: We examined all HCCs diagnosed on partial hepatectomy or liver explant specimens obtained at our institution during a recent 3.5-year period, with special attention to the presence of "steatohepatitis-like" features within neoplastic tissue. A total of 119 viable HCC cases were reviewed. The underlying liver diseases included alcoholic and non-alcoholic cirrhosis, viral hepatitis and others. Tumors were classified as SH-HCC if all features of steatohepatitis were present in >50% of the tumor; otherwise, the tumor was classified as "typical" HCC. Clinical information regarding diagnostic criteria for MS (increased body mass index, hypertriglyceridemia, low HDL cholesterol, hypertension, and diabetes) was retrieved from medical records.

Results: SH-HCC was identified in a total of 16 of 119 cases (13.4%). Underlying SH (alcoholic or non-alcoholic) was found in 93.7% (15/16) of SH-HCC cases, compared to 27.5% (22/80) of typical HCC cases (P<0.0001). The SH-HCC group had a significantly higher MS score (2.44 vs 1.46; P=0.008) and a higher % of patients with ≥ 3 MS components (50% vs 21.2%; P=0.03). Steatosis was present in the non-neoplastic liver of 81.2% of SH-HCC cases compared to 38.7% of typical HCCs (P=0.004), while SH was present in 68.7% and 10% of cases, respectively (P=0.0001). Immunohistochemically, there was diffuse loss of cytoplasmic CK8/18 and increased numbers of activated hepatic stellate cells within SH-HCC, in a pattern identical to that seen in steatohepatitis in non-neoplastic liver.

Conclusions: HCCs with the "steatohepatitic" histologic phenotype (SH-HCC) are strongly associated with underlying SH and MS. This association further suggests a possible direct role of SH/MS in human hepatocarcinogenesis. The impact of such a concept is considerable in light of the current global epidemic of obesity and fatty liver disease.

1586 Use of S100P, IMP3 and pVHL Immunopanel To Aid in the Interpretation of Bile Duct Biopsies with Atypical Histology or Suspicious for Malignancy.

MT Schmidt, F Chung, F Lin, H Xu, HL Wang. Cedars-Sinai Medical Center, Los Angeles, CA; Geisinger Medical Center, Danville, PA; University of Rochester, NY.

Background: Histological evaluation of small bile duct biopsies is a known challenge. Our prior studies have shown that S100P, the insulin-like growth factor 2 mRNA binding protein 3 (IMP3) and the von Hippel-Lindau gene product (pVHL) are a useful immunopanel for the distinction between adenocarcinoma and benign biliary epithelium (Levy et al. Hum Pathol 41:1210-9, 2010). The current study aimed to determine if this panel could be useful in making a more confident diagnosis for challenging bile duct biopsies with atypical histology or suspicious for malignancy.

Design: A total of 14 histologically challenging bile duct biopsies were immunohistochemically stained for S100P, IMP3 and pVHL. Nuclear staining for S100P, cytoplasmic staining for IMP3 and membranous staining for pVHL were considered positive. The staining intensity for pVHL was also evaluated to determine if it was reduced in the cells of interest in comparison with histologically unremarkable biliary epithelium present in the same biopsies. Clinical, surgical, radiologic and pathologic follow up data were obtained for all 14 cases.

Results: Follow up data showed 9 cases to be adenocarcinomas and 5 cases to be benign. In the malignant group, the following staining patterns in atypical or suspicious cells in the initial bile duct biopsies were observed: S100P-positive/IMP3-positive/pVHL-negative or reduced (n=5), S100P-positive/IMP3-negative/pVHL-negative or reduced (n=3), and S100P-positive/IMP3-positive/pVHL-positive (n=1). In the benign group, 2 biopsies showed a S100P-positive/IMP3-negative/pVHL-positive pattern. In the remaining 3 biopsies that showed a S100P-positive/IMP3-positive/pVHL-negative or reduced pattern, the atypical cells were histologically dysplastic.

Conclusions: Bile duct adenocarcinoma frequently shows positive IMP3 staining and negative or reduced pVHL staining. This staining pattern can also be seen in dysplastic epithelium in the absence of invasive carcinoma. When IMP3 is negative, positive S100P with reciprocal loss or reduction of pVHL staining is also indicative of malignancy. On the contrary, benign biliary epithelium typically lacks IMP3 staining and retains normal pVHL expression. These results indicate that an immunopanel consisting of S100P, IMP3 and pVHL can be helpful in aiding in the interpretation of bile duct biopsies with atypical histology or suspicious for malignancy.

1587 Identification of eIF3f as a New Tumor Suppressor in Pancreatic Cancer.

J Shi, F Wen, R Zhou, A Bhattacharyya. University of Arizona, Tucson; Fifth People's Hospital of Shanghai, Shanghai, China.

Background: Misregulated mRNA translation is one of the most important factors in cancer development and progression in humans. Prominent nucleoli have been recognized to be one of the key features of many malignant cells in pathology for decades, which implicates increased ribosome generation and translation. However translational control mechanisms in cancer development are poorly understood. Previously, we identified the translation initiation factor eIF3f as a protein involved in apoptotic signaling. We were the first to report a decreased expression of eIF3f in more than 90% of the pancreatic cancer cases. Restoration of eIF3f expression in cancer cells led to ribosomal RNA degradation, decreased translation and increased apoptosis.

Design: In the present study, we stably silenced eIF3f expression in the immortalized normal human pancreatic ductal epithelial (HPDE) cells using lentiviral RNAi to assess whether the benign epithelial cells can be transformed to malignant cells. We have also established an in vitro 3D-cell culture model to better mimic the in vivo growth environment and tissue architecture.

Results: The eIF3f-silenced HPDE cells showed increased cell size, nuclear pleomorphism, aneuploidy, mesenchymal morphology, proliferation, clonogenicity, apoptotic and chemotherapy drug resistance, and migration compared to the control HPDE cells. We also demonstrated by 3D-culture that eIF3f-silenced HPDE cells formed masses that recapitulate malignant tumors (loss of normal epithelial cell orientation and architecture, disruption of the intact basement membrane shown by laminin V staining). On the contrary, the control HPDE cells developed into a single layer epithelial hollow spheres resembling normal pancreatic ductal structure.

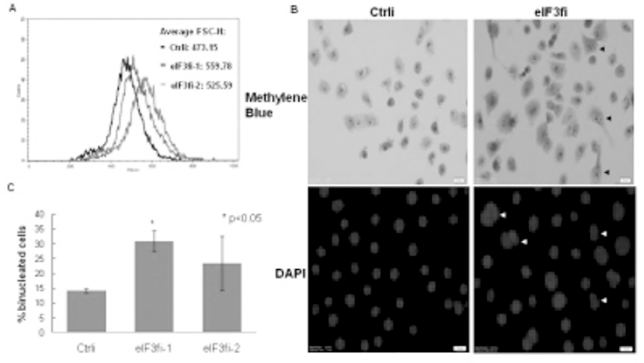

Fig. 1. eIF3f-silenced HPDE cells have an increased cell size, nuclear pleomorphism and binucleated cells (arrow head). (**A**) Cell sizes of 2 different eIF3f-silenced and a control RNAi HPDE cell line were measured by flow cytometry. (**B**) eIF3f-silenced and control HPDE cells are stained with methylene blue or DAPI. Representative images are shown. (**C**) Binucleated cells are counted in 2 different eIF3f-silenced clones and a control HPDE cell line.

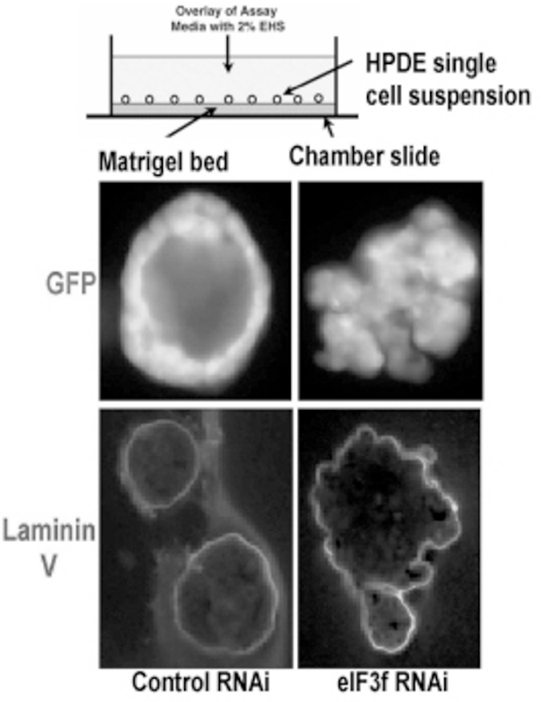

Fig 2. Stable knock down of eIF3f induced malignant features in HPDE cells. Control and eIF3f RNAi HPDE cells were stably transduced with a GFP lentivirus and positive cells were sorted. These cells were used in a 3D-culture on matrigel and labeled with laminin V antibody tagged with Texas Red.

Conclusions: Decreased eIF3f expression in pancreatic ductal epithelial cells led to malignant transformation. These data support our hypothesis that eIF3f is a tumor suppressor in pancreatic ductal adenocarcinoma.

1588 Reticulin Loss in Benign Fatty Liver: An Important Diagnostic Pitfall When Considering a Diagnosis of Hepatocellular Carcinoma.

AD Singhi, D Jain, S Kakar, T-T Wu, MM Yeh, M Torbenson. Johns Hopkins, Baltimore, MD; Yale, New Haven, CT; UCSF, San Francisco, CA; Mayo, Rochester, MN; U. of Wash., Seattle.

Background: Reticulin stains are commonly used when diagnosing hepatocellular carcinomas (HCC) and typically demonstrate diminished or loss of reticulin fibers. Reticulin is particularly helpful on small biopsies and difficult cases. However, an under-recognized diagnostic pitfall is that non-neoplastic liver tissues can show decreased staining in areas of fatty change. To better clarify the histological correlates of this diagnostic pitfall, we evaluated the extent of reticulin loss in a variety of non-cancerous settings.

Design: 96 cases with varying grades of macrovesicular steatosis (mild, 5-33%; moderate, 34-66%; and marked, >66%) were collected from 5 academic centers: 49 cases had steatosis alone, 35 cases with NASH and 12 hepatic adenomas with fatty change. The following were evaluated: steatosis grade, inflammation, ballooning, and fibrosis. The number of foci with diminished reticulin staining in 10 high power fields (hpf) was calculated. A focus was scored positive when the extent of reticulin loss was similar to that seen in HCC.

Results: Diminished reticulin staining was observed in steatosis, NASH, and fatty adenomas. In hepatic steatosis without NASH, the extent of reticulin loss was associated with the grade of steatosis. For mild steatosis, reticulin loss was rare with the number of foci of reticulin loss per 10 hpf averaging 0.8 (range 0-3), but increased for moderate steatosis, mean 3.0 (range 0-5), and most prominent with marked steatosis, mean 5.8 (range 5-8). The same overall pattern was more evident in cases of NASH: mild steatosis had an average of 1 hpf, moderate 2.9, and marked steatosis 5.8. Overall, reticulin loss was not associated with inflammation, balloon cell change and fibrosis stage. In hepatic adenomas, decreased reticulin staining paralleled the amount of steatosis with marked steatosis showing the highest with an average of 6.0 hpf. Reticulin loss in hepatic adenomas was seen only in areas of fatty change and normal reticulin patterns were retained in the non-fatty areas.

Conclusions: Reticulin loss that focally reaches the levels seen in HCC can be seen in benign liver tissues with fatty change. Overall, reduction of reticulin is more common and more extensive with marked fatty change and does not appear to be linked to inflammation or fibrosis. Increased awareness of this important diagnostic pitfall will help prevent over-calling reticulin loss when evaluating specimens with fatty change.

1589 Diagnostic Utility of CD10 in Benign and Malignant Bile Duct Lesions.

M Tretiakova, M Westerhoff, T Antic, J Mueller, E Himmelfarb, H Wang, S-Y Xiao. University of Chicago, IL; Cedars-Sinai Medical Center, Los Angeles.

Background: CD10, a cell surface enzyme with neutral metalloendopeptidase activity, is widely accepted as a useful brush border marker of the small intestine. In a few reports it was also shown that CD10 is present in normal bile duct and gallbladder epithelium. However, the expression profile of CD10 in benign and malignant bile duct epithelial lesions has not been studied.

Design: A total of 16 biopsies, 9 resections and 7 cell blocks prepared from fine needle aspiration biopsies from 32 patients were included in our study. The majority of cases contained normal intact biliary epithelium (27/32, 84%), and multiple lesions of both benign and malignant nature in various combinations. Benign lesions included reactive atypia (n=8), low-grade dysplasia of unknown significance (n=9), and adenoma (n=1). Malignant lesions included high grade dysplasia (n=20) and adenocarcinoma (n=15) (see table). All specimens were examined by immunohistochemistry for CD10 (Novocastra Labs, dilution 1:20).

Results: Normal biliary epithelium was strongly positive in all cases with characteristic continuous staining of the brush border. Benign lesions were also CD10 positive in all cases except for one, but the staining pattern was discontinuous with positive cells varying from 20 to 60%. None of malignant lesions showed reactivity with CD10 except for one case of high grade dysplasia with focal staining (see table). Pearson chi square statistical analysis showed significant difference in CD10 expression between all study groups ($p<0.001$). Importantly, presence of inflammatory cells did not obscure interpretation and served as an internal positive control.

CD10 positivity in 53 benign and malignant biliary lesions

Localization	Benign (n=18)	Malignant (n=35)
Intrahepatic bile ducts	1/1	0/4
Extrahepatic bile ducts	15/16	1/29
Gallbladder	1/1	0/2
Total	17/18 (94%)	1/35 (3%)

Conclusions: The histopathologic distinction between benign and malignant bile duct epithelial lesions on biopsies and cytology specimens can be extremely challenging because of limited material, crush artifact, and frequent inflammatory/reactive changes. In our study, continuous strong CD10 reactivity of normal epithelium was contrasted by discontinuous CD10 expression in benign lesions and absence of CD10 in malignant lesions. This lack of CD10 expression is associated with microvilli loss during malignant transformation of biliary epithelial cells; hence, CD10 can serve as a useful marker to aid in the evaluation of bile duct biopsies.

1590 Interaction of *p53* Mutation and *B-Catenin* Mutation with CK19 Expression on Early Tumor Recurrence and Prognosis of Hepatocellular Carcinoma.

J-H Tsai, Y-M Jeng, R-H Hu, P-H Lee, H-C Hsu. National Taiwan University Hospital, Taipei, Taiwan; National Taiwan University, Taipei, Taiwan; College of Medicine, National Taiwan University, Taipei, Taiwan.

Background: Cytokeratin 19 (CK19), a molecular marker of hepatic progenitor cells and cholangiocytes, is not expressed in normal hepatocytes but expressed in hepatocellular carcinomas (HCC). However, its role in HCC progression, especially when interacted with *p53* and β-*catenin* mutations, remained largely unknown.

Design: From January 1983 to December 1997, 210 surgically resected, unifocal, primary HCCs were studied retrospectively. CK19 protein expression was detected by immunohistochemistry while mutations of *p53* and β-*catenin* genes were detected by direct sequencing.

Results: CK19 protein expression was detected in 35.7% (75/210), *p53* mutation in 47.2% (83/176) and β-*catenin* mutation in 14.5% (27/186). The tumor size ($p=0.0023$), grade ($p=0.00093$), tumor stage ($p<1x10^{-7}$), high α-fetoprotein (AFP) ($p=0.0004$), *p53* mutation ($p=0.024$), absence of β-*catenin* mutation ($p=0.0013$), and CK19 expression ($p=3x10^{-5}$) were markers predictive of early tumor recurrence (ETR). The CK19 expression, stage and ETR were strong indicators of poor prognosis (all $p<0.0001$). Importantly, combination analysis showed an additive unfavorable prognostic interaction of CK19 expression and *p53* mutation. On the contrary, concurrent CK19 expression and β-*catenin* mutation was rare and CK19 expression abolished the suppression effect of β-*catenin* mutation on HCC progression.

Conclusions: CK19 expression is associated with more aggressive HCC. CK19 cooperates with *p53* mutation toward advanced disease. In contrast, CK19 expression and β-*catenin* mutation appear to be mutually excluded, and they play dramatic opposite roles in vascular invasion, ETR and prognosis of HCC.

1591 Immunoprofile of Pediatric Liver Tumors.

K Van Patten, M Robert, D Jain, K Mitchell. Yale University, New Haven.

Background: Liver tumors are rare in children and include hepatoblastomas (HB), hepatocellular carcinoma (HCC) and focal nodular hyperplasia (FNH). Little published data exists on immunohistochemical profiles of these tumors in children. We examined the expression of a panel of markers that have been shown to be useful in evaluating liver tumors in adults.

Design: We identified available tissue from 4 needle biopsies and 13 resections of liver masses in children (< 18 years) between 1985 and 2010 at our institution. These were stained with reticulin, CD34, AFP, pCEA, HepPar, GP3, HSP70 and Arg-1. The staining pattern of each marker was recorded as negative (no staining), patchy (<30% of tumor cells), moderate (30-60%) and diffuse (>60%), while intensity was scored as weak, moderate or strong, (Arg-1 and GPC3). AFP and HSP-70 were scored by absolute percent positive cells.

Results: Sixteen cases, 10 males and 6 females, (HB=7, HCC=6, FLC =2, FNH=3) from patients of age range 4 months to 16 years were examined. Of the carcinomas, 2 were of fibrolamellar type (FHCC) with the typical large tumor cells with cytoplasmic pale bodies within abundant fibrous stroma. Of the HBs 4 were epithelial and 3 epithelial/mesenchymal. The results are shown in Table 1.

Staining profile of pediatric liver tumors

Lesion	Cd34	LR	%AFP	Hep	Arg	%HSP	GP3
CHCC	P	I	60	D	D/S	10	M/M
CHCC	P	I	40	D	D/S	0	P/M
CHCC	P	I	1	D	D/M	10	D/M
CHCC	D	M	1	P	D/S	2	D/S
FHCC	D	I	0	M	D/W	0	N
FHCC	D	I	0	D	D/W	0	N
HB	D	P	80	M	D/M	0	D/S
HB	M	D	50	M	D/S	1	D/S
HB	M	I	0	N	P/M	0	P/M
HB	D	I	10	M	M/S	70	D/S
HB	D	D	60	P	M/S	30	D/S
HB	D	D	20	M	M/S	0	D/S
HB	M	D	70	P	M/S	0	D/S
FNH	M	I	0	D	D/S	0	N
FNH	M	I	0	D	D/S	0	N
FNH	M	I	0	D	D/S	80*	N

N-negative, LR- lost reticulin, P-patchy, M-moderate, D-diffuse, S-strong, W-weak, *- nuclear only

Arg was a sensitive marker of hepatocytes, benign and malignant. Hepar was also a sensitive marker with less consistent staining in HB. PCEA is a poor marker of liver lineage in HB (positive in 1/7).

Conclusions: GPC3 distinquished benign from malignant hepatic lesions in this population of pediatric tumors. In contrast to adults, in pediatric HCC, CD34 and reticulin stains were not useful in this distinction. These findings provide further evidence of the utility of GPC3 staining in the diagnosis of hepatocellular tumors and is the first study to explore the use of this antibody in pediatric populations and also show the potential utility of HSP. This data also supports the distinct difference in immunoprofile between CHCC and FHCC.

1592 Hepatocellular Carcinoma in Tyrosinemia Related Cirrhosis.

K Van Patten, K Mitchell. Yale University, New Haven.

Background: Hereditary tyrosinemia type I is a rare autosomal recessive disorder resulting in the accumulation of toxic tyrosine metabolites in the liver and kidneys with progressive organ damage. Tyrosinemia has a documented rate of neoplastic transformation that is significantly greater than that of other liver diseases with cirrhosis, both in the adult and pediatric population. Classification of liver nodules is difficult from both a radiologic and pathologic perspective. The goal of our study was to evaluate the imunohistochemical profile of nodules in the setting of tyrosinemia-related cirrhosis for features of dysplastic nodules and hepatocellular carcinoma (HCC).

Design: Three patients who underwent orthotopic liver transplant in 2010 for tyrosinemia were identified from the pathology database. The demographic data, gross photographs and microscopic slides were reviewed. Reticulin, CD34, polyclonal CEA, AFP, heat-shock protein-70 (HSP-70, Abcam) and glypican-3 (Cell Marque) were performed on dominant nodules. Two pathologists reviewed the morphology of each case and scored each stain. Greater than 10% staining was considered positive.

Results: All livers had mixed micronodular/macronodular cirrhosis, with one predominantly macronodular. Case 1 was a 1 year old boy who had a 2.8 cm dominant nodule with marked steatosis, focal pseudoacinar formation and small and large cell changes. This nodule was AFP and HSP-70 positive with rare positivity observed in nodules without obvious atypia. Case 2 was a 2 year old boy who had three dominant nodules, up to 1.9. Within these nodules, there were areas of small cell change, nuclear atypia and pleomorphism and steatosis as well as subcentimeter nodules with similar changes. HSP-70 was positive only in atypical nodules. Case 3 was a 5 month old boy with three dominant nodules, up to 1.4 cm in diameter with moderate pleomorphism. AFP was positive in these atypical nodules. All 3 cases showed intact reticulin network with patchy peripheral CD34 staining, while GPC3 was positive in atypical nodules in all three. GPC3 was also positive in numerous nodules in cases 2 and 3.

Conclusions: Nodules in tyrosinemia show a spectrum of changes ranging from bland cirrhosis to well defined HCC. We have demonstrated that AFP, GPC3 and HSP are helpful in identifying foci of HCC within the liver and in dysplastic nodules, while CD34 and reticulin are not. The staining of these reported markers of neoplasia in nodules without significant atypia supports that the rate of neoplastic progression may be accelerated in tyrosinemia even in early stages of cirrhosis.

1593 Non-Neoplastic Polyps of the Gallbladder: Incidence, Histologic Types, and Clinicopathologic Associations in an Analysis of 162 Cases.

CE Vance, JC Roa, N Dursun, O Tapia, L Ducato, B Saka, K-T Jang, H Losada, J Sarmiento, S Bandyopadhyay, N Adsay. Emory, GA; UFRO, Temuco, Chile; WSU, MI.

Background: The data on the pathologic characteristics and clinicopathologic associations of *non-neoplastic* GB polyps (NNP) is highly limited.

Design: Cases that had been designated as "polyp" in the authors' files were retrieved. Additionally, 2206 consecutive cholecystectomies were systematically analyzed.

Results: 162 NNPs were identified with an incidence of 2.2% (46 in 2206 systematically reviewed GBs). Only 10 (6%) were ≥1.0 cm (the cut-off used widely as cholecystectomy indication). In comparison, identified in the same review were 92 intracholecystic papillary tubular neoplasms (ICPN) and 29 polypoid invasive carcinomas ≥1.0 cm. The average age of NNPs was 52 (vs 64 for ICPN and 47 for cholecystitis); F/M=2.6.

Histopathologic types: *I.* Fibromyoglandular polyp(n=90;Fig A): Broad-based polyps composed of lobules of small pyloric-like glands separated by fibroblastic stroma with

variable amounts of smooth muscle. They were small (mean=0.4 cm; largest, 1.3 cm), often multiple(48%), and almost always associated with stones (98%) and significant inflammation (77%). Dysplastic changes were identified in 14%. 2. Cholesterol-type polyps(n=64,Fig B): Pedunculated, arborizing papillary lesions lined by normal GB epithelium, with edematous cores mostly devoid of glands and often (85%) but not always showing cholesterol-laden macrophages. Only 25% were associated with cholesterolosis in the uninvolved GB. 33% occurred in males. 3% showed overt dysplastic changes as a focal finding. 3. Inflammatory and stromal polyps: 2 granulation tissue, 2 xanthogranulomatous, and 2 lymphoid.

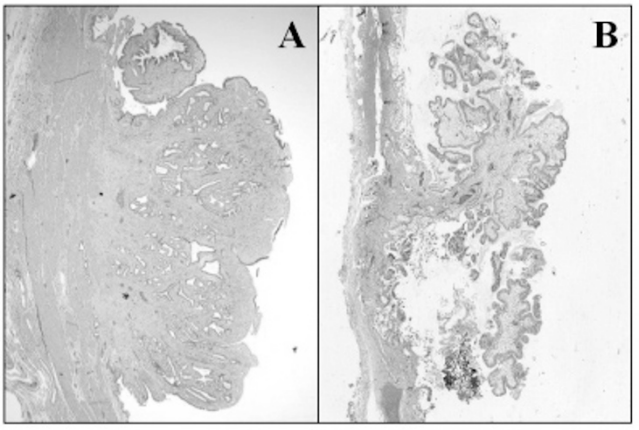

Conclusions: I. NNPs are seen in 2.2% of cholecystectomies but most (93%) are small (<1 cm) and incidental. **II.** Among clinically significant (≥1 cm) polyps, only 8% are NNPs. **III.** Focal dysplasia is seen in 9% of otherwise classic NNPs, and some show transitional features with ICPN, suggesting a progression phenomenon. **IV.** Cholesterol-type polyps are defined by a distinctive morphology rather than cholesterolosis. **V.** What we propose to designate as fibromyoglandular polyps are distinctive lesions that are often multiple, associated with stones and inflammation, and harbor focal dysplasia in 14%.

1594 Visual and Image Cytometric Analysis of Apoptosis in Hepatocellular Carcinoma: Correlation with Proliferation, Prognostic Parameters, and Survival.

J Wang, NK Saxena, C Cohen. Emory University School of Medicine, Atlanta.

Background: The incidence of hepatocellular carcinoma (HCC) is increasing worldwide. Programmed cell death, named apoptosis in the 1970s, has led to various therapeutic efforts. The caspase and BCL2 family of proteins are fundamental to the molecular cascade necessary for apoptosis. In the BCL2 family, Bax promotes cell death while BCL2 itself encourages survival. Caspase 3 is necessary for the caspase cascade which, upon activation, is responsible for the morphologic changes characteristic of apoptosis. Survivin, a member of the inhibitor of apoptosis gene family, inhibits apoptosis and is implicated in the regulation of mitosis and promotion of angiogenesis.

Design: 135 HCCs in 3 tissue microarrays with 2 1mm cores of each tumor were immunostained for survivin, activated caspase 3, Bax, and BCL2 expression and scored as intensity 0-3+ and % + cells. Results were compared to proliferation (mitoses/10HPF, MIB-1 visual mean, visual high and labeling index [LI], phosphohistone-3[PPH3] visual mean, visual high and LI), prognostic parameters (size, grade, stage, angiolymphatic invasion [ALI], metastases, focality, local recurrence [LR]), and survival. LI was determined with the ACIS III Image Cytometer (Dako).

Results: Positive staining is defined as 2-3+ intensity. Of the 135 HCCs, 58 (43%) had + nuclear survivin, 112 (83%) + cytoplasmic survivin, 85 (63%) + caspase 3, 109 (81%) + Bax and 4 (3%) + BCL2 expression. Statistically significant correlations are summarized as follows:

Significant Correlations

	Inverse	Direct	p-value
Survivin - Nuclear	Focality		0.04
	Cirrhosis		0.01
	PPH3 LI		0.02
		Histologic Grade	0.001
		Nuclear Grade	0.003
		Stage	0.02
		pT	0.002
		ALI	0.02
		LR	0.01
		Mitoses	0.005
Survivin - Cytoplasmic	MIB LI		0.05
Caspase 3		Mitoses	0.01
		MIB Visual Mean	0.05
		MIB Visual High	0.03
Bax	LR		0.03
		Cirrhosis	0.02
		Survival	0.01

BCL2 expression revealed no statistically significant relationships.

Conclusions: Survivin expression, especially nuclear, consistent with its role as an inhibitor of apoptosis, is associated with aggressive prognostic parameters (grade, stage, ALI, LR) and increased proliferation (mitoses). Caspase 3, indicating increased apoptosis, is associated with increased proliferation (mitoses, MIB-1), which may represent an overall increase in cell turnover. Bax, consistent with its pro-apoptotic role, is associated with decreased LR and increased survival.

1595 Histopathologic Characterization of 29 Explanted Livers Containing Treated Hepatocellular Carcinoma.

M Wang, S Rao, X Lin, Z-ME Chen. Northwestern University Feinberg School of Medicine, Chicago, IL.

Background: In patients with non-resectable hepatocellular carcinoma (HCC), downstaging therapy has been used as a bridge to subsequent transplant. The current available therapeutic modalities include arterial Yttrium-90 (^{90}Y) microsphere radioembolization, chemoembolization, and radiofrequency ablation (RFA). Morphologic features of treated tumors and adjacent liver parenchyma have not been carefully compared among the different modalities.

Design: A case search from 2004-2010 for explanted livers with treated HCC was performed. 14 cases (11 male and 3 female patients, mean age 63) were found to be treated with ^{90}Y microspheres (duration between treatment and transplant ranging from 1-18 months, mean 7 months), and 15 cases (13 male and 2 female patients, mean age 59) were identified featuring treatment with RFA, chemoembolization, or both (duration between treatment and transplant ranging from 3-6 months, mean 4 months). The histopathologic characteristics of tumor and adjacent liver parenchyma were evaluated, and the results were statistically analyzed by Fisher exact test.

Results: 8 of 14 (57%) ^{90}Y-treated livers had residual tumor with viability ranging from 5-90%, while 6 of 15 (40%) livers treated by other modalities had residual viable tumor ranging from 5-80% (p=0.29). All (100%) ^{90}Y-treated livers demonstrated acute lobular injury in the adjacent liver parenchyma, characterized by hepatocyte necrosis, chronic inflammation, and regenerative ductular proliferation. In contrast, only 6 (40%) of the 15 non-^{90}Y treated livers showed such changes, which were milder by comparison. Additionally, all (100%) ^{90}Y-treated livers demonstrated marked cytologic atypia in bile ducts surrounding treated tumor. These bile ducts often showed angulated borders, occasional cribriforming patterns, and associated marked stromal fibrosis, thereby mimicking malignancy. Such changes were only noted in one (6.7%) of the livers treated by other modalities.

Conclusions: Both ^{90}Y microsphere radioembolization and non-^{90}Y treatment modalities appear to induce equivalent degrees of tumor necrosis. However, acute lobular changes and marked duct epithelial atypia were more common in the ^{90}Y-treated cases. While the clinical significance of this difference remains elusive, recognizing the unique hepatocyte and bile duct morphology is helpful in histopathologic analysis of explanted livers.

1596 The Expression of FOXL2 in Pancreatic, Hepatobiliary, and Renal Tumors with Ovarian-Type Stroma.

M Westerhoff, M Tretiakova, L Hovan, J Hart, K Gwin, T Antic. University of Chicago, IL.

Background: FOXL2, a gene encoding a member of the fork-head-winged-helix family of transcription factors, is one of the earliest expressed genes during female gonadal development. It is required for folliculogenesis and is expressed in ovarian stroma. FOXL2 also opposes testicular development by suppressing the counteracting transcription factor SOX9. Moreover, FOXL2 is expressed in ovarian neoplasms with granulosa cell lineage.

Non-ovarian tumors such as pancreatic mucinous cystic neoplasms (PMC), hepatobiliary cystadenomas (HBC), and renal mixed epithelial stromal tumors (MEST), share the distinctive feature of having ovarian-type stroma. Given the expression of FOXL2 in normal human ovaries, the aim of our study was to further characterize the stroma in these non-ovarian tumors.

Design: 20 PMC, 5 HBC, and 3 MEST were retrieved from the surgical pathology database. H&E sections were reviewed and immunohistochemical (IHC) staining with FOXL2 (goat IgG, IMAENEX), estrogen receptor (ER), and progesterone receptor (PR) were assessed for nuclear IHC positivity in the tumor stroma.

Results: There were 26 females and 2 males (both PMC), with an age range of 35-71 years. All cases (20/20 PMC, 3/3 MEST, and 5/5 HBC) demonstrated strong nuclear reactivity for FOXL2 in the subepithelial stromal cells. ER and PR demonstrated nuclear reactivity in 12/20 PMC, 2/3 MEST, and 4/5 HBC, but staining intensity was generally weaker and patchier. The sensitivity of FOXL2 (100%) was superior to that of ER and PR (64%).

Clinical information was available for 20 patients. In 17/20 there was a history of obesity, chronic tamoxifen use, or oral contraceptive use. The 2 male patients had histories significant for morbid obesity and chronic alcoholism.

Conclusions: FOXL2 is expressed from the early stages of ovarian development and has been shown to be mandatory for normal ovarian function. We have shown that it is also expressed in the aberrant ovarian-type stroma characteristic of PMC, HBC, and MEST. It is more sensitive than ER and PR in demonstrating the stromal elements by IHC. The majority of such patients, including the rare male patients, have risk factors for hormonal abnormalities, such as morbid obesity and hormonal replacement therapy. There is no well-delineated explanation for the presence of ovarian-type stroma in PMC, HBC, and MEST. FOXL2 may be useful not only as an adjunct diagnostic marker, but in the elucidation of the embryologic origin/pathogenesis of the stroma in these tumors.

1597 The Presence of IGG4 Positive Plasma Cells in PSC/AIH as Compared to Other Autoimmune Liver Diseases.

M Westerhoff, J Hart. University of Chicago, IL.

Background: It has recently been recognized that some patients with autoimmune pancreatitis develop a hepatic IgG4 associated disease which clinically and histologically resembles sclerosing cholangitis. It is not clear whether this disease, termed IgG4-associated cholangitis, can also occur in patients without autoimmune pancreatitis.

Design: In order to determine whether IgG4 positive plasma cells are present in a variety of autoimmune liver disease, we performed immunohistochemical staining for IgG4 on needle core biopsies from 47 patients diagnosed by standard histologic and clinical criteria as autoimmune hepatitis (AIH), primary biliary cirrhosis (PBC), AMA negative PBC, AIH/PBC overlap, primary sclerosing cholangitis (PSC), and PSC/AIH overlap. No patients had autoimmune pancreatitis or any other IgG4 related disorder. The total number of IgG4 reactive plasma cells was counted, and the highest number per portal tract was scored as: 0 (none), 1 (1-3), and 2 (greater than 3).

Results: Absent or rare scattered single IgG4 reactive plasma cells were present in portal tracts (score 0 or 1) in the patients with PBC (n=12), AMA negative PBC (n=7), PBC/AIH overlap (n=7), AIH, (n=7), and PSC (n=6). In contrast, biopsies from six of eight patients with PSC/AIH overlap contained numerous IgG4 reactive cells (see chart).

PSC/ AIH	Total # of IgG4 cells	IgG4 score	Colonoscopy	ANA	Alk phos	AST/ALT	MRCP/ ERCP
48 F	44	2+	No IBD	1:320	472	37/39	Negative
54 F	20	2+	Not done	1:640	68	77/161	Not done
28 F	82	2+	Not done	1:640	236	182/263	Not done
28 M	68	2+	IBD	1:640	366	502/692	Negative
19 M	65	2+	Not done	Not done	N/A	N/A	Negative
27 M	34	2+	IBD	1:2560	190	1083/1300	Negative
5 M	1	1+	No IBD	1:640	3415	325/358	Not done
16 M	3	1+	IBD	1:320	3415	17/13	Negative

Conclusions: IgG4 reactive plasma cells are not present in the liver biopsies of patients with AIH, PBC, AMA negative PBC, AIH/PBC overlap or PSC. In contrast, a majority of patients with PSC/AIH overlap have significant infiltrates of IgG4 plasma cells. These patients appear to have a small duct form of PSC (ERCP negative) with fibrotic biliary changes that may be an IgG4-associated feature. Serum levels of IgG4 should be obtained from PSC/AIH patients to further characterize this overlap syndrome.

1598 IPMNS of the Pancreas and Associated Small Duct Lesions – Analysis of the Distribution of High Grade Dysplasia.

GQ Young, N Katabi, E Vakiani, UK Bhanot, DS Klimstra. Memorial Sloan-Kettering Cancer Center, New York, NY.

Background: Pancreatic intraductal papillary mucinous neoplasms (IPMNs) are preinvasive neoplastic lesions that are increasingly recognized. IPMNs can be associated with small ductal lesions (SDL), both close to and distant from the main cystic lesion (MCL). The differential diagnosis of SDLs includes pancreatic intraepithelial neoplasia (PanIN), which often demonstrates similar histologic features. In some cases the degree of dysplasia may vary throughout all of the intraductal neoplasia, but the relevance of the degree of dysplasia in SDLs has not been addressed. Our goal was to evaluate IPMNs with associated SDLs, comparing their morphologic features to determine if a relationship exists.

Design: Among 46 reviewed cases of IPMNs, 18 cases were identified with SDLs separately identified from the MCL (39%). Only cases lacking an invasive carcinoma component were selected. Clinical information was retrieved. Histologic analysis of the MCL, the SDLs, and margin sections was performed.

Results: Half of the IPMNs were located in the pancreatic head. The size ranged from 0.4-8.0 cm, (mean, 2.99 cm). 56% (n=10) were branch duct type, and the remainder were either main duct type or combined type. 72% of IPMNs (n=13) had gastric type (GT) epithelium, while intestinal and pancreatobiliary types numbered 3 and 2, respectively. 78% (14/18) cases had high grade dysplasia (HGD) somewhere in the pancreas, and among these, 9 cases (64%) showed HGD in the MCL, while 5 cases (36%) showed HGD only in the SDLs. All cases with a higher grade of dysplasia in the SDLs versus the MCL were GT IPMNs. Evaluation of the margin showed 2 cases with HGD, 7 with moderate dysplasia and 6 with low grade dysplasia. Margin section slides were not available for 3 cases. IPMN was favored at the margin in 3/15 cases, PanIN was favored at the margin in 6/15 cases, while 6/15 cases were deemed indeterminate for IPMN vs. PanIN.

Conclusions: IPMNs can be associated with SDLs and the interpretation of these smaller lesions can be difficult. In 36% of cases, a higher grade of dysplasia was found in SDLs than in the MCL. Whether SDLs are an extension of the IPMN or separate foci of PanIN is difficult to determine by morphology alone. This problem is often encountered in the evaluation of resection margins; in 40% of cases, margin status remained indeterminate. IHC and molecular studies may help in accurately classifying these lesions. The finding of higher grades of dysplasia in non-cystic ducts away from the MCL has implications for sampling of these specimens.

1599 Autoimmune Pancreatitis (AIP) Type 1 and Type 2: An International Consensus Study on Histopathologic Diagnostic Criteria.

L Zhang, S Chari, T Smyrk, V Deshpande, G Kloppel, M Kojima, X Liu, D Longnecker, M Mino-Kenudson, K Notohara, M Rodriguez-Justo, A Srivastava, G Zamboni, Y Zen. Mayo Clinic, Rochester; Massachusetts General Hospital, Boston; University of Kiel, Germany; National Cancer Center Hospital East, Kashiwa Chiba, Japan; Cleveland Clinic; Dartmouth-Hitchcock Medical Center, Lebanon; Kurashiki Central Hospital, Japan; University College London, United Kingdom; University of Verona, Italy; King's College London, London, United Kingdom.

Background: There is lack of consensus among pathologists regarding diagnostic criteria and typing of AIP. The goal of this study was to develop and validate consensus diagnostic criteria for AIP and its types.

Design: As a part of the AIP International Co-operative Study Group, 13 pathologists from five countries participated in this two-phase study to develop diagnostic criteria for AIP types 1 and 2 (Phase I) and validate them (Phase II). A virtual library of 40 resected pancreata of AIP and other forms of chronic pancreatitis (CP) was constructed at PathXchange.org. All slides were reviewed online. Readers filled out a questionnaire for key histopathologic findings, final diagnosis and AIP type.

Results: AIP had distinguishing features from alcoholic and obstructive forms of CP, including periductal lymphoplasmacytic infiltrate, inflamed cellular stroma with storiform fibrosis, obliterative phlebitis, and granulocytic epithelial lesion (GEL). Although there was overlap, two types (type 1 and type 2) were recognized. Type 1 AIP had dense periductal lymphoplasmacytic infiltrate with storiform fibrosis and obliterative phlebitis, while type 2 was distinguished from type 1 by GEL and less prominent lymphoplasmacytic infiltrate and storiform fibrosis. Diagnostic criteria for AIP and its types were proposed according to the results from the top 5 reviewers in phase I. The inter-observer agreement was significantly improved in phase II study. The multi-rater Kappa statistic among all reviewers for diagnosing AIP and distinguishing its types were increased from 0.59 to 0.7 and from 0.08 to 0.54 respectively. For the top 5 reviewers, there was almost perfect agreement for diagnosing AIP in both phases, and the Kappa statistic for distinguishing its types was increased from 0.39 to 0.80.

Conclusions: In resected pancreata, AIP can be distinguished from other forms of CP with substantial interobserver agreement. There are two distinct histopathologic types of AIP. The histopathologic diagnostic criteria for AIP and its types proposed by this international consensus study can be used as guidelines by general pathologists.

1600 Pancreatic Carcinoma with Concurrent, Autoimmune-Like Chronic Pancreatitis – Clinical Implications.

X Zhang, M Westerhoff, J Hart, S-Y Xiao. University of Chicago Medical Center, IL.

Background: Autoimmune pancreatitis (AIP) accounts for about 2-6% of idiopathic chronic pancreatitis and is a well-known mimic of pancreatic adenocarcinoma. It is crucial to distinguish AIP from pancreatic carcinoma to avoid unnecessary surgery; however, it remains unclear whether a diagnosis of AIP excludes that of carcinoma. In this study, we investigate the potential incidence of AIP-like changes concurrent with pancreatic carcinoma.

Design: Sixty pancreatectomies for carcinoma that also exhibit chronic pancreatitis were reviewed. Periductal/lobular lymphoplasmacytic infiltration, fibrosis, and ductal obstruction were scored on a scale of 0-3. The presence of granulocytic epithelial lesions, obliterative phlebitis, and germinal centers were also recorded. Immunohistochemistry for IgG4 was performed on cases with features suggestive of AIP and on cases without features of AIP as controls. IgG4+ plasma cells were counted in three HPFs (40x) in each case and an average was calculated.

Results: Eight cases showed features suggestive of AIP as characterized by moderate to severe (scored 2-3/3) periductal lymphoplasmacytic infiltration and/or periductal fibrosis. In five of these, IgG4+ plasma cells were more than 20/HPF (25, 30, 51, 75, 120/HPF respectively). All five cases showed germinal centers, three with granulocytic epithelial lesions, and two with obliterative phlebitis. Overall, 8.3% (5/60) of the reviewed cases were found to have histologic and immunohistochemical features of AIP. Most control cases had no or scattered IgG4 + plasma cells (median 2/HPF, ranged 0-65/HPF, $p<0.05$ vs those with features of AIP). Although three control cases exhibited an increased number of IgG4+ plasma cells (23, 26, 65/HPF respectively), no morphological features of AIP were present in these cases.

Conclusions: Features consistent with AIP were observed in 8.3% of pancreatectomy cases containing carcinoma that also showed concurrent chronic pancreatitis. Therefore, the presence of chronic pancreatitis with features consistent with AIP on core biopsy specimens may not completely exclude a coexisting pancreatic carcinoma. Clinical correlation and close follow up is necessary in this scenario. Furthermore, an increased number of IgG4+ plasma cells alone should not be used as a diagnostic criterion for AIP.

1601 Involvement of the Cytosolic Phospholipase A_2 alpha Signaling Pathway in Spontaneous and Transforming Growth Factor-beta Induced Hepatic Stellate Cell Activation.

L Zhao, Z-H Gao. University of Calgary and Calgary Laboratory Services, AB, Canada.

Background: Activated hepatic stellate cells (HSCs) play a pivotal role in liver fibrogenesis. The aim of the study is to evaluate the involvement of cytosolic phospholipase A_2 alpha ($cPLA_2\alpha$) signaling pathway in spontaneous and transforming growth factor-beta (TGF-β) induced HSC activation.

Design: Rat HSCs were isolated, purified, cultured, and stimulated with TGF-β1 in the presence or absence of the selective $cPLA_2\alpha$ inhibitor, arachidonyltrifluoromethyl ketone ($AACOCF_3$). The activation status of HSC was evaluated by immunofluorescent staining of alpha-smooth muscle actin (α-SMA) and by measuring the expression of $cPLA_2\alpha$, cyclooxygenase 2 (COX-2) and peroxisome proliferator-activated receptor beta/delta (PPAR-β/d) using Western blot analysis.

Results: Rapid and significant increase in the expression of $cPLA_2\alpha$ was observed during spontaneous activation of HSCs. These events preceded the elevation of PPAR-β/d and α-SMA. Elevated expression of $cPLA_2\alpha$, but not COX-2, was also observed during TGF-β induced HSC activation. The TGF-β induced α-SMA expression was blocked by the selective $cPLA_2$ inhibitor, $AACOCF_3$. Furthermore, transfection of $cPLA_2\alpha$ expression vector enhanced the transcription activity of PPAR- β/d and the expression of α-SMA in HSCs.

Conclusions: These data demonstrated a novel intracellular signaling pathway in spontaneous and TGF-β induced activation of HSCs that involves $cPLA_2\alpha$ mediated induction of PPAR-β/d. Therefore, inhibiting this signaling pathway may represent a novel therapeutic approach for the treatment of liver fibrosis.

1602 Pathologic Complete Response Is Associated with Good Prognosis in Patient with Pancreatic Ductal Adenocarcinoma Who Received Neoadjuvant Chemoradiation and Pancreatectomy.

Q Zhao, A Rashid, Y Gong, M Katz, J Lee, R Wolf, C Charnsangavej, G Varadhachary, P Pisters, E Abdalla, J-N Vauthey, H Wang, H Gomez, J Fleming, J Abbruzzese, H Wang. MD Anderson Cancer Center, Houston, TX.

Background: Patients with pancreatic ductal adenocarcinoma (PDA) has poor prognosis. To improve the clinical outcome, most patients with PDA are treated with neoadjuvant chemoradiation prior to surgery at our institution. In this group of patients, pathologic complete response (PCR) is rarely observed in subsequent pancreatectomies. However, the prognostic significance of PCR is not clear.

Design: Among 442 patients with PDA who received neoadjuvant chemoradiation and pancreatectomy from 1995 to 2010, 11 (2%) patients with PCR were identified. The cytologic diagnosis on pre-therapy tumor was reviewed and PCR in pancreatectomies was confirmed in all patients. Clinical and follow-up information were extracted from the medical records. Survival analysis was performed using the Kaplan-Meier method.

Results: There were 6 men and 5 women with age ranging from 43y to 75y (median: 61y). 4/11 (36%) patients had prior history of or synchronous extrapancreatic cancers, including one with lung cancer, one with breast cancer, one with prostate cancer and one with renal cell carcinoma. 5 patients received neoadjuvant chemotherapy followed by chemoradiation and 6 patient received chemoradiation. 10 patients had pancreaticoduodenectomy (PD) and one had distal pancreatectomy. These specimens were well sampled by histology and the entire pancreas was submitted for histology in 9 cases. On review, scar with fibrosis and chronic pancreatitis were present in all eleven cases. Carcinoma in situ was present in 2 cases and PanIN3 or PanIN2 in 4 cases. However, no residual viable invasive carcinoma cells or lymph node metastasis was identified in all cases. Follow-up information was available in 9/11 patients. Follow-up time ranges from 6M to 181M (median, 49M). During follow-up, four patients died, including one from brain metastasis of prior lung cancer, one from bone metastasis of breast cancer, one from sepsis, and one developed a second primary or recurrent PDA in the tail of pancreas at 84 M after PD and died of PDA at 105 M after the diagnosis of the initial PDA. The last patient had carcinoma in situ in the initial PD specimen. The other 5 patients were alive with no evidence of disease. Patients with PCR had better survival compared to the 240 patients who had residual viable PDA in pancreatectomy specimens after neoadjuvant therapy ($p<0.001$).

Conclusions: Patients with PDA who received neoadjuvant chemoradiation and had PCR in pancreatectomy is rare and is associated with better prognosis.

1603 Hepatocellular Carcinomas Occasionally Express Neuroendocrine Markers While Neuroendocrine Tumors Metastatic to the Liver Do Not Show Hepatocellular Expression.

X Zhou, MM Yearsley, KS Jones, WL Frankel. The Ohio State University, Columbus.

Background: Neuroendocrine tumors (NETs) of gastrointestinal tract are generally slow growing but frequently metastasize to the liver, ranking second to colorectal carcinoma as a source of liver metastases. Distinction between NET and hepatocellular carcinoma (HCC) can be challenging on a small biopsy because both can show nested and trabecular patterns. In addition, immunostaining for neuroendocrine markers has been observed occasionally in HCCs. Utilizing immunohistochemistry for hepatocyte, glypican-3, CD56, synaptophysin (Syn) and chromogranin A (Chr), we analyzed the staining profile in HCCs and NETs to determine how often the tumors show an overlapping pattern of expression.

Design: Tissue microarrays were constructed from formalin-fixed, paraffin-embedded blocks of 48 NETs metastatic to the liver and 114 HCCs from our archives and stained for hepatocyte, glypican-3, CD56, Syn and Chr. Immunostaining was evaluated by two pathologists; > 5% immunoreactivity was considered positive and intensity was scored for each (1+, weak; 2+, strong).

Results: Of the 114 HCCs, 107 (94%) were positive for hepatocyte or glypican-3, 92 (81%) for hepatocyte, 67 (59%) for glypican-3, and 52 (46%) for both. Seven HCCs (6%) showed positivity for CD56 (4 focal, 3 diffuse, 2 weak and 5 strong), of which 3 (3%) were also positive for Syn (all focal, 1 weak and 2 strong). All 7 HCCs positive for CD56 or Syn expressed hepatocyte or glypican-3 and none were fibrolamellar type. None of the HCCs expressed Chr. All 48 NET liver metastases expressed at least one neuroendocrine marker. All but one (98%) NETs were positive for Syn, 40 (83%) for Chr and 39 (81%) for CD56. Thirty-four NETs (71%) expressed all neuroendocrine markers. No hepatocyte or glypican-3 expression was present in the NET liver metastases.

Positive immunostaining in HCCs and NETs metastatic to the liver

	Hepatocyte	Glypican-3	Synaptophysin	Chromogranin A	CD56
HCC (n = 114)	92	67	3	0	7
NET (n = 48)	0	0	47	40	39

HCC, hepatocellular carcinoma; NET, neuroendocrine tumor.

Conclusions: Occasional HCCs express CD56 and Syn, while all express either hepatocyte or glypican-3. NETs metastatic to the liver do not express hepatocyte or glypican-3 and almost always express Syn, while Chr and CD 56 are seen in most cases. Utilizing a limited immunohistochemistry panel, including hepatocyte, glypican-3, Syn and Chr, can efficiently distinguish HCC from NET liver metastases and help avoid diagnostic pitfalls on small biopsies.

Neuropathology

1604 Nestin, an Important Marker for Differentiating Oligodendroglioma from Astrocytic Tumors.

SH Abu-Farsakh, IA Sbeih, HA Abu-Farsakh. Jordan University, Amman, Jordan; Ibn Hytham Hospital, Amman, Jordan; First Medical Lab, Amman, Jordan.

Background: Nestin is an acronym for neuroepithelial stem cell protein. It is an intermediate filament protein expressed in proliferating cells during the developmental stages in a variety of embryonic and fetal tissues. It is also expressed in some adult stem/progenitor cell populations, such as newborn vascular endothelial cell. Differentiation between astrocytic tumors and oligodenoglioma tumor is of paramount importance because of different lines of treatment and different prognosis.

Design: We performed Nestin immunostaining on paraffin blocks of 16 cases of astrocytomas of various grades (3 Glioblastoma, 3 anaplastic astrocytoma, 3 fibrillary astrocytoma and 7 Pilocytic astrocytoma) and on 12 oligodendroglioma (6 grade II, and 6 grade III). All cases of oligodendroglioma has confirmation by FISH for 1p 19q.

Results: Nestin staining was seen in all astrocytic tumors. The strongest staining was in glioblastomas and in Anaplastic astrocytomas.

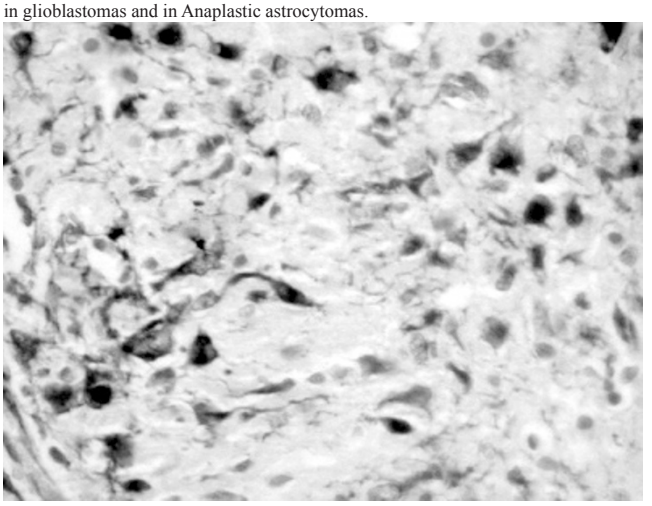

Pilocytic astrocytomas show mostly focal and weak staining with strong staining of Rosenthal fibers. Grade II astrocytoma shows weak but more intense staining than pilocytic astrocytoma. No Nestin immunostaining was seen in any of the oligodendroglioma tumor cells, but Nestin stained the endothelial cells in oligodendroglioma as a positive internal control.

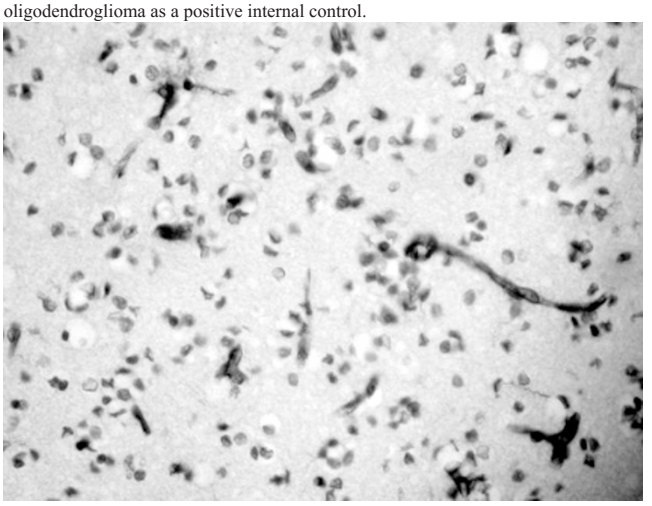

Conclusions: Nestin is an important immunohistochemical marker in differentiating oligodendroglioma from astrocytic tumors. Nestin, also, is helpful in grading astrocytoma.

1605 Analysis of Glioma Stem Cell Markers and Genomic Alterations in Primary and Recurrent Glioblastomas.

CL Appin, MJ Schniederjan, E Van Meir, GM Mastrogianakis, DJ Brat. Emory University School of Medicine, Atlanta, GA.

Background: Glioblastoma (GBM) is an aggressive primary CNS tumor, with a median survival of one year following standard therapy. Previous studies demonstrated an association between the glioma stem cell (GSC) compartment and biologic aggressiveness. Moreover, recurrent post-radiation GBMs are enriched for GSCs in animal models. Here we investigate whether stem cell markers are increased in recurrent human GBMs compared to the primary and also examine whether genetic alterations are associated with the expression of GSC markers.

Design: Primary and recurrent GBMs from 13 patients (29-67 yrs-old; 4F, 9M) were included. Paraffin-embedded slides were stained for CD133, Sox2, Nestin, c-Myc and